

**NASA CONTRACTOR
REPORT**



NASA CR-1906

2.1

006,1030



NASA CR-1906

**LOAN COPY: RETURN TO
AFWL (DOUL)
KIRTLAND AFB, N. M.**

**COMPARISON OF VARIOUS METHODS
OF MATHEMATICAL ANALYSIS OF THE
FOUCAULT KNIFE-EDGE TEST PATTERN
TO DETERMINE OPTICAL IMPERFECTIONS**

by B. E. Gatewood

Prepared by

THE OHIO STATE UNIVERSITY RESEARCH FOUNDATION

Columbus, Ohio 43212

for Langley Research Center

NATIONAL AERONAUTICS AND SPACE ADMINISTRATION • WASHINGTON, D. C. • NOVEMBER 1971



0061030

1. Report No. NASA CR-1906	2. Government Accession No.	3. Recipient's Catalog No.	
4. Title and Subtitle COMPARISON OF VARIOUS METHODS OF MATHEMATICAL ANALYSIS OF THE FOUCAULT KNIFE-EDGE TEST PATTERN TO DETERMINE OPTICAL IMPERFECTIONS		5. Report Date November 1971	6. Performing Organization Code
		8. Performing Organization Report No. RF Project 3050 A1	
7. Author(s) B. E. Gatewood		10. Work Unit No.	
9. Performing Organization Name and Address The Ohio State University Research Foundation 1314 Kinnear Road Columbus, Ohio 43212		11. Contract or Grant No. NGR-36-008-153	
		13. Type of Report and Period Covered	
12. Sponsoring Agency Name and Address National Aeronautics and Space Administration Washington, D.C. 20546		14. Sponsoring Agency Code Contractor Report	
		15. Supplementary Notes	
16. Abstract <p>The linearized integral equation for the Foucault test of a solid mirror is solved by various methods: power series, Fourier series, collocation, iteration, and inversion integral. The case of the Cassegrain mirror is solved by a particular power series method, collocation, and inversion integral. The inversion integral method appears to be the best overall method for both the solid and Cassegrain mirrors. Certain particular types of power series and Fourier series are satisfactory for the Cassegrain mirror. Numerical integration of the nonlinear equation for selected surface imperfections shows that results start to deviate from those given by the linearized equation at a surface deviation of about 3 percent of the wavelength of light. Several possible procedures for calibrating and scaling the input data for the integral equation are described.</p>			
17. Key Words (Suggested by Author(s)) Foucault Knife-Edge Test Integral Equations Large Orbiting Telescope Active Optics Deformable Mirror		18. Distribution Statement Unclassified - Unlimited	
19. Security Classif. (of this report) Unclassified	20. Security Classif. (of this page) Unclassified	21. No. of Pages 106	22. Price* \$3.00



SUMMARY

The linearized integral equation for the Foucault test of a solid mirror is solved by various methods: power series, Fourier series, collocation, iteration, and inversion integral. The case of the Cassegrain mirror is solved by a particular power series method, collocation, and inversion integral. The inversion integral method appears to be the best overall method for both the solid and Cassegrain mirrors. Certain particular types of power series and Fourier series are satisfactory for the Cassegrain mirror. Numerical integration of the nonlinear equation for selected surface imperfections shows that results start to deviate from those given by the linearized equation at a surface deviation of about three percent of the wavelength of light. Several possible procedures for calibrating and scaling the input data for the integral equation are described.

TABLE OF CONTENTS

<u>Section</u>	<u>Page</u>
I INTRODUCTION	1
II DERIVATION OF INTEGRAL EQUATIONS	2
III RESTRAINT CONDITIONS ON SOLUTION OF THE LINEAR EQUATIONS	7
IV POWER SERIES SOLUTIONS	10
V FOURIER SERIES SOLUTIONS	16
VI COLLOCATION SOLUTION	26
VII ITERATION SOLUTIONS	29
VIII INVERSION INTEGRAL SOLUTION	34
IX COMPARISON OF THE VARIOUS SOLUTIONS FOR SELECTED EXAMPLES	48
X SOLUTIONS FOR CASE OF A CENTRAL HOLE	62
XI NONLINEAR NUMERICAL INTEGRATION FOR ASSUMED SOLUTIONS	75
XII SCALE FACTOR PROBLEMS	81
XIII CONCLUSIONS AND RECOMMENDATIONS	82
REFERENCES	84
 <u>Appendix</u>	
A Approximation in Sense of Least Squares for a System of Simultaneous Equations	85
B Evaluation of an Integral in Fourier Series Solution	89
C G Matrix for Inversion Integral Method	91
D Computer Program for Inversion Integral Method (Cassegrain Mirror)	97

I - INTRODUCTION

The Foucault knife-edge test method is a widely used method of testing astronomical mirrors and other high-quality optical systems of large aperture during the final figuring. It would appear to be especially suited for testing the mirror of a large telescope in orbit because of its sensitivity and minimal equipment requirements and because its essential requirement of a perfectly uniform test beam can be satisfied in space by pointing the telescope at a star. Even if the telescope is free of imperfections when first built, temperature variations and structural relaxation or creep may subsequently introduce distortions so that some such method for occasionally testing the telescope optics is desirable. If the primary mirror is adjustable, it would be especially desirable that the test method be capable of providing quantitative information on the distortion that must be corrected.

This problem of the quantitative determination of the distortion of the mirror by means of the Foucault knife-edge test is considered here. The analysis is based on the work of Linfoot (Ref. 1), who derived expressions for the distribution of the light intensity seen in the knife-edge test for both perfect and imperfect mirrors as a function of the mirror surface distortion. For a uniformly reflecting mirror with small surface imperfections, the change in the light distribution from that of a perfect mirror is given by a linear integral expression involving the phase distortion of the converging wave front at the mirror. The solution for this phase distortion, which is directly related to the mirror surface distortion, involves the inversion of this integral expression.

Thus, the problem of the determination of the mirror imperfections from the knife-edge observations reduces to the problem of solving an integral equation. In the work herein reported, various methods of solution were studied. Five function methods involving power series and Fourier series, a collocation solution, two iteration solutions, and an inversion integral solution are presented and compared for selected examples. Three of the more suitable methods were applied to the Cassegrain type of mirror, or mirror with a central hole. In addition to describing and discussing the advantages and disadvantages of these various methods, this report also presents some nonlinearized calculations of the knife-edge test intensities for distortions of increasing size, in order to help the user estimate the limitations of the linearized solutions.

II - DERIVATION OF INTEGRAL EQUATIONS

The optical arrangement in the knife-edge test is shown in the sketch, Fig. 2-1. The knife-edge passes through the focus of the mirror and the lens focuses the mirror surface onto the image plane of the lens. This image plane may be the location of the observers eye or may be the location of a group of light sensors. Linfoot (Ref. 1) showed that when the observer looks past the knife-edge toward the mirror, the observed distribution of light intensity at the mirror along any line normal to the knife-edge depends only on the mirror figure along that line. Thus, with the knife-edge normal to the plane of the sketch in Fig. 2-1, only a line of sensors in, or parallel to, the plane of the sketch is needed in the image plane of the lens. To completely test the mirror, several lines of sensors would be needed. Katzoff (Ref. 2) discusses possible arrangements of the sensors for a complete test of the mirror. He also examines the problem of precise location of the knife-edge when the mirror has imperfections.

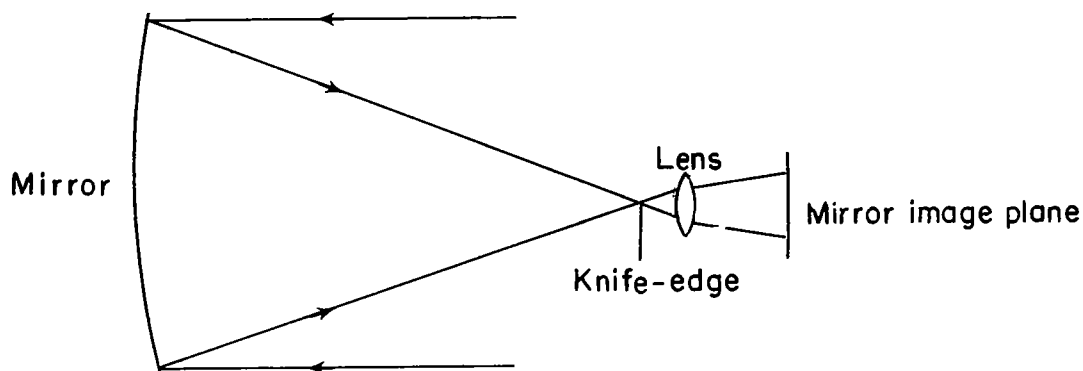


Fig. 2-1. Optical Arrangement in Knife-Edge Test

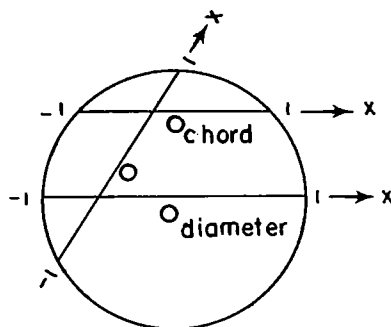


Fig. 2-2. Definition of x for Lines on the Mirror

Since the light intensity along a line across the mirror normal to the knife-edge depends only on the shape of the mirror along that line, let x be the distance along this line. Let $x = -1$ and $x = +1$ represent the points where the line crosses the edges of the mirror, regardless of whether the line is a diameter or a chord of the mirror (see Fig. 2-2). Linfoot (Ref. 1) derived the following basic equation for $D(x)$, the

$$2\pi D(x) = \pi E(x) + i \int_{-1}^{+1} \frac{E(t)}{t - x} dt \quad (2-1)$$

complex displacement at the image plane of the lens, where $E(x)$ is the complex displacement of the converging wave front just as it leaves the mirror, and t is a running variable corresponding to the variable x . The observed distribution of light intensity along the line is

$$I(x) = 4\pi^2 |D(x)|^2 \quad (2-2)$$

$I(x)$ and $D(x)$ are functions of x in the sense that the observer looking past the knife-edge sees $I(x)$ as the apparent brightness at point x .

The conditions or restrictions on Eqs. (2-1) and (2-2) are (see p. 138, Ref. 1):

- (a) the diameter of the mirror subtends only a small angle at the focal point;
- (b) the errors of figure of the mirror, though they may amount to many wavelengths, are small compared to the focal distance;
- (c) the errors of slope in the mirror surface are small; and
- (d) the function $E(x)$ is continuous and differentiable except at the edge of the mirror.

Under these conditions, the equations are valid for mirrors of arbitrary edge contour, including central piercings as for a Cassegrain arrangement, and of variable reflecting power.

The function $E(x)$ can be taken in the form

$$E(x) = |E(x)| \exp \left[- \frac{2\pi i}{\lambda} \varphi(x) \right] \quad (2-3)$$

where $\exp \left[- \frac{2\pi i}{\lambda} \varphi(x) \right]$ is a phase function which describes the imperfections on the surface of the mirror; λ is the wavelength of light. For the perfect mirror, $\varphi(x) = 0$ and $E(x) = 1$, so that

$$2\pi D_0(x) = \pi + i \log \left(\frac{1-x}{1+x} \right), \text{ perfect mirror,} \quad (2-4)$$

and

$$I_0 = 4\pi^2 |D_0(x)|^2 = \pi^2 + \log^2 \left(\frac{1-x}{1+x} \right), \quad -1 < x < 1, \quad (2-5)$$

where the subscript 0 indicates the perfect mirror. For the case of the distorted mirror, take

$$\eta(x) = -\phi(x)/\lambda$$

$$E(x) = \exp[2\pi i \eta(x)] = \cos 2\pi \eta(x) + i \sin 2\pi \eta(x) \quad (2-6)$$

where $\eta(x)$ is the phase error, in wavelengths, on the converging wave front where it leaves the mirror. It is twice the error, in wavelengths of the mirror surface at that location. The phase error $\eta(x)$ is positive when the imperfection on the mirror surface is raised toward the observer.

If Eq. (2-6) for $E(x)$ is substituted into Eqs. (2-1) and (2-2), then

$$\begin{aligned} 2\pi D(x) &= \pi [\cos 2\pi \eta(x) + i \sin 2\pi \eta(x)] \\ &+ i \int_{-1}^1 \frac{\cos 2\pi \eta(t) dt}{t-x} - \int_{-1}^1 \frac{\sin 2\pi \eta(t) dt}{t-x} \end{aligned} \quad (2-7)$$

and

$$\begin{aligned} I(x) &= \pi^2 + \left[\int_{-1}^1 \frac{\cos 2\pi \eta(t) dt}{t-x} \right]^2 + \left[\int_{-1}^1 \frac{\sin 2\pi \eta(t) dt}{t-x} \right]^2 \\ &+ 2\pi \sin 2\pi \eta(x) \int_{-1}^1 \frac{\cos 2\pi \eta(t) dt}{t-x} \\ &- 2\pi \cos 2\pi \eta(x) \int_{-1}^1 \frac{\sin 2\pi \eta(t) dt}{t-x} \end{aligned} \quad (2-8)$$

If $\eta(x)$ is sufficiently small so that

$$\cos 2\pi \eta(x) \sim 1.0, \quad \sin 2\pi \eta(x) \sim 2\pi \eta(x)$$

$$[\eta(x)]^2 \sim 0.0$$

then Eq. (2-8) can be linearized approximately to give

$$I - I_0 = 4\pi^2 \eta(x) \log \left(\frac{1-x}{1+x} \right) - 4\pi^2 \int_{-1}^1 \frac{\eta(t)}{t-x} dt \quad (2-9)$$

This is the basic linear integral equation for $\eta(x)$. Take

$$f(x) = 4\pi^2 \eta(x), F(x) = I - I_0 \quad (2-10)$$

so that the basic Eq. (2-9) is

$$F(x) = f(x) \log \left(\frac{1-x}{1+x} \right) - \int_{-1}^1 \frac{f(t)}{t-x} dt. \quad (2-11)$$

For some of the solutions to be given later in this report, it is preferable to write Eq. (2-11) in the form

$$F(x) = - \int_{-1}^1 \frac{f(t) - f(x)}{t-x} dt \quad (2-12)$$

When the mirror has a central hole of radius R , the linearization of Eq. (2-8) gives

$$F(x) = I - I_0 = f(x) \log \left| \frac{1-x}{1+x} \frac{x+R}{x-R} \right| - \int_{-1}^{-R} \frac{f(t)dt}{t-x} - \int_R^1 \frac{f(t)dt}{t-x} \quad (2-13)$$

where

$$I_0 = \pi^2 + \log^2 \left| \frac{1-x}{1+x} \frac{x+R}{x-R} \right| \quad (2-14)$$

for any diameter. However, as in Fig. 2-2, the line on the mirror may be any chord so that R in Eq. (2-13) may vary from $R = 0$, the case of Eq. (2-11) when the chord line does not cross the hole, up to $R = \text{radius}$ of the hole. Thus, in Eq. (2-13), $x = -1$ and $x = 1$ refer to the edges of the mirror for any line and $x = \pm R$, with R properly scaled to the x length, refer to the edges of the hole if the line crosses the hole (see Fig. 2-3).

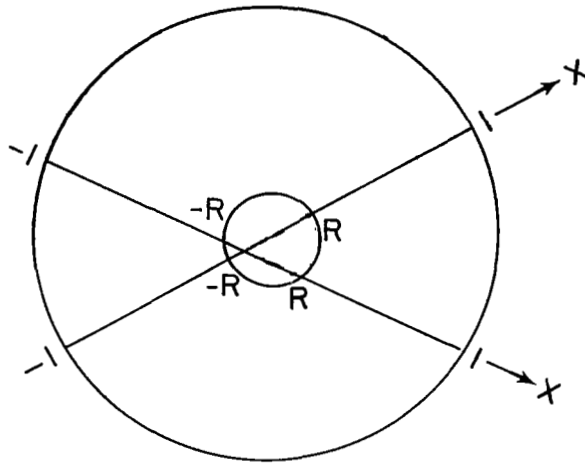


Fig. 2-3. Knife-Edge Test Lines for Cassegrain Mirror System

For later use, Eq. (2-13) can be written in the form

$$F(x) = - \int_{L_2} \frac{f(t) - f(x)}{t - x} dt \quad (2-15)$$

where L_2 consists of the two line segments, -1.0 to $-R$ and R to 1.0 .

The problem now is reduced to solving these integral equations for $f(x)$ or $\eta(x)$. Since little can be done about solving the nonlinear integral Eq. (2-8) for $\eta(x)$, the work of this report is concentrated on solving the linear integral Eqs. (2-11) or (2-12) and (2-13) or (2-15) for $f(x)$. Some results for the exact Eq. (2-8), obtained by numerical integration, are given in Sec. XI for assumed values of $\eta(x)$. Before presenting the various methods of solving the linear equations, some discussion of the general restraint conditions, homogeneous solutions, numerical integration difficulties and computer limitations for these equations is given in the following section.

III - RESTRAINT CONDITIONS ON SOLUTION OF THE LINEAR EQUATIONS

There are several factors that must be considered in attempting to solve the integral equations (2-11), (2-12), (2-13), and (2-15). The problems of (a) point values of $F(x)$, (b) numerical integration, (c) function methods with numerical integration, (d) discontinuities at the edges of the mirror, (e) homogeneous solutions, (f) rigid body rotations of the mirror and (g) computer limitations are described below.

(a) Point values of $F(x)$. Since $F(x) = I(x) - I_0(x)$, the change in light intensity due to a distortion in the mirror and must be obtained by sensors from the knife-edge test, it will be known only at selected points on selected lines on the mirror (unless it is measured with a scanning sensor). Thus, with $F(x)$ given at points only, the equations must be solved numerically. Regardless of what method of solution is used, numerical integrations will have to be made, either directly or indirectly. Since these equations may be singular, with the integrand becoming infinite when the integration variable t crosses x , there may be difficulties with the numerical integration. As the particular type of numerical integration will depend upon the method of solution, the specific problems with the integration are discussed later, where the different methods of solution are described. Some general comments on numerical integration are given in item (b).

(b) Numerical integration. In the numerical integration for the various methods of solution described later in this report, it will be assumed that readings of $F(x)$ from the knife-edge test will be at equally spaced points in a line across the mirror. For this case of equal intervals, the Newton-Cotes quadrature formulas (Ref. 3, p. 397) are probably the most suitable for the numerical integration. These formulas give weight coefficients H_j , or the Cotes numbers, to multiply the ordinates of the integrand for the integration. Thus

$$\int_0^1 f(x)dx = \sum_{j=1}^J H_j f(x_j) \quad (3-1)$$

The two-point formula is the same as the trapezoid rule, the three-point formula is Simpson's rule. The H_j numbers up to a 21 point rule are given on pages 536-538 in Ref. 3. The error in the numerical integration using these formulas is proportional to a certain derivative of the integrand at some point. For example, the error in the trapezoid rule is proportional to the second derivative; in Simpson's rule, to the fourth derivative; in the nine-point rule, to the tenth derivative. As pointed out by Kopal, (Ref. 3), whether a higher-order rule is better than a lower-order rule depends upon the behavior of the derivatives. This factor is important in the solution of the subject integral equations. In some of the methods discussed later, it will be shown that

the higher order derivatives involved in the numerical integration errors are extremely large and may be infinite at some points. This results in the trapezoid rule giving the best results in some methods of solution.

(c) Function methods with numerical integration. The function method of solution assumes that the unknown function $f(x)$ can be approximated by a finite sum of known functions with unknown multiplying constants, as

$$f(x) = \sum_{i=1}^N a_i p_i(x) \quad (3-2)$$

The $p_i(x)$ functions may be x^i terms, trigometric terms or any selected group of functions. The constants a_i are to be determined for the solution. The determination of these constants normally involves the evaluation of certain integrals containing $F(x)$ and $p_i(x)$. In the present case, these integrations must be performed numerically. This introduces a second approximation into the function solution in Eq. (3-2). Not only is there a finite number of the a_i , they are also approximate and no better than the numerical integration used to evaluate them. It is evident that if the numerical integration is quite accurate, then the accuracy in $f(x)$ in Eq. (3-2) will be limited only by the number and type of selected functions $p_i(x)$. Since the larger the number of points used in the integration the better the results are, as many points as possible should be used. The number of points used depends not only on the behavior of $f(x)$ but also on the selected $p_i(x)$. If the $p_i(x)$ are cyclic, more points will be needed if the number of terms in Eq. (3-2) is large, (p. 408, Ref. 3). In fact, the number of points in the numerical integration should be at least equal to the number of constants in Eq. (3-2). Preferably, the number of points should be many times the number of constants for cyclic $p_i(x)$, but from practical limitations of the computer, twice as many points as constants seems to be a good compromise. In order to compare the various methods discussed later, the number of points on the mirror for all numerical integrations has been selected as

$$\begin{array}{l} 40 \text{ equal intervals, } 41 \text{ points for} \\ \text{mirror without hole} \end{array} \quad (3-3)$$

$$\begin{array}{l} 40 \text{ equal intervals, } 20 \text{ on each side,} \\ 42 \text{ points for mirror with hole} \end{array} \quad (3-4)$$

The number of constants used in the function methods of solution has been selected as

$$20 \text{ constants for function methods.} \quad (3-5)$$

Further discussion of the numerical integration in the function methods will be given for each of the particular function methods.

(d) Discontinuities at edges of mirror. In Eqs. (2-11) and (2-13) the log terms become infinite at the edges of the mirror and the edges of the central hole. This may mean that $f(x)$ must be zero at the edges or $F(x)$ must be infinite at the edges. Since $F(x)$ is a change in light intensity, it is not infinite at the edges. However, since the mirror may have a distortion at the edge, it is not desirable to make $f(x) = 0$ at the edges. Thus, these factors must be considered in the solutions so as not to restrict the solutions more than necessary. It should be noted that this problem can be avoided in those methods which make use of Eqs. (2-12) and (2-15).

(e) Homogeneous solutions. It is evident from Eqs. (2-12) and (2-15) that

$$f(x) = C_1 \quad (3-6)$$

with C_1 a constant, makes $F(x) = 0$ so that this $f(x)$ is a homogeneous solution of the equations. This solution represents a uniform change in phase of the entire wave front and has no physical significance as the reference phase is arbitrary. However, the method of solution must include a reference point or condition for this constant.

It can be verified that Eq. (2-15) for the hole case has another homogeneous solution

$$f(x) = \frac{C_2}{x} \quad , \quad (3-7)$$

which makes $F(x) = 0$. This is a possible physical distortion of the Cassegrain type mirror that the knife-edge test is unable to detect, as no change in light intensity is produced by this distortion. The evaluation of C_2 by using restraint conditions on the mirror is considered in Section X.

(f) Rigid body rotation of mirror. In Eq. (2-12), it is easy to show that

$$f(x) = C_3 x \text{ gives } F(x) = -2C_3 \quad , \quad (3-8)$$

which indicates that a uniform change in the light intensity implies a rotation of the line on the mirror being observed. However, since the reference scale for the light intensity may be arbitrary, the rotation in Eq. (3-8) may be an apparent rigid body rotation of the entire mirror and not a real distortion of the mirror. If a group of parallel lines on the mirror all gave the same rotation, then it would undoubtedly represent an apparent rigid body rotation. It is evident that the method of solution for $f(x)$ in the equations should not include restraints

at the edges or elsewhere that would keep the method from giving the solution in Eq. (3-8). That is, the solution must handle the problem described in item (d) above. Further discussion of the scale factor problems on $F(x)$ is given in Section XII.

(g) Computer limitations. Since most of the methods studied in this report involve the inversion of matrices of large order (either 41 by 41, 42 by 42, or 20 by 20 from Eqs. (3-3) to (3-5)), the question of the accuracy of the inversion on the digital computer must be considered. On the IBM 360 system used, single precision arithmetic uses 8 digits and double precision arithmetic uses 16 digits. It was found that the 8-digit arithmetic was insufficient for several methods, so that it was decided to do all the calculations in the report using 16-place arithmetic. Even so, one method of solution could not be completed because 16 digits was insufficient.

The above listed factors influencing the solution of the equations will be considered in each method of solution in the following sections. Several function methods using power series and Fourier series, a collocation method, an iteration procedure, and an inversion integral solution are described. In each case, the solution is set up in matrix form using forty (40) equal intervals across the mirror. In the solution form

$$[f] = [G][F] \quad (3-9)$$

where $[f]$ is a 41 by 1 matrix for the mirror distortion at 41 points on the mirror, including edge points, and $[F]$ is 41 by 1 for the same 41 points (as observed in the knife-edge test on the line). The $[G]$ matrix (41 by 41) is derived as a product of various matrices for each method of solution. The results given by all the methods for selected $F(x)$ functions as well as the $[G]$ matrices are compared in Section IX for the case of no hole in the mirror. The Cassegrain type of mirror is considered in Section X.

IV - POWER SERIES SOLUTIONS

The integration in the integral equation (2-12), or

$$F(x) = - \int_{-1}^1 \frac{f(t) - f(x)}{t - x} dt \quad , \quad (4-1)$$

is simple to perform if $f(x)$ is assumed as a power series

$$f(x) = \sum_{j=1}^J A_j x^j \quad (4-2)$$

whence

$$\begin{aligned}
 F(x) &= - \sum_{j=1}^J A_j \int_{-1}^1 \frac{t^j - x^j}{t - x} dt \\
 &= - \sum_{j=1}^J A_j \int_{-1}^1 [t^{j-1} + t^{j-2}x + \dots + tx^{j-2} + x^{j-1}] dt \\
 &= - \sum_{j=1}^J A_j \left[\frac{1 - (-1)^j}{j} + \frac{1 - (-1)^{j-1}}{j-1} x + \dots + 2x^{j-1} \right] \\
 &= - \sum_{j=1}^J A_j \sum_{k=1}^j \frac{[1 - (-1)^{j-k+1}] x^{k-1}}{j - k + 1} \tag{4-3}
 \end{aligned}$$

$$= - \sum_{j=1}^J x^{j-1} \sum_{k=j}^J \frac{[1 - (-1)^{k-j+1}] A_k}{k - j + 1} \tag{4-4}$$

Note that the form for $f(x)$ in Eq. (4-2) makes the C_1 constant in the homogeneous solution, Eq. (3-6), zero.

Since Eq. (4-3) has no zeros in the denominator, it should be a simple form to solve for the A_j constants. Three different methods of solution were made, as described below.

Method A. Expand $F(x)$ in a power series

$$F(x) = \sum_{j=1}^J B_{j-1} x^{j-1} \tag{4-5}$$

so that Eq. (4-4), for like powers of x , gives

$$B_{j-1} = - \sum_{k=j}^J \frac{[1 - (-1)^{k-j+1}] A_k}{k - j + 1} \tag{4-6}$$

The A_j constants can be obtained from the B_j constants in Eq. (4-6) by a back recursion, in which

$$\begin{aligned}
A_J &= -\frac{1}{2} B_{J-1} \\
A_{J-1} &= -\frac{1}{2} B_{J-2} \\
A_{J-2} &= -\frac{1}{2} \left[B_{J-3} + \frac{2}{3} A_J \right] \\
A_{J-3} &= -\frac{1}{2} \left[B_{J-4} + \frac{2}{3} A_{J-1} \right] \\
&\vdots \\
A_{J-i+1} &= -\frac{1}{2} \left[B_{J-i} + \sum_{k=1}^{i-1} \frac{1 - (-1)^{i+1-k}}{i+1-k} A_{J-k+1} \right] \quad (4-7) \\
&\quad i = 2, 3, \dots, J
\end{aligned}$$

In matrix form

$$\left. \begin{aligned}
[C][A] &= [B] \\
C_{ij} &= 0, \quad j < i \\
C_{ij} &= \frac{-[1 - (-1)^{j-i+1}]}{j-i+1}, \quad j \geq i \\
[A] &= [C]^{-1}[B]
\end{aligned} \right\} \quad (4-8)$$

To calculate the B_j constants multiply Eq. (4-5) by x^{i-1} and integrate to get

$$\int_{-1}^1 x^{i-1} F(x) dx = \sum_{j=1}^J B_{j-1} \frac{1 - (-1)^{i+j-1}}{i+j-1} \quad (4-9)$$

or

$$\sum_{j=1}^{M+1} x_j^{i-1} F(x_j) H_j \Delta x = \sum_{j=1}^J B_{j-1} \frac{1 - (-1)^{i+j-1}}{i+j-1} \quad (4-10)$$

where H_j are the Cotes numbers for the numerical integration. In matrix form, Eq. (4-10) is

$$\frac{2}{M} [X][H][F] = [D][B], \quad M \text{ equal intervals,} \quad (4-11)$$

where [B] is a J by 1 matrix for the $B_0, B_1, \dots; B_{J-1}$ constants, [D] is J by J with the elements

$$D_{ij} = \frac{1 - (-1)^{i+j-1}}{i + j - 1}, \quad (4-11a)$$

[F] is (M + 1) by 1 for the value of F(x) at the (M + 1) equally spaced points, [H] is a (M + 1) by (M + 1) diagonal matrix with the H_j numbers on the diagonal, [X] is a J by (M + 1) matrix with elements

$$X_{ij} = x_j^{i-1} \quad (4-11b)$$

The matrix [D] is ill-conditioned and could not be inverted for the case of twenty constants ($J=20$) using sixteen place arithmetic on the computer. However, the [D] matrix is similar to the Hilbert matrix. By changing the x variable to make the interval of integration from 0 to 1 rather than -1 to 1, the resulting [D] matrix is exactly the Hilbert matrix with

$$D_{ij} = \frac{1}{i + j - 1}$$

From page 139 of Ref. 4, the elements of the inverse of the Hilbert matrix are (matrix size J by J)

$$ID_{ij} = \frac{(-1)^{i+j} (J+i-1)! (J+j-1)!}{(i+j-1) [(i-1)! (j-1)!]^2 (J-i)! (J-j)!} \quad (4-12)$$

For the case of $J = 20$, the numerator and denominator for some elements in Eq. (4-12) were too large for the computer to handle, so that a recursion multiplying factor had to be used, starting from $ID_{11} = J^2$. This gave the elements, but they varied from $ID_{11} = 400$ to $ID_{15,15} = 3.6(10)^{27}$ for the case of $J = 20$. With these elements in $[D]^{-1}$ for

$$[B] = [D]^{-1}[X][H][F] \quad (4-13)$$

it is evident that a sixteen place computer cannot produce values of B_j of the order of 1.0. In fact, it gave B_j of order 10^{11} as might be expected (order 27 minus order 16 = order 11).

This result shows that a numerical function cannot be expanded directly into a power series with large order terms by regular computers with a limited number of digits in the calculations. Naturally, if the function and its derivatives are known, then the expansion is the Maclaurin series with the B_j being given by the derivatives at $x = 0$.

Since the solution could not be obtained for a sufficiently large number of constants using the available computers, method A has not been completed in this report.

Method B. Multiply Eq. (4-3) by x^{i-1} and integrate to get

$$\sum_{j=1}^J K_{ij} A_j = E_i, \quad i = 1, 2, \dots, J \quad (4-14)$$

where

$$E_i = \int_{-1}^1 x^{i-1} F(x) dx \quad (4-15)$$

$$K_{ij} = - \sum_{k=1}^J \frac{[1 - (-1)^{j-k+1}][1 - (-1)^{i+k-1}]}{(j-k+1)(k+i-1)} \quad (4-16)$$

This method expands $F(x)$ in a power series but does not calculate the B_j in Eq. (4-5) directly. Instead, the A_j are calculated directly from Eq. (4-14). If desired, the B_j can then be obtained from Eq. (4-6).

In matrix form, Eq. (4-14) is

$$[K][A] = [E] = \frac{2}{M} [X][H][F] \quad (4-17)$$

where Eqs. (4-15) and (4-10) have been used. Here $[A]$ is J by 1 for the J unknown A_j constants, $[K]$ is J by J with elements in Eq. (4-16), and $[X]$, $[H]$, $[F]$ are as for Eq. (4-11). Now Eq. (4-2) gives

$$[f] = [Y][A] \quad (4-18)$$

where $[f]$ is $(M+1)$ by 1 for the results at the $(M+1)$ equally spaced points, and $[Y]$ is $(M+1)$ by J with the elements

$$Y_{ij} = x_i^j \quad (4-19)$$

Now, if Eq. (4-17) is solved for $[A]$ and the result put in Eq. (4-18), there results

$$[f] = [G][F] \quad (4-20)$$

$$[G] = \frac{2}{M} [Y][K]^{-1}[X][H] \quad (4-21)$$

where $[G]$ is $(M+1)$ by $(M+1)$ and operates on the $(M+1)$ values of $F(x_j)$ to produce the $(M+1)$ values of $f(x_j)$ at the same points.

For the case of $J = 20$ constants for the A_j in Eq. (4-2), it was found that the largest terms in the 20 by 20 $[K]^{-1}$ were of the order of 10^{13} , which is much better than the terms of order 10^{27} in Method A. However, with 16-place calculations in the computer, there appears to be some round-off error in the $[K]^{-1}$ matrix so that 20 constants probably represent the maximum number that can be used in a 16-digit machine for this Method B solution.

Results for $f(x)$ using Eq. (4-20) for selected $F(x)$ functions or point data are given in Section IX together with a discussion of the results.

Method C. Take Eq. (4-3) as

$$F_i = F(x_i) = \sum_{j=1}^J A_j B_j(x_i) = \sum_{j=1}^J B_{ij} A_j \quad (4-22)$$

where

$$B_{ij} = B_j(x_i) = - \sum_{k=1}^j \frac{[1 - (-1)^{j-k+1}] x_i^{k-1}}{j - k + 1} \quad (4-23)$$

$$i = 1, 2, \dots, M + 1 \quad \text{for } (M+1) \text{ points}$$

Solve for A_j directly without expanding $F(x)$ in a power series. This is a collocation solution for Eq. (4-3). In matrix form

$$[F] = [B][A] \quad (4-24)$$

where $[A]$ is J by 1 for the J constants A_j , $[B]$ is $(M+1)$ by J with elements in Eq. (4-23), and $[F]$ is $(M+1)$ by 1 for the $(M+1)$ point values of F . Unless the same number of points as constants are used $[B]$ is a rectangular matrix and cannot be inverted to give $[A]$. However, if Eq. (4-24) is multiplied by $[B]^T$, the transpose of $[B]$, then $[B]^T[B]$ is a square matrix with positive diagonal terms that can be inverted. Thus

$$[B]^T[F] = [B]^T[B][A]$$

whence

$$[A] = [B^T B]^{-1} [B]^T [F] \quad (4-25)$$

If this [A] is put into Eq. (4-18) there follows

$$[f] = [G][F] \quad (4-26)$$

$$[G] = [Y][B^T B]^{-1}[B]^T \quad (4-27)$$

where [Y] is defined by Eq. (4-19) and [B] by Eq. (4-23).

This procedure of using the transpose of the matrix to obtain a solution is equivalent to solving Eq. (4-24) in the sense of least squares. See Appendix A for the proof of this statement.

It should be pointed out that this power series Method C is the only method of solution presented herein that does not involve a numerical integration. However, multiplication by $[B]^T$ is equivalent to an indirect numerical integration using the trapezoid rule. This operation is similar to the multiplication by x^{i-1} in Method B, followed by a numerical integration.

For the case of $J = 20$ constants for the A_j , it was found that the largest terms in the 20 by 20 $[B^T B]^{-1}$ matrix were of the order of 10^{12} , which is an improvement over the Method B inverse matrix. Results given by Eq. (4-26) for power series Method C are described in Section IX.

V - FOURIER SERIES SOLUTIONS

By making a change of variable

$$x = \cos \theta \quad , \quad t = \cos \varphi \quad (5-1)$$

it is possible to solve the integral equations (2-11) or (2-12) by using Fourier series expansions. One procedure is to change the variable in the power series form in Eq. (4-3) and obtain the relation between the constants for both $f(x)$ and $F(x)$ in Fourier cosine series. Katzoff has used this method in Ref. 2. A brief description of the procedure using matrices is given below as Fourier series Method B. Another procedure is to expand $f(x)$ in a sine series and $F(x)$ in a cosine series, in which case the integrations for Eq. (2-11) can be made directly. This method is described below as Method A.

Method A. Use the change of variable in Eq. (5-1) and take

$$f(x) = f(\cos \theta) = \sum_{n=1}^N A_n \sin(n\theta) \quad (5-2)$$

Since

$$x = -1 \text{ gives } \theta = \pi, \quad x = 1 \text{ gives } \theta = 0 \quad (5-3)$$

the form (5-2) restrains $f(x)$ to be zero at the ends. If $f(x) \neq 0$ at the ends, then $f(x)$ must be regarded as discontinuous at the ends, which requires many more terms in the series to obtain convergence. Equation (2-11) now becomes

$$\begin{aligned} F(\theta) &= 2 \log \left(\frac{\sin \theta}{1 + \cos \theta} \right) \sum_{n=1}^N A_n \sin(n\theta) \\ &\quad - \sum_{n=1}^N A_n \int_0^\pi \frac{\sin(n\varphi) \sin \varphi}{\cos \varphi - \cos \theta} d\varphi \end{aligned} \quad (5-4)$$

By using the identity

$$2 \sin(n\varphi) \sin \varphi = \cos(n-1)\varphi - \cos(n+1)\varphi \quad (5-5)$$

the integral in Eq. (5-4) can be changed to the form of the Glauert integral (Ref. 5, p. 92-93)

$$\int_0^\pi \frac{\cos(m\varphi) d\varphi}{\cos \varphi - \cos \theta} = \frac{\pi \sin(m\theta)}{\sin \theta} \quad (5-6)$$

which occurs in thin-airfoil theory and finite-wing theory of aerodynamics. This gives

$$\begin{aligned} \int_0^\pi \frac{\sin(n\varphi) \sin \varphi d\varphi}{\cos \varphi - \cos \theta} &= \frac{\pi}{2} \frac{\sin(n-1)\theta - \sin(n+1)\theta}{\sin \theta} \\ &= -\pi \cos(n\theta) \end{aligned} \quad (5-7)$$

so that

$$F(\theta) = 2 \log \left(\frac{\sin \theta}{1 + \cos \theta} \right) \sum_{n=1}^N A_n \sin n\theta + \pi \sum_{n=1}^N A_n \cos n\theta \quad (5-8)$$

Expand $F(\theta)$ in a cosine series by multiplying Eq. (5-8) by $\cos m\theta$ and integrating from 0 to π . Thus

$$A_m + \sum_{n=1}^N K_{mn} A_n = E_m, \quad m = 0, 1, \dots, N-1, \quad (5-9)$$

where

$$E_m = \frac{2}{\pi^2} \int_0^\pi F(\theta) \cos m\theta d\theta \quad (5-10)$$

$$K_{mn} = \frac{4}{\pi^2} \int_0^\pi \log \left(\frac{\sin \theta}{1 + \cos \theta} \right) \sin n\theta \cos m\theta d\theta \quad (5-11)$$

$$A_0 = 0 \quad .$$

The integral for K_{mn} in Eq. (5-11) is evaluated in Appendix B to give

$$\left. \begin{aligned} K_{mn} &= 0, \quad \text{for } m+n \text{ odd} \\ K_{mm} &= -\frac{4}{m\pi^2} \sum_{k=1}^m \frac{1}{2k-1}, \quad m=n, \\ K_{mn} &= -\frac{8}{\pi^2(m+n)} \sum_{k=1}^{(m+n)/2} \frac{1}{2k-1} \\ &\quad + \frac{8}{\pi^2(m-n)} \sum_{k=1}^{|(m-n)/2|} \frac{1}{2k-1}, \quad \text{for } m+n \text{ even} \end{aligned} \right\} (5-12)$$

Since there is no A_0 term in Eqs. (5-2) and (5-9) but $F(\theta)$ may have a constant term, it is necessary to use care in writing Eq. (5-9) in matrix form so as to properly include the $m=0$ case. If the $m=0$ equation in (5-9) is put in the last row rather than the first row, then the matrix equation takes the simple form

$$[I + K][A] = [E] \quad (5-13)$$

where $[I]$ is the N by N identity matrix with element $I_{NN} = 0$, $[K]$ is N by N with the elements in Eq. (5-12) but with row N having $m=0$ or

$$\left. \begin{aligned}
K_{Nn} &= 0 \text{ for } n \text{ odd} \\
&= -\frac{16}{n\pi^2} \sum_{k=1}^{n/2} \frac{1}{2k-1} \text{ for } n \text{ even}
\end{aligned} \right\} \quad (5-14)$$

and $[E]$ is N by 1 for the values of the integral in Eq. (5-10) for $m = 1, 2, \dots, N-1, 0$, respectively. $[A]$ represents the N unknown constants.

The matrix form of E_m for the numerical integration for point values of $F(\theta)$ is

$$[E] = \frac{2}{\pi^2} [C][H][F] \quad (5-15)$$

where $[C]$ is N by M (N constants and M points for the numerical integration) with elements

$$C_{ij} = -\cos i\theta_j, \quad \cos N\theta_j = -1, \quad (5-16)$$

$[H]$ is the M by M weighting matrix for the numerical integration, and $[F]$ is M by 1 for the M point values of F . Here $\theta_1 = \pi$ for $x = -1$ so that the numerical integration starts at the upper limit in Eq. (5-10).

Put Eq. (5-15) into Eq. (5-13) to get the constants A_n in Eq. (5-2)

$$[A] = \frac{2}{\pi^2} [I+K]^{-1} [C][H][F] \quad (5-17)$$

The matrix form of Eq. (5-2) is

$$[f] = [S][A]$$

where $[S]$ is M by N with elements

$$S_{ij} = \sin j\theta_i \quad (5-18)$$

Finally,

$$[f] = [G][F] \quad (5-19)$$

$$[G] = \frac{2}{\pi^2} [S][I+K]^{-1}[C][H] \quad (5-20)$$

where $[G]$ is M by M and operates on the M values of $F(\theta_j)$ to produce the M values of $f(\theta_j)$.

Equal Δx and Equal $\Delta\theta$ Intervals. Since a change of variable (Eq. 5-1) is used in the Fourier series analysis, there arises the question of what intervals to use in Eqs. (5-19) and (5-20). If equal Δx intervals are used, then the $\Delta\theta$ intervals will be unequal. On the other hand, if equal $\Delta\theta$ intervals are used, then the Δx intervals will be unequal. Since the other methods of solution presented herein use equal Δx intervals, it is desirable to calculate $f(x_j)$ at equal Δx intervals in order to make a direct comparison with the other methods in Section IX. This was done by using θ_i in Eq. (5-18) at the equal Δx intervals. On the other hand, the numerical integration involving Eq. (5-15) can be done either way by using θ_j in Eq. (5-16) for equal Δx or equal $\Delta\theta$ with the corresponding values of $F(\theta_j)$, either calculated in selected cases or interpolated in actual cases. The case of equal Δx is given in Section IX for this Method A using the trapezoid rule for the matrix $[H]$.

Special Numerical Integration Procedure. As pointed out in paragraph (c) of Section III difficulties may occur in the numerical integration for function methods, particularly for cyclic functions. For the case of 20 constants and 41 points used in this report, it was found that the trapezoid rule for the matrix $[H]$ in Eq. (5-20) gave poor results for both equal Δx and equal $\Delta\theta$. (see Sec. IX for Δx results). In order to improve the numerical integration in Eq. (5-10), the cosine function was integrated across each interval (both for equal Δx and equal $\Delta\theta$) with $F(\theta)$ being held constant over the interval. Thus

$$\int_{(\theta_i+\theta_{i-1})/2}^{(\theta_i+\theta_{i+1})/2} F(\theta) \cos m\theta d\theta = F(\theta_i) \left[\frac{\sin m\theta}{m} \right]_{(\theta_i+\theta_{i-1})/2}^{(\theta_i+\theta_{i+1})/2}$$

$$= \frac{F(\theta_i)}{m} \left[\sin \frac{m}{2} (\theta_i+\theta_{i+1}) - \sin \frac{m}{2} (\theta_i+\theta_{i-1}) \right] \quad (5-21)$$

The matrix $[C][H]$ in Eqs. (5-15) and (5-20) is replaced by a matrix

$$[D] = [C][H] \quad (5-22)$$

where, from Eq. (5-21), the elements of $[D]$ are $(\theta_1 = \pi, \theta_M = 0)$

$$\left. \begin{aligned}
D_{N1} &= \frac{1}{2} (\pi - \theta_2) \quad , \quad D_{NM} = \frac{1}{2} \theta_{M-1} \\
D_{Nj} &= -\frac{1}{2} (\theta_{j+1} - \theta_{j-1}) \quad , \quad j = 2, 3, \dots, M-1, \\
D_{iM} &= \frac{1}{i} \sin \left(\frac{i}{2} \theta_{M-1} \right) \quad , \quad i = 1, 2, 3, \dots, N-1 \\
D_{i1} &= (-1)^i D_{iM} \quad , \quad i = 1, 2, 3, \dots, N-1 \\
D_{ij} &= -\frac{1}{i} \left[\sin \frac{i}{2} (\theta_j + \theta_{j+1}) - \sin \frac{i}{2} (\theta_j + \theta_{j-1}) \right], \\
&\quad i \neq N, \quad j \neq 1, M
\end{aligned} \right\} \quad (5-23)$$

The [G] matrix in Eq. (5-20) becomes

$$[G] = \frac{2}{\pi^2} [S][I+K]^{-1}[D] \quad (5-24)$$

where the elements of [S], [K], and [D] are given in Eqs. (5-18), (5-12), (5-14) and (5-23), respectively. Also, $I_{NN} = 0$ in [I].

The matrix [D] in Eq. (5-24) can be calculated for equal Δx or for equal $\Delta \theta$. Results for the Δx case are shown in Section IX for Method A.

Method B. This method uses the change of variable in Eq. (5-1) in the power series method after integration, Eq. (4-3), and relates the Fourier cosine series constants for $f(x)$ and $F(x)$. The details of the procedure is given by Katzoff in Ref. 2. A brief outline of the method in matrix form is given below so as to set up a form similar to the other methods in order that results of all the methods can be compared directly. Put Eq. (5-1) into Eq. (4-5) to get

$$F(\theta) = \sum_{j=1}^J B_{j-1} (\cos \theta)^{j-1} \equiv B_0 + \sum_{j=1}^{J-1} (\cos \theta)^j B_j \quad (5-25)$$

Take the Fourier cosine expansion of $F(\theta)$ as

$$F(\theta) = \frac{P_0}{2} + \sum_{j=1}^{J-1} P_j \cos j\theta \quad (5-26)$$

where the P_j may be regarded as known,

$$P_j = \frac{2}{\pi} \int_0^\pi F(\theta) \cos j\theta d\theta \quad (5-27)$$

Now the B_j constants in Eq. (5-25) can be obtained in terms of the known P_j constants in Eq. (5-26) by using the summation form of Eq. (7) in Ref. 2:

$$\left. \begin{aligned} \cos n\theta &= \sum_{i=0}^K \frac{(-1)^i n(n-i-1)! (2)^{n-2i-1} (\cos \theta)^{n-2i}}{(n-2i)! i!} \\ K &= \frac{n-1}{2}, \quad \text{for } n \text{ odd} \\ K &= \frac{n}{2}, \quad \text{for } n \text{ even} \end{aligned} \right\} (5-28)$$

Substitute Eq. (5-28) into Eq. (5-26) and equate the result for $F(\theta)$ to the form for $F(\theta)$ in Eq. (5-25). The coefficients of corresponding $(\cos \theta)^j$ terms on both sides of the resulting equation must be equal so that

$$\left. \begin{aligned} B_0 &= \frac{P_0}{2} + \frac{1}{2} \sum_{j=1}^{J-1} [1 - (-1)^{j+1}] (-1)^{j/2} P_j \\ B_m &= \sum_{j=m}^{J-1} \frac{(-1)^{(j-m)/2} [1 - (-1)^{j+m+1}] 2^{m-2} (j) \left(\frac{j+m-2}{2}\right)! P_j}{m! \left(\frac{j-m}{2}\right)!} \\ m &= 1, 2, \dots, J-1 \end{aligned} \right\} (5-29)$$

In matrix form, Eq. (5-29) is

$$[B] = [R][P] \quad (5-30)$$

where the elements of [R] are

$$\left. \begin{aligned}
 R_{ij} &= 0, \quad j < i, \\
 R_{ij} &= \frac{(-1)^{(j-i)/2} [1 - (-1)^{j+i+1}] 2^{i-3} (j-1) \left(\frac{j+i-4}{2}\right)!}{(i-1)! \left(\frac{j-i}{2}\right)!}, \\
 &\quad j \geq i, \\
 R_{11} &= \frac{1}{2}.
 \end{aligned} \right\} \quad (5-31)$$

The A_j constants in Eq. (4-2) are related to the B_j constants by Eq. (4-8) as

$$[A] = [Q]^{-1}[B] \quad (5-32)$$

where the Q_{ij} elements are

$$\left. \begin{aligned}
 Q_{ij} &= 0, \quad j < i \\
 Q_{ij} &= - \frac{[1 - (-1)^{j-i+1}]}{j - i + 1}, \quad j \geq i
 \end{aligned} \right\} \quad (5-33)$$

Hence, the A_j constants can be expressed in terms of the P_j constants by putting Eq. (5-30) into (5-32) to get

$$[A] = [Q]^{-1}[R][P] \quad (5-34)$$

The numerical integration for the P_j constants in Eq. (5-27) is similar to that for the E_j constants in Eqs. (5-10) and (5-15) for Method A. Thus

$$[P] = \frac{2}{\pi} [C][H][F] = \frac{2}{\pi} [D][F] \quad (5-35)$$

for the special form in Eqs. (5-22) and (5-23). However, the last row in [D] should be transferred to the first row in the [D] for Eq. (5-35) in order that the [P] matrix be compatible with the [R] matrix in Eq. (5-34).

Since it is desirable to calculate $f(x_j)$ at equal Δx intervals in order to compare the results to the other methods, Eq. (4-2) or (4-18) can be used for $f(x)$ to give

$$[f] = [G][F] \quad (5-36)$$

$$[G] = \frac{2}{\pi} [Y][Q]^{-1}[R][D] \quad (5-37)$$

where Eqs. (4-18), (5-34), and (5-35) have been combined. Here, the $[Y]$ matrix should be calculated from Eq. (4-19) for equal Δx intervals, but the $[D]$ matrix should be calculated for equal $\Delta\theta$ intervals (Eq. (5-23) with row N used as row 1. This requires that $[F]$ in Eq. (5-36) be known at equal $\Delta\theta$ intervals. If the F_j values are given at equal Δx intervals, then an interpolation matrix can be used to calculate F_j at the equal $\Delta\theta$ intervals. For this case $[G]$ in Eq. (5-37) becomes

$$[G] = \frac{2}{\pi} [Y][Q]^{-1}[R][D][IM] \quad (5-38)$$

with $[IM]$ an interpolation matrix. Results are given in Section IX for a straight line interpolation matrix and for exact F_j at equal $\Delta\theta$, using a selected F function.

To calculate f_j at equal $\Delta\theta$ intervals, as Katzoff does in Ref. 2, a further modification can be made to the $[G]$ matrix in Eq. (5-37). If $f(\theta)$ is expanded in a Fourier cosine series without the constant term, as

$$f(\theta) = \sum_{j=1}^J H_j \cos j\theta \quad , \quad (5-39)$$

then a relation between the A_j constants in Eq. (4-2) and the H_j constants can be obtained in the same manner as above for the relation between the B_j and P_j constants in Eq. (5-30). Thus

$$[A] = [S][H] \quad (5-40)$$

where

$$\left. \begin{aligned} S_{ij} &= 0 \quad , \quad \text{for } j < i \quad , \\ S_{ij} &= \frac{(-1)^{(j-i)/2} [1 - (-1)^{j+i+1}] 2^{i-2}(j) \left(\frac{j+i-2}{2}\right)!}{i! \left(\frac{j-i}{2}\right)!} \quad , \end{aligned} \right\} \quad (5-41)$$

$j \geq i \quad .$

Put Eqs. (5-40) and (5-30) into Eq. (5-32) to get

$$\text{or} \quad [S][H] = [Q]^{-1}[R][P] \quad (5-42)$$

$$[H] = [S]^{-1}[Q]^{-1}[R][P]$$

It can be shown that

$$[S]^{-1}[Q]^{-1}[R] = \frac{1}{2} [Q]^{-1} \quad (5-43)$$

so

$$[H] = \frac{1}{2} [Q]^{-1}[P] \quad (5-44)$$

which corresponds to the relation given by Katzoff in Ref. 2. This Eq. (5-44) gives the constants in the Fourier cosine series for $f(\theta)$ in terms of the constants in the Fourier cosine series for $F(\theta)$. Thus, for f_j at equal $\Delta\theta$ intervals

$$[f_i] = [\cos j\theta_i][H_j] \quad (5-45)$$

whence

$$[f] = [G][F] \\ [G] = \frac{1}{\pi} [T][Q]^{-1}[D] \quad (5-46)$$

where the elements of $[T]$ are

$$T_{ij} = \cos j\theta_i \quad (5-47)$$

and $[Q]^{-1}$ and $[D]$ are the same as in Eq. (5-37).

In Ref. 2, Katzoff uses the same number of points as constants, does not include the end points, and uses the trapezoid rule so that his $[D]$ matrix has the elements

$$D_{ij} = \cos (i-1)\theta_j, \quad i, j = 1, 2, 3, \dots, N \quad (5-48)$$

with $[D]$ being a square matrix.

VI - COLLOCATION SOLUTION

In Sections IV and V, function methods of solution of Eqs. (2-11) or (2-12) using power series and Fourier series have been described. Another method of solution, which is simple to apply, is a direct collocation on Eqs. (2-11) or (2-12). Take Eq. (2-12) in the form

$$F(x_i) = - \int_{-1}^1 \frac{f(t) - f(x_i)}{t - x_i} dt \quad (6-1)$$

which gives M equations for M x_i points. Now, a numerical integration can be made on the unknown function $f(t)$. Since $f(x_i)$ occurs under the integral, it is necessary to use the same points in the numerical integration as in the Eqs. (6-1) in order to get a determinate system (see p. 455, Ref. 3).

The question arises as to which of Eqs. (2-11) or (2-12) to use in the collocation. It is evident that the edge points cannot be used in Eq. (2-11), as the log term becomes infinite at the ends. Also, the integrand in the integral in Eq. (2-11) becomes infinite at $t = x$. However, this problem can be handled by using the Cauchy principal value for the integration. It was also found that the collocation solution using Eq. (2-11) gave a rigid body rotation to the $f(x)$ solution (item (f), Section III). This rotation apparently resulted from the first term in Eq. (2-11) being exact, while the integral was approximate. Now, if $f(x)$ is continuous, these problems do not arise in Eq. (2-12). This can be shown by expanding $f(t)$ into a Taylor's series about $t = x$:

$$f(t) = f(x) + f'(x)(t-x) + \frac{f''(x)}{2!} (t-x)^2 + \dots \quad (6-2)$$

This gives the integrand in Eq. (2-12) as

$$g(t,x) \equiv \frac{f(t) - f(x)}{t - x} = f'(x) + \frac{f''(x)}{2!} (t-x) + \dots \quad (6-3)$$

Thus, for $t = x$,

$$g(x,x) = f'(x), \quad t = x \quad (6-4)$$

and the integrand is finite and continuous at $t = x$, if $f'(x)$ is continuous.

Further, from Eq. (6-3)

$$g'(x,x) = \frac{1}{2} f''(x), \quad g''(x,x) = \frac{1}{3} f'''(x), \quad t = x \quad . \quad (6-5)$$

This indicates that for any derivative of $f(x)$ that is discontinuous, the next lower derivative of $g(x,x)$ will be discontinuous, and the corresponding derivative of $g(x,x)$ will be infinite. As pointed out in paragraph (b) of Section III, the behavior of these derivatives will affect the numerical integration in Eq. (6-1). Further discussion of these derivatives in the collocation solution is given for selected functions in Section IX.

On the basis of the above discussion, Eq. (2-12) or Eq. (6-1) will be used in the collocation solution. With numerical integration, Eq. (6-1) becomes

$$\sum_{j=1}^M (\Delta x) H_j \frac{f(x_j) - f(x_i)}{x_j - x_i} = - F(x_i) \quad (6-6)$$

where the H_j are the Cotes numbers for equal intervals in the integration (paragraph (b), Sec. III). For the M points and $M-1$ intervals on $x = -1$ to $x = 1$,

$$\left. \begin{aligned} x_j &= (j-1)\Delta x - 1, & x_i &= (i-1)\Delta x - 1 \\ \Delta x &= \frac{2}{M-1} \end{aligned} \right\} \quad (6-7)$$

and Eq. (6-6) becomes

$$\sum_{j=1}^M H_j \frac{f_j - f_i}{j - i} = - F_i; \quad i = 1, 2, \dots, M; \quad j \neq i \quad (6-8)$$

As $j \rightarrow i$, Eq. (6-4) gives

$$\begin{aligned} \frac{f_j - f_i}{j - i} &\rightarrow f'(x_i) \Delta x \\ &= \frac{f_{i+1} - f_{i-1}}{2}, \quad i \neq 1, M \end{aligned} \quad (6-9)$$

At the end points, $i = 1$ and M , the three point Lagrangian differentiation formula (p. 516, Ref. 3) gives

$$f'_1 = \frac{-3f_1 + 4f_2 - f_3}{2(\Delta x)}$$

$$f'_M = \frac{f_{M-2} - 4f_{M-1} + 3f_M}{2(\Delta x)} \quad (6-10)$$

These Eqs. (6-8)-(6-10) can be combined into a matrix equation

$$[A][f] = - [F] \quad (6-11)$$

where $[A]$ is M by M for M points with the elements

$$\left. \begin{aligned} A_{1,2} &= 2H_1 + H_2 \quad , \quad A_{1,3} = \frac{1}{2} (H_3 - H_1) \quad , \\ A_{M,M-1} &= -2H_M - H_{M-1} \quad , \quad A_{M,M-2} = \frac{1}{2} (H_M - H_{M-2}) \quad , \\ A_{i,i-1} &= -H_{i-1} - \frac{1}{2} H_i \\ A_{i,i+1} &= H_{i+1} + \frac{1}{2} H_i \\ A_{ij} &= \frac{H_j}{j-i} \quad , \quad i \neq j \quad , \quad \text{except above values,} \\ A_{ii} &= - \sum_{j=1, j \neq i}^M A_{ij} \quad , \quad \text{see Eq. (6-8) .} \end{aligned} \right\} \quad (6-12)$$

Since the diagonal elements A_{ii} are the negative sum of all other elements in each row, it is evident that when $f(x)$ is constant, $F(x)$ will be zero as required by the homogeneous solution in paragraph (c), Section III. This result is not given exactly by Eq. (2-11), since the log term on the diagonal is only approximated by the negative sum of the other elements in each row.

Since all rows of the $[A]$ matrix in Eq. (6-12) add to zero, the matrix $[A]$ is a singular and cannot be inverted. It is necessary to add a boundary condition on $f(x)$ to obtain the homogeneous solution in

Eq. (3-6). To correspond to the power series solution in Section IV, which made $f(0) = 0$, the restraint condition

$$f(0) \equiv f_{(M+1)/2} = 0 \quad (6-13)$$

was selected. Now the system of equations in (6-11) and (6-13) has $M + 1$ equations in M unknowns. To solve such a system, multiply by the matrix transpose, as in power series Method C above. In this case, the resulting system of M equations for the M unknowns can be expressed as

$$[B][f] = - [A]^T[F] \quad (6-14)$$

$$[B] = [A]^T[A] + [C] \quad (6-15)$$

where the elements of $[C]$ are

$$C_{i,j} = 0 \quad , \quad C_{(M+1)/2,(M+1)/2} = 1.0 \quad (6-16)$$

The $[B]$ matrix is nonsingular so that

$$[f] = - [B]^{-1}[A]^T[F] = [G][F] \quad (6-17)$$

$$[G] = - [B]^{-1}[A]^T \quad (6-18)$$

Results given by Eq. (6-17) for selected functions of $F(x)$ are shown in Section IX and compared to the results of the other methods. The $[G]$ matrix in Eq. (6-18) is also compared to the other $[G]$ matrices in Section IX.

VII - ITERATION SOLUTIONS

Iteration is a classical procedure for solving integral equations. However, when numerical integration is involved in the iteration and the equation has singular points, difficulties can arise. As pointed out in Section VI on the collocation solution Eq. (2-11) has infinities in the log term at the end points and has a singularity at $t = x$. Yet Eq. (2-11) is in the form needed for iteration so that it should be used rather than Eq. (2-12).

Equation (2-11) can be written in two forms for iteration

$$f_m(x) = \frac{1}{\log\left(\frac{1-x}{1+x}\right)} \left[F(x) + \int_{-1}^1 \frac{f_{m-1}(t)dt}{t-x} \right] \quad (7-1)$$

$$\int_{-1}^1 \frac{f_m(t)dt}{t-x} = -F(x) + f_{m-1}(x) \log\left(\frac{1-x}{1+x}\right) \quad (7-2)$$

$$\equiv -G_{m-1}(x)$$

The form in Eq. (7-1) requires a direct integration to get the next $f_m(x)$ while the form in Eq. (7-2) requires the solution of a well-known integral equation for which the inversion integral is known. The form in Eq. (7-1) was found to be divergent so that the following discussion is restricted to Eq. (7-2).

The solution of Eq. (7-2) for $f_m(x)$ is given as an example in Section VIII. From Eq. (8-40)

$$f_m(x) = \frac{X(x)}{\pi^2} \int_{-1}^1 \frac{G_{m-1}(t)dt}{X(t)(t-x)} + \phi_h(x) \quad (7-3)$$

where the possible forms of $X(x)$ and $\phi_h(x)$ from Eqs. (8-41)--(8-44) are

$$\left. \begin{aligned} X_1(x) &= \frac{1}{\sqrt{1-x^2}}, \quad \phi_{h_1}(x) = \frac{C_0}{\sqrt{1-x^2}}, \\ f_m(x) &\text{ may be unbounded at } x = \pm 1; \end{aligned} \right\} \quad (7-4)$$

$$\left. \begin{aligned} X_2(x) &= \sqrt{\frac{1-x}{1+x}}, \quad \phi_{h_2}(x) = 0, \\ f_m(x) &\text{ may be unbounded at } x = -1; \end{aligned} \right\} \quad (7-5)$$

$$\left. \begin{aligned} X_3(x) &= \sqrt{\frac{1+x}{1-x}}, \quad \phi_{h_3}(x) = 0, \\ f_m(x) &\text{ may be unbounded at } x = 1; \end{aligned} \right\} \quad (7-6)$$

$$\left. \begin{aligned}
 X_4(x) &= \sqrt{1 - x^2} \quad , \quad \phi_{h_4}(x) = 0 \quad , \\
 f_m(x) &\text{ is bounded, but Eq. (8-45)} \\
 &\text{restricts } G_{m-1}(t).
 \end{aligned} \right\} \quad (7-7)$$

Since $f(x)$ is actually bounded in the problem under consideration, any of the four forms in Eqs. (7-4)-(7-7) may be used for $X(x)$ and $X(t)$ in Eq. (7-3). For the numerical integration in Eq. (7-3), the form $X_1(x)$ will make the integrand zero at the ends while the other forms will make it infinite at one or both ends. Necessarily, the end points must be omitted in the calculations, but the total area in the integral must be included. A reasonably accurate representation of the area near the ends can be obtained for the X_1 form, but only a rough approximation can be obtained for the other forms. The matrix form for all the cases is as follows.

Start with $f_0 = 0$ as the first approximation in the iteration procedure so that

$$f_1(x) = \frac{X(x)}{\pi^2} \int_{-1}^1 \frac{F(t)dt}{X(t)(t-x)} \quad (7-8)$$

where $\phi_h(x) = 0$ for all cases. In matrix form

$$[f_1] = \frac{1}{\pi^2} [X_D][A_I][X_D]^{-1}[F] \quad (7-9)$$

where the same points are used for x and t and

$$X_D(i,j) = 0 \quad , \quad X_D(i,i) = X(x_i) \quad (7-10)$$

$$\left. \begin{aligned}
 A_I(i,j) &= A_{ij} \quad \text{in Eq. (6-12)} \quad , \quad i \neq j \\
 A_I(i,i) &= 0 \quad , \quad A_{12} = H_2, \quad A_{13} = \frac{1}{2} H_3 \\
 A_{M,M-1} &= -H_{M-1}, \quad A_{M,M-2} = -\frac{1}{2} H_{M-2}
 \end{aligned} \right\} \quad (7-11)$$

The numerical integration matrix $[A_I]$ is taken in the same form as that for the collocation method in Section VI.

For the iteration from Eq. (7-2) and Eq. (7-3)

$$\begin{aligned}
 f_2(x) &= \frac{X(x)}{\pi^2} \left[\int_{-1}^1 \frac{F(t)dt}{X(t)(t-x)} - \int_{-1}^1 \frac{f_1(t) \log\left(\frac{1-t}{1+t}\right)}{X(t)(t-x)} dt \right] \\
 &= f_1(x) - \frac{X(x)}{\pi^2} \int_{-1}^1 \frac{f_1(t) \log\left(\frac{1-t}{1+t}\right)dt}{X(t)(t-x)}
 \end{aligned} \tag{7-12}$$

or

$$\begin{aligned}
 [f_2] &= \frac{1}{\pi^2} [X_D][A_I][X_D]^{-1}[F] - \frac{1}{\pi^2} [X_D][A_I][L][X_D]^{-1}[f_1] \\
 &= \left[\frac{1}{\pi^2} [X_D][A_I][X_D]^{-1} - \frac{1}{\pi^4} [X_D][A_I][L][A_I][X_D]^{-1} \right] [F] \\
 &= \frac{1}{\pi^2} [X_D][I + J][A_I][X_D]^{-1}[F]
 \end{aligned} \tag{7-13}$$

where [I] is the identity matrix and

$$\left. \begin{aligned}
 [J] &= -\frac{1}{\pi^2} [A_I][L] \\
 L_{ij} &= 0 \quad , \quad L_{ii} = \log\left(\frac{1-x_i}{1+x_i}\right)
 \end{aligned} \right\} \tag{7-14}$$

The form for $f_3(x)$ is

$$f_3(x) = f_1(x) - \frac{X(x)}{\pi^2} \int_{-1}^1 \frac{f_2(t) \log\left(\frac{1-t}{1+t}\right)dt}{X(t)(t-x)}$$

or

$$[f_3] = \frac{1}{\pi^2} [X_D][I + J + J^2][A_I][X_D]^{-1}[F] \quad .$$

After m iterations,

$$[f_m] = [G_m][F] \tag{7-15}$$

$$[G_m] = \frac{1}{\pi^2} [X_D][I + J + J^2 + \dots + J^{m-1}][A_I][X_D]^{-1} \tag{7-16}$$

It should be noted that as $m \rightarrow \infty$ in Eq. (7-16),

$$[G_m] \rightarrow [G] = \frac{1}{\pi^2} [X_D][I - J]^{-1}[A_I][X_D]^{-1}, \quad m \rightarrow \infty. \quad (7-17)$$

However, this limit value of $[G]$ is just the $[G]$ for a collocation solution of Eq. (7-3) with $\phi_h = 0$, $f_m = f_{m-1}$. That is, Eq. (7-3) becomes

$$\frac{\pi^2 f_m(x)}{X(x)} = \int_{-1}^1 \frac{F(t) dt}{X(x)(t-x)} - \int_{-1}^1 \frac{f_m(t) \log\left(\frac{1-t}{1+t}\right) dt}{X(t)(t-x)}$$

or

$$[X_D]^{-1}[f_m] + \frac{1}{\pi^2} [A_I][L][X_D]^{-1}[f_m] = \frac{1}{\pi^2} [A_I][X_D]^{-1}[F],$$

or, by use of Eq. (7-14),

$$[I - J][X_D]^{-1}[f_m] = \frac{1}{\pi^2} [A_I][X_D]^{-1}[F],$$

whence

$$[f_m] = [G][F] \quad (7-18)$$

where $[G]$ is given by Eq. (7-17). This indicates that the iteration solution can only approach a collocation solution of Eq. (7-3) with $G_{m-1}(t)$ given by Eq. (7-2) and $f_{m-1} = f_m$ at convergence. Because of the log term and the $X(t)$ term in Eq. (7-3), it appears that a collocation solution of Eq. (7-3) would be less accurate than the collocation solution in Section VI for the original Eq. (6-1). Thus, there is little justification for using a collocation solution on a modified equation or for an iteration solution in this particular problem, as compared to a collocation solution of the original equation. However, to get some idea of the behavior of the iterations and of the different forms of the $X(x)$ function, the Eqs. (7-15) and (7-16) are used for five iterations on a selected function in Section IX for the X_1 and X_2 forms, Eqs. (7-4) and (7-5), and the results compared to the other methods. For the X_2 form in which the integrand in Eq. (7-3) becomes infinite at $x = 1$, the $[A_I]$ matrix in Eq. (7-11) was modified to include the approximate integrated area over the interval adjoining $x = 1$. Examination of the powers of the $[J]$ matrix in Eq. (7-16) shows for both X_1 and X_2 that up to the fourth power, most of the elements are decreasing but some are oscillating and some are actually increasing. Because of the approximations in the numerical integration it does not appear that all the elements in J^{m-1} will become zero for a practical number of m iterations. This error accumulation can be avoided by using the limit form in Eq. (7-17), but

then this is not an iteration solution but a collocation solution. Further discussion of the iteration results is given in Section IX.

VIII - INVERSION INTEGRAL SOLUTION

It is possible to obtain a solution for both the solid mirror, Eq. (2-11), and the mirror with a central hole, Eq. (2-13), in an integral form by using methods described by Muskhelishvili in Ref. 6. Although the formula from which the solutions can be obtained is given on page 328 of Ref. 6, the definitions, conditions, and derivations leading up to this particular formula are spread throughout the book. The derivations are made for the complex plane and the equations are in terms of the complex variables z and t . A brief outline of the derivation of the solution is given below.

Consider the limiting value of the Cauchy integral

$$\phi(z) = \frac{1}{2\pi i} \int_L \frac{\phi(t) dt}{t - z} \quad (8-1)$$

as z approaches t_0 on the arc or contour L . If $\phi(t)$ satisfies a Hölder condition on L of the form

$$|\phi(t_2) - \phi(t_1)| \leq A |t_2 - t_1|^k, \quad \text{H condition}, \quad (8-2)$$

where A and k are positive constants, then Muskhelishvili (Ref. 6) shows that $\phi(z)$ is continuous on L from the left and from the right, with the exception of those ends at which $\phi(t) \neq 0$. Further, $\phi(z)$ tends uniformly to the limits

$$\phi^+(t_0) = \frac{1}{2} \phi(t_0) + \frac{1}{2\pi i} \int_L \frac{\phi(t) dt}{t - t_0} \quad (8-3)$$

$$\phi^-(t_0) = -\frac{1}{2} \phi(t_0) + \frac{1}{2\pi i} \int_L \frac{\phi(t) dt}{t - t_0} \quad (8-4)$$

from the left of L and from the right of L , respectively. Here, L may be a union of smooth, non-intersecting arcs or contours, L_1, L_2, \dots, L_q , with definite positive directions with the $+$ region on the left. These equations can be written in the form

$$\Phi^+(t_0) - \Phi^-(t_0) = \varphi(t_0) \quad (8-5)$$

$$\Phi^+(t_0) + \Phi^-(t_0) = \frac{1}{\pi i} \int_L \frac{\varphi(t) dt}{t - t_0} = 2\varphi(t_0) \quad (8-6)$$

The function $\Phi(z)$, holomorphic in the complex plane, except possibly at infinity, and continuous on L from the left and from the right with the possible exception of the ends b_k , near which the inequality

$$|\Phi(z)| < \frac{\text{const.}}{|z - b_k|^p}, \quad 0 \leq p < 1 \quad (8-7)$$

holds, is called sectionally holomorphic with the line of discontinuity L or boundary L .

From Eq. (8-5), it is evident that the Cauchy integral formula solves an important boundary value problem. That is, it is required to find a sectionally holomorphic function $\Phi(z)$, zero at infinity, and satisfying the given boundary condition

$$\Phi^+(t) - \Phi^-(t) = \varphi(t) \quad \text{on } L \quad . \quad (8-8)$$

If $\varphi(t)$ satisfies the H condition, Eq. (8-2), the solution for $\Phi(z)$ is given by Eq. (8-1).

In his book on "Singular Integral Equations," (Ref. 6) Muskhelishvili develops this procedure of solving boundary value problems and applies it to various boundary value problems and integral equations. To arrive at the integral equation form that is suitable for the subject problem (Eqs. 2.11 and 2.13), it is necessary to first consider the Hilbert boundary value problem for both the homogeneous and nonhomogeneous cases.

Homogeneous Hilbert Problem

The homogeneous Hilbert problem can be stated as : To find a sectionally holomorphic function $\Phi_h(z)$ of finite degree at infinity satisfying the boundary condition

$$\Phi_h^+(t) = G(t)\Phi_h^-(t) \quad \text{on } L \quad , \quad (8-9)$$

where $G(t)$ is a given non-vanishing function on L , satisfying the H condition.

Take logarithms on both sides of Eq. (8-9) to get

$$\log \Phi_h^+(t) - \log \Phi_h^-(t) = \log G(t) \quad (8-10)$$

which has the form of Eq. (8-8) above. Thus, the formal solution for $\log \Phi_h$ is given by Eq. (8-1) as

$$\log \Phi_h(z) = \frac{1}{2\pi i} \int_L \frac{\log G(t) dt}{t - z} \quad (8-11)$$

or

$$\Phi_h(z) = e^{P(z)}, \quad P(z) = \frac{1}{2\pi i} \int_L \frac{\log G(t)}{t - z} dt \quad (8-12)$$

There are two difficulties with this solution for $\Phi_h(z)$ in Eq. (8-12). The function $\log G(t)$ is multivalued and the solution for Φ_h may not obey Eq. (8-7) at the ends of the arcs L_j ($j = 1, \dots, q$) of L . These difficulties are resolved by Muskhelishvili (pp. 230-234, Ref. 6) in the following manner.

Near any end b_k ($k = 1, \dots, 2q$), $P(z)$ in Eq. (8-12) can be written in the form

$$P(z) = \mp \frac{\log G(b_k)}{2\pi i} \log(z - b_k) + P_0(z) \quad (8-13)$$

where $P_0(z)$ remains bounded near b_k . Thus

$$e^{P(z)} = (z - b_k)^{a_k + ic_k} Q(z) \quad (8-14)$$

near b_k , where a_k and c_k are real constants given by

$$a_k + ic_k = \mp \frac{\log G(b_k)}{2\pi i} \quad (8-15)$$

and $Q(z)$ is a non-vanishing function bounded near b_k . Now select integers λ_k , satisfying the conditions

$$-1 < a_k + \lambda_k < 1 \quad (8-16)$$

and put

$$T(z) = (z - b_1)^{\lambda_1} (z - b_2)^{\lambda_2} \dots (z - b_{2q})^{\lambda_{2q}} \quad (8-17)$$

Then the function

$$X(z) = T(z)e^{P(z)} \quad (8-18)$$

satisfies Eqs. (8-7) and (8-9) and is a solution of the homogeneous Hilbert problem.

Since Eq. (8-16) may permit two values of λ_k for some k values, the solution $X(z)$ is not necessarily unique. Its form will depend upon what requirements are placed upon the solution at the end points. If the solution is to be bounded at certain end points, then one form results. If it is permissible for the solution to become infinite at some end points (under condition (8-7)), then a different form of the solution results. Muskhelishvili (p. 231, Ref. 6) divides the solutions into classes on basis of the end point requirements and shows that the most general solution in a certain class has the form

$$\Phi_h(z) = X(z)R(z) \quad (8-19)$$

where $R(z)$ is a arbitrary polynomial of order depending upon the desired behavior of the function at infinity. Thus the solution of the homogeneous Hilbert problem has the form

$$\Phi_h(z) = T(z)R(z)e^{P(z)} \quad (8-20)$$

where $P(z)$ and $T(z)$ are defined by Eqs. (8-12) and (8-17), respectively, and $R(z)$ is a polynomial with arbitrary constants.

Nonhomogeneous Hilbert Problem

The nonhomogeneous Hilbert Problem may be stated as: To find a sectionally holomorphic function $\phi(z)$, having finite degree at infinity, for the boundary condition

$$\phi^+(t) = G(t)\phi^-(t) + g(t) \quad \text{on } L \quad (8-21)$$

where $G(t)$ and $g(t)$ are given functions with at most finite discontinuities on L and $G(t) \neq 0$ on L . As for the homogeneous problem, L may be a union of smooth nonintersecting arcs.

The solution of the nonhomogeneous problem can be obtained from the homogeneous solution. From Eq. (8-9)

$$G(t) = \frac{\Phi_h^+(t)}{\Phi_h^-(t)} = \frac{X^+(t)}{X^-(t)} \quad (8-22)$$

where $X(t)$ is $\Phi_h(t)$ in Eq. (8-20) with the unknown polynomial $R(t)$ omitted, or

$$X(t_0) = T(t_0)e^{P(t_0)} \quad (8-23)$$

With $\phi = \log G$ and $\phi = \log X$, it follows from Eqs. (8-5) and (8-6) that

$$\left. \begin{aligned} X^+(t_0) &= \sqrt{G(t_0)} X(t_0) \quad , \\ X^-(t_0) &= X(t_0)/\sqrt{G(t_0)} \quad . \end{aligned} \right\} \quad (8-24)$$

Put $G(t)$ from Eq. (8-22) into Eq. (8-21) to get

$$\frac{\phi^+(t)}{X^+(t)} - \frac{\phi^-(t)}{X^-(t)} = \frac{g(t)}{X^+(t)} \quad \text{on } L \quad (8-25)$$

This Eq. (8-25) is of the form of Eq. (8-8) so that from Eq. (8-1)

$$\frac{\phi(z)}{X(z)} = \frac{1}{2\pi i} \int_L \frac{g(t)}{X^+(t)(t-z)} dt \quad (8-26)$$

Thus

$$\phi(z) = \frac{X(z)}{2\pi i} \int_L \frac{g(t)}{X^+(t)(t-z)} dt + \phi_h(z) \quad (8-27)$$

where any homogeneous $\phi_h(z)$ has been included. By using Eq. (8-24), the solution (8-27) can be written as

$$\phi(z) = \frac{X(z)}{2\pi i} \int_L \frac{g(t)}{X(t)\sqrt{G(t)}(t-z)} dt + \phi_h(z) \quad (8-28)$$

which is the general solution of the nonhomogeneous Hilbert problem with $X(t)$ given by Eq. (8-23).

This solution (8-28) can be used to solve various singular integral equations, including the integral equations (2-11) and (2-13) under investigation in this report.

Integral Equations Solutions

The integral equation discussed in Section 107 of Ref. 6 can be adapted to the problems involved in this report. The equation has the form

$$A(t_0)f(t_0) + \frac{B(t_0)}{\pi i} \int_L \frac{f(t)}{t - t_0} dt = F(t_0) \quad , \quad \text{on } L, \quad (8-29)$$

with $A(t)$, $B(t)$, $F(t)$ satisfying the H condition, Eq. (8-2). If $f(t_0)$ corresponds to $\phi(t_0)$, then Eqs. (8-5) and (8-6) can be used to express the unknown $f(t_0)$ in terms of an unknown function $\phi(z)$ and the Eq. (8-29) can be written in the form

$$\begin{aligned} A(t_0)[\phi^+(t_0) - \phi^-(t_0)] + B(t_0)[\phi^+(t_0) + \phi^-(t_0)] \\ = F(t_0) \quad \text{on } L \end{aligned} \quad (8-30)$$

or

$$\phi^+(t_0) = G(t_0)\phi^-(t_0) + \frac{F(t_0)}{A(t_0) + B(t_0)} \quad (8-31)$$

$$G(t_0) = \frac{A(t_0) - B(t_0)}{A(t_0) + B(t_0)} \quad (8-32)$$

This Eq. (8-31) corresponds to the nonhomogeneous Hilbert problem in Eq. (8-21) so that if $\phi(z)$ is determined for this problem then the solution of the integral equation (8-29) is simply

$$f(t_0) = \phi^+(t_0) - \phi^-(t_0) \quad (8-33)$$

From Eqs. (8-28), (8-31), and (8-32)

$$\begin{aligned} \phi(z) &= \frac{X(z)}{2\pi i} \int_L \frac{F(t)dt}{\sqrt{G(t)} X(t)[A(t) + B(t)](t-z)} + \phi_h(z) \\ &= \frac{X(z)}{2\pi i} \int_L \frac{F(t)dt}{X(t)\sqrt{A^2 - B^2}(t-z)} + \phi_h(z) \end{aligned} \quad (8-34)$$

Use Eqs. (8-3) and (8-4) for $\phi(z)/X(z)$ in Eq. (8-34) and take $t_0 = x$, $\phi(t) = F(t)/X(t)\sqrt{A^2-B^2}$, to get

$$\begin{aligned} \phi^+(x) &= \frac{1}{2} \frac{X^+(x)F(x)}{X(x)\sqrt{A^2-B^2}} + \frac{X^+(x)}{2\pi i} \int_L \frac{F(t)dt}{X(t)\sqrt{A^2-B^2} (t-x)} \\ &+ \phi_h^+(x) \end{aligned} \quad (8-35)$$

$$\begin{aligned} \phi^-(x) &= -\frac{1}{2} \frac{X^-(x)F(x)}{X(x)\sqrt{A^2-B^2}} + \frac{X^-(x)}{2\pi i} \int_L \frac{F(t)dt}{X(t)\sqrt{A^2-B^2} (t-x)} \\ &+ \phi_h^-(x) \end{aligned} \quad (8-36)$$

Since, from Eq. (8-24),

$$\left. \begin{aligned} X^+ + X^- &= \left(\sqrt{G} + \frac{1}{\sqrt{G}} \right) X = \frac{2AX}{\sqrt{A^2-B^2}} \\ X^+ - X^- &= \frac{-2BX}{\sqrt{A^2-B^2}} \\ \phi_h^+ - \phi_h^- &= (X^+ - X^-)R(x) = -\frac{2B}{\sqrt{A^2-B^2}} \phi_h \end{aligned} \right\} \quad (8-37)$$

it follows from Eqs. (8-33), (8-35) and (8-36) that

$$\begin{aligned} f(x) &= \frac{A(x)F(x)}{A^2(x) - B^2(x)} - \frac{B(x)X(x)}{\pi i \sqrt{A^2-B^2}} \int_L \frac{F(t)dt}{X(t)\sqrt{A^2-B^2} (t-x)} \\ &- \frac{2B(x)}{\sqrt{A^2-B^2}} \phi_h(x) \end{aligned} \quad (8-38)$$

This is the general solution of the integral equation (8-29) with $\phi_h(x)$ given by Eq. (8-20) and $X(x)$ given by Eq. (8-23). The solution can be used for the particular integral equation used in the iteration method in Section VII as well as for the integral equations (2-11) and (2-13).

Integral Equation Solution for Iteration Method

In Eq. (8-29) take $A(t_0) = 0$, $B(t_0) = -\pi i$, and $x = t_0$, whence

$$\int_L \frac{f(t)dt}{t-x} = -F(x) \quad (8-39)$$

is the integral equation to be solved. From Eq. (8-38) the solution is

$$f(x) = \frac{X(x)}{\pi^2} \int_L \frac{F(t)}{X(t)(t-x)} dt + \Phi_h(x) \quad (8-40)$$

To find $X(x)$ in Eq. (8-23) and $\Phi_h(x)$ in Eq. (8-20), get $G(t) = -1$ from Eq. (8-32), $\log G(b_k) = \pi i$ in Eq. (8-15) so that $a_1 = -\frac{1}{2}$ at $x = -1$, $a_2 = \frac{1}{2}$ at $x = 1$ with L the line $-1 \leq x \leq 1$. Thus in Eq. (8-16), $\lambda_1 = 0$ or 1 , $\lambda_2 = 0$ or -1 . In Eq. (8-20), with $G = -1$,

$$P(x) = \frac{1}{2} \log \left(\frac{1-x}{1+x} \right)$$

whence

$$X(x) = (1+x)^{\lambda_1} (1-x)^{\lambda_2} \sqrt{\frac{1-x}{1+x}}$$

$$X_1(x) = \frac{1}{\sqrt{1-x^2}}, \quad \lambda_1 = 0, \quad \lambda_2 = -1 \quad (8-41)$$

$$X_2(x) = \sqrt{\frac{1-x}{1+x}}, \quad \lambda_1 = 0, \quad \lambda_2 = 0 \quad (8-42)$$

$$X_3(x) = \sqrt{\frac{1+x}{1-x}}, \quad \lambda_1 = 1, \quad \lambda_2 = -1 \quad (8-43)$$

$$X_4(x) = \sqrt{1-x^2}, \quad \lambda_1 = 1, \quad \lambda_2 = 0 \quad (8-44)$$

For these four possible forms of $X(x)$, the homogeneous solutions $\Phi_h(x)$ have the value 0 except for $\Phi_{h1}(x) = C_0/\sqrt{1-x^2}$ (pp. 240-242, Ref. 6). For the case of X_4 with both ends bounded there is a restriction on $F(t)$

$$\int_{-1}^1 \frac{F(t)}{\sqrt{1-t^2}} dt = 0 \quad (8-45)$$

The proper form of $X(x)$ to be used in Eq. (8-40) depends upon the desired behavior of the solution at the end points. For example, in thin airfoil theory of aerodynamics where $f(t)$ in Eq. (8-39) represents the pressure distribution, it is desired that $f(1) = 0$ at $x = 1$ to satisfy the Kutta condition while $f(-1)$ may be infinite. Thus the form $X_2(x)$ is used in Eq. (8-40) for this problem.

Solution of the Foucault Test Integral Equation

The Eq. (2-11) for the solid mirror is the same as Eq. (8-29) with

$$A(x) = \log \frac{1-x}{1+x}, \quad B(x) = -\pi i, \quad x = t_0, \quad (8-46)$$

and the solution from Eq. (8-38) is

$$f(x) = \frac{F(x) \log \left(\frac{1-x}{1+x} \right)}{D^2(x)} + \frac{X(x)}{D(x)} \int_{-1}^1 \frac{F(t) dt}{X(t)D(t)(t-x)} + \frac{\Phi_h(x)}{D(x)},$$

$$D(x) = \sqrt{\pi^2 + \log^2 \left(\frac{1-x}{1+x} \right)} \quad (8-47)$$

To find $X(x)$ in Eq. (8-23) and $\Phi_h(x)$ in Eq. (8-20), start with (see Eq. 8-32)

$$G(t) = \frac{\log \left(\frac{1-t}{1+t} \right) + \pi i}{\log \left(\frac{1-t}{1+t} \right) - \pi i}$$

$$= e^{2i\theta(t)} \quad (8-48)$$

where

$$\theta(t) = \arctan \left[\frac{\pi}{\log \left(\frac{1-t}{1+t} \right)} \right] \quad (8-49)$$

Now $\theta(t) = 0$ at $t = -1$, and $\theta(t) = \pi$ at $t = 1$ so that in Eq. (8-15)

$$\log G(-1) = 0 \quad , \quad \log G(1) = 2\pi i$$

whence $a_1 = 0$ at $x = -1$, $a_2 = 1$ at $x = 1$. From Eq. (8-16), $\lambda_1 = 0$, $\lambda_2 = -1$ and from Eq. (8-17)

$$T(z) = (1-z)^{-1} \tag{8-50}$$

In Eq. (8-12)

$$\begin{aligned} P(x) &= \frac{1}{2\pi i} \int_{-1}^1 \frac{2i\theta(t)}{t-x} dt \\ &= \frac{1}{\pi} \int_{-1}^1 \frac{\theta(t)}{t-x} dt \\ &= \frac{1}{\pi} \left[\theta(t) \log(t-x) \right]_{-1}^1 - 2 \int_{-1}^1 \frac{\log(t-x) dt}{(1-t^2) \left[\pi^2 + \log^2 \left(\frac{1-t}{1+t} \right) \right]} \\ &= \log(1-x) + Q(x) \end{aligned} \tag{8-51}$$

where

$$Q(x) = -2 \int_{-1}^1 \frac{\log(t-x)}{(1-t^2) \left[\pi^2 + \log^2 \left(\frac{1-t}{1+t} \right) \right]} dt$$

To evaluate $Q(x)$, differentiate and change variables:

$$\begin{aligned} \frac{dQ(x)}{dx} &= 2 \int_{-1}^1 \frac{dt}{(1-t^2) \left[\pi^2 + \log^2 \left(\frac{1-t}{1+t} \right) \right]} (t-x) \\ &= - \int_{-\infty}^{\infty} \frac{du}{(\pi^2 + u^2) \left(\frac{1 - e^u}{1 + e^u} - x \right)} \end{aligned}$$

where

$$\left. \begin{aligned} e^u &= \frac{1-t}{1+t}, \quad t = -\tanh \frac{u}{2} \\ dt &= -\frac{1}{2} \operatorname{sech}^2 \frac{u}{2} du \\ 1-t^2 &= \operatorname{sech}^2 \frac{u}{2} \end{aligned} \right\} \quad (8-52)$$

Take

$$e^v = \frac{1-x}{1+x} \quad (8-53)$$

whence

$$\begin{aligned} \frac{dQ}{dx} &= \frac{1}{1+x} \int_{-\infty}^{\infty} \frac{(1+e^u)}{(e^u-e^v)(\pi^2+u^2)} du \\ &= \frac{1}{1+x} \int_{-\infty}^{\infty} \frac{du}{\pi^2+u^2} + \frac{2}{(1+x)^2} \int_{-\infty}^{\infty} \frac{du}{(e^u-e^v)(\pi^2+u^2)} \\ &= \frac{1}{1+x} \left[\frac{1}{\pi} \arctan \frac{u}{\pi} \right]_{-\infty}^{\infty} + S(x) \\ &= \frac{1}{1+x} + S(x) \end{aligned}$$

The integral $S(x)$ has poles in the upper plane at

$$u = i\pi, \quad u = v + 2ni\pi, \quad 0 \leq n \leq \infty$$

so that

$$\begin{aligned} S(x) &= \frac{2}{(1+x)^2} 2\pi i \sum \text{Residues} \\ &= \frac{4\pi i}{(1+x)^2} \left[\frac{1}{-2\pi i(1+e^v)} + \frac{1}{e^v} \sum_{n=0}^{\infty} \frac{1}{\pi^2 + (v+2ni\pi)^2} \right] \\ &= \frac{-1}{1+x} + \frac{4\pi i}{1-x^2} \sum_{n=0}^{\infty} \frac{1}{\pi^2 + (v+2ni\pi)^2} \end{aligned}$$

where Eq. (8-53) has been used to simplify the results. Use partial fractions and evaluate the sum to get

$$\begin{aligned}
 S(x) &= -\frac{1}{1+x} + \frac{4\pi i}{1-x^2} \sum_{n=0}^{\infty} \frac{i}{2\pi} \left[\frac{1}{v + (2n+1)\pi i} - \frac{1}{v + (2n-1)\pi i} \right] \\
 &= -\frac{1}{1+x} + \frac{2}{1-x^2} \left(\frac{1}{v - \pi i} \right) \\
 &= -\frac{1}{1+x} + \frac{2}{1-x^2} \frac{v + \pi i}{v^2 + \pi^2}
 \end{aligned}$$

Thus

$$\frac{dQ}{dx} = \frac{2}{1-x^2} \frac{v + \pi i}{v^2 + \pi^2}$$

or by Eq. (8-53)

$$\begin{aligned}
 Q &= \int \frac{v}{\pi^2 + v^2} dv + \pi i \int \frac{dv}{\pi^2 + v^2} \\
 &= \log \sqrt{\pi^2 + v^2} + \pi i \theta + C_1
 \end{aligned}$$

and from Eq. (8-51)

$$P(x) = \log(1-x) + \log \sqrt{\pi^2 + \log^2 \left(\frac{1-x}{1+x} \right)} + C_1 \quad (8-54)$$

where the $\pi i \theta$ term has been dropped from the real $P(x)$; this term represents the $G(t)$ term already included in Eq. (8-24). Now from Eqs. (8-23), (8-50), (8-54)

$$\begin{aligned}
 X(x) &= \frac{C_2}{1-x} (1-x) \sqrt{\pi^2 + \log^2 \left(\frac{1-x}{1+x} \right)} \\
 &= C_2 D(x) \quad (8-55)
 \end{aligned}$$

where $D(x)$ is defined in Eq. (8-47). In this case, the only homogeneous solution for $f(x)$ is a constant (see paragraph (e) in Sec. III) so that in Eq. (8-20)

$$\begin{aligned}\Phi_h(x) &= C_3 X(x) \\ &= C_4 D(x)\end{aligned}\tag{8-56}$$

The solution (8-47) now becomes

$$\begin{aligned}f(x) &= \frac{F(x) \log\left(\frac{1-x}{1+x}\right)}{D^2(x)} + \int_{-1}^1 \frac{F(t)}{D^2(t)(t-x)} + C_4 \\ D^2(x) &= \pi^2 + \log^2\left(\frac{1-x}{1+x}\right)\end{aligned}\tag{8-57}$$

which is the inversion integral solution of Eq. (2-11).

There may be a question about this solution (8-57) since $A(x)$ in Eq. (8-46) for this problem does not satisfy the H condition at the end points $x = \pm 1$, as required in Eq. (8-29). Also, this $A(x)$ term in $D^2(x)$ in Eq. (8-57) forces the first term to be 0 at $x = \pm 1$, which is a undesired restriction on $f(x)$. To avoid these difficulties, $\log(1-x)/(1+x)$ can be taken as some finite value at $x = \pm 1$, or $f(x)$ can be calculated up to $\pm 1 \mp \Delta x$. Since $F(t)$ is known only at specified points, it is necessary to use numerical integration in the calculation of $f(x)$ in Eq. (8-57) so that the end points can be omitted or approximated. Since the $\log(1-x)/(1+x)$ term is almost bounded and has a rapid change to infinity for a very small Δx at the end points any approximation for the end points will have little effect on the values of $f(x)$ at other points.

Numerical Integration for Inversion Integral

For the calculation of $f(x)$ in Eq. (8-57) by numerical integration, the same procedure, except at end points, as for the collocation method in Sec. VI was used. The trapezoid rule was used and all $\log(1-x)/(1+x)$ terms in Eq. (8-57) were approximated by

$$\log \frac{1-x_i}{1+x_i} \approx -A_{i1}\tag{8-58}$$

as given in Eq. (6-12). Thus

$$D_i^2 = \pi^2 + (A_{i1})^2\tag{8-59}$$

and

$$f(x_i) = \sum_{j=1}^M H_j \left[\frac{\frac{F(x_j)}{D_j^2} + \frac{F(x_i)}{D_i^2}}{x_j - x_i} \right] (\Delta x) + C_4 \quad (8-60)$$

In matrix form, Eq. (8-60) is

$$\{f\} = [G_0]\{F\} + C_4[1] \quad (8-61)$$

$$\left. \begin{aligned} A_{12} &= H_2, \quad A_{13} = \frac{1}{2} H_3, \quad A_{M,M-1} = -H_{M-1}, \quad A_{M,M-2} = -\frac{1}{2} H_{M-2}, \\ G_{0ij} &= \frac{A_{ij}}{D_j^2}; \quad G_{0ii} = -\frac{A_{ii}}{D_i^2}, \quad [1] = \text{column of ones} \\ D_1^2 &= 30.0 = D_M^2, \end{aligned} \right\}$$

where A_{ij} and A_{ii} are defined in Eq. (6-12) except as noted above. To evaluate the constant C_4 , the condition $f(0) = 0$ was used so that

$$C_4 = -[G_{0,21,j}]\{F_j\} \quad (8-63)$$

and

$$\{f\} = [G]\{F\} \quad (8-64)$$

with

$$\left. \begin{aligned} G_{ij} &= G_{0ij} - G_{0,21,j}, \\ G_{11} &= 0.2032 = -G_{MM}, \\ G_{21} &= -0.0250 = -G_{M-1,M}. \end{aligned} \right\} \quad (8-65)$$

The special values of D_1^2 , G_{11} , and G_{21} were arrived at by a special integration over the interval -0.975 to -1.0 . At $x = -1$, the integrand in the integral in Eq. (8-57) becomes infinite as $t \rightarrow -1$. The value for G_{11} , which represents this area from -0.975 to -1.0 with $F = \text{constant}$ was obtained by a numerical integration from -0.975 to -0.999 and by

$$\int_{-1}^{-0.999} \frac{dt}{(1+t) \log^2 \left(\frac{1+t}{2} \right)} = \left[\frac{1}{\log \left(\frac{1+t}{2} \right)} \right]_{-1}^{-0.999} = 0.132, \quad ,$$

where the π^2 term in (8-57) was dropped as small compared to the \log^2 term. The same result holds at $x = 1$, $t = 1$. For all x_1 points $\neq \pm 1$, as $t \rightarrow \pm 1$, the integrand is 0. The integration over -0.975 to -1.00 for these points was approximated by the D_1^2 in Eq. (8-62) and by G_{21} in Eq. (8-65).

It should be noted that the solution in Eq. (8-57) is not necessarily unique. A more restricted solution, making $f(x)$ zero at both ends, can be obtained by taking $X(x) = \text{constant}$ in Eq. (8-55). This gives the solution

$$f(x) = \frac{F(x) \log\left(\frac{1-x}{1+x}\right)}{D^2(x)} + \frac{1}{D(x)} \int_{-1}^1 \frac{F(t) dt}{D(t)(t-x)} \quad (8-66)$$

which differs from that in Eq. (8-57). This constant value for $X(x)$ can be obtained by considering $G(t)$ in Eq. (8-48) as a real variable expression so that, with $\log(-1) = \pi i$,

$$G(t) = \frac{\log(-1) \left(\frac{1-t}{1+t}\right)}{\log\left(\frac{1}{-1}\right) \left(\frac{1-t}{1+t}\right)} = 1 \quad (8-67)$$

Thus, $\theta = 0$ in Eq. (8-49) and $X(x)$ is constant.

If $f(x)$ is actually zero at the ends, then both solutions (8-57) and (8-66) may be the same. This was found to be true in the example of the hump discussed in Section IX.

IX - COMPARISON OF THE VARIOUS SOLUTIONS FOR SELECTED EXAMPLES

In Sections IV-VIII various solutions of the integral equations (2-11) or (2-12) have been obtained. All of the solutions have been expressed in the form

$$[f] = [G][F] \quad (9-1)$$

where $[G]$ is a matrix that operates on a set of known values of the $F(x)$ function to produce a set of values of the unknown $f(x)$ function. The elements of the $[G]$ matrix depend upon the method of solution. Since all of the solutions are approximate because of numerical integration or because of a finite functional representation or because of both of these

approximations, there is no reason to expect the [G] matrix to be unique or to expect any two solutions to have exactly the same elements in the [G] matrix. However, if the solutions given by the various methods are to agree for a broad class of F(x) functions, then there should not be much variation among the elements of the [G] matrices for the same boundary conditions on f(x).

In order to evaluate the various solutions, several examples have been selected for which the exact solutions are known. The solutions given by the various methods are then compared to each other and to the exact solution for these examples. The methods of solution that do all the examples the best and which appear to cover the largest class of F(x) functions may then be considered to be the better methods of solution. Also, a comparison of two selected rows of the [G] matrices is made for the methods in order to establish criteria as to which method of solution may be better.

In order to identify all of the methods of solution, a summary (Table I) is presented below, which gives the form of the [G] matrix for each method and gives the reference equations for each matrix in [G]. Reference will be made to this table in the following discussion.

To compare results given by the [G] matrices in Table I when used in Eq. (9-1), all calculations were made for 40 equal intervals on the line across the mirror, giving 41 points. Thus the [G] matrices are all 41 by 41 (except method 8, iteration, where the end points were omitted, and method 6 which was not calculated as it gives results at unequal Δx intervals). Examples using method 6 are given in Ref. 2.

Example of Hump. Assume that on a line across the mirror, an imperfection in the form of a local hump occurs with the shape given by

$$\left. \begin{aligned} f(x) &= (1 - z^2)^2, & z^2 \leq 1, \\ &= 0, & z^2 \geq 1 \\ z &= \frac{x - a}{b}, & a \text{ and } b \text{ are selected constants.} \end{aligned} \right\} \quad (9-2)$$

This particular type of imperfection was used by Linfoot in Ref. 1, except he assumed a symmetrical case with two humps. Substitute this f(x) into Eq. (2-11) and integrate to get

Table I - Summary of [G] Matrices for All Solutions

Method		[G] Matrix		Reference Eqs. for Matrices in [G]
No.	Title	Eq. No.	Formula	
1	Power Series B	(4-21)	$\frac{2}{M} [Y]^T [K]^{-1} [X] [H]$	4-19, 4-16, 4-11b, 3-1
2	Power Series C	(4-27)	$[Y] [B^T B]^{-1} [B]^T$	4-19, 4-23
3	Fourier Series A, trapezoid rule	(5-20)	$\frac{2}{\pi^2} [S] [I + K]^{-1} [C] [H]$	5-18, 5-12, 5-13, 5-14, 5-16, 3-1
4	Fourier Series A, special rule	(5-24)	$\frac{2}{\pi^2} [S] [I + K]^{-1} [D]$	5-18, 5-12, 5-13, 5-14, 5-23
5	Fourier Series B, special rule	(5-38)	$\frac{2}{\pi^2} [Y] [Q]^{-1} [R] [D] [IM]$	4-19, 5-33, 4-8, 5-31 5-23, 5-35, 5-38
6	Fourier Series B, Katzoff procedure	(5-46)	$\frac{1}{\pi} [T] [Q]^{-1} [D]$	5-47, 5-33, 4-8, 5-48
7	Collocation	(6-18)	$- [B]^{-1} [A]^T$	6-15, 6-12
8	Iteration	(7-16)	$\frac{1}{\pi^2} [X_D] [I + J + J^2 + \dots + J^{m-1}] [A_I] [X_D]^{-1}$	7-10, 7-14, 7-11
9	Inversion Integral	(8-65)	$G_{o_{ij}} - G_{o_{21,j}}$	8-62, 8-59, 6-12

$$\left. \begin{aligned}
 F(x) &= -2z^3 + \frac{10}{3}z - (1 - z^2)^2 \log \left| \frac{1 - z}{1 + z} \frac{1 + x}{1 - x} \right|, \quad z^2 < 1, \\
 &= \pm \frac{4}{3}, \quad z = \pm 1, \quad \text{respectively,} \\
 &= \frac{2}{3z} + \frac{2}{3z^3} - (z^2 - 1)^2 \left[\frac{2}{z} + \frac{2}{3z^3} + \log \left| \frac{z - 1}{z + 1} \right| \right], \quad z^2 > 1
 \end{aligned} \right\} \quad (9-3)$$

The form for $z^2 > 1$ has been changed from that given by the integration in order to obtain a form which is more accurate for large values of z . Graphs of Eqs. (9-2) for $f(x)$ and (9-3) for $F(x)$ with $a = 0.6$ and $b = 0.2$ are shown in Fig. 9-1.

Because of the numerical integration in the various methods, as has been pointed in paragraph (b) of Section III and in Eqs. (6-4) and (6-5), the derivatives of the function $f(x)$ in Eq. (9-2) should be examined. Now from Eq. (9-2)

$$\left. \begin{aligned}
 \frac{df}{dx} &= -\frac{4z}{b}(1 - z^2), \quad z^2 \leq 1, \\
 &= 0, \quad z^2 > 1,
 \end{aligned} \right\} \quad (9-4)$$

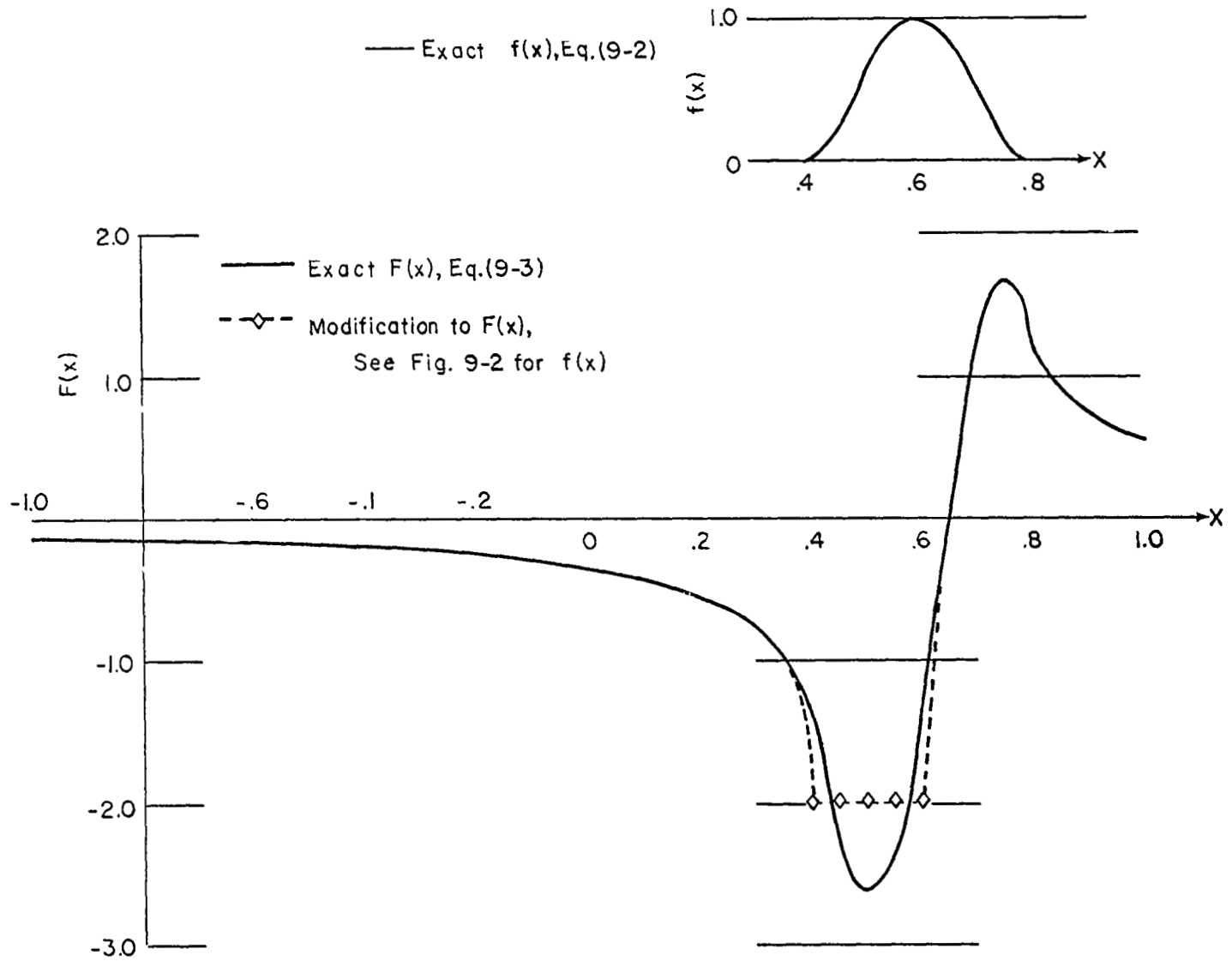
whence $f'(x)$ is continuous for $-1 \leq x \leq 1$. Thus, from Eq. (6-4), the integrand in Eq. (2-12) is continuous. However, the second derivative is discontinuous at $z = \pm 1$,

$$\left. \begin{aligned}
 \frac{d^2f}{dx^2} &= -\frac{4}{b^2} + \frac{12z^2}{b^2}, \quad z^2 \leq 1, \\
 &= 0, \quad z^2 > 1,
 \end{aligned} \right\} \quad (9-5)$$

whence from Eq. (6-5), the first derivative of the integrand in Eq. (2-12) is discontinuous at $z = \pm 1$, and the higher derivatives are infinite at $z = \pm 1$.

In order to examine the derivatives of the integrand

$$g(t, x) \equiv \frac{f(t) - f(x)}{t - x} \quad (9-6)$$

Fig. 9-1. Exact $F(x)$ and $f(x)$ for Hump Case

in Eq. (2-12) for the $f(x)$ in Eq. (9-2) in the neighborhood of $z = \pm 1$, take

$$z = \frac{t - a}{b} , \quad y = \frac{x - a}{b} \quad (9-7)$$

so that

$$g(t,x) = h(z,y) = \frac{(1-z^2)^2 - (1-y^2)^2}{b(z-y)} , \quad z^2 < 1 , \quad y^2 < 1 , \quad (9-8)$$

$$= \frac{(1-z^2)^2}{b(z-y)} , \quad z^2 < 1 , \quad y^2 \geq 1 , \quad (9-9)$$

$$= - \frac{(1-y^2)^2}{b(z-y)} , \quad z^2 \geq 1 , \quad y^2 < 1 , \quad (9-10)$$

$$= 0 , \quad z^2 \geq 1 , \quad y^2 \geq 1 . \quad (9-11)$$

Take the case of Eq. (9-10) and differentiate with respect to t , whence

$$\frac{dg}{dt} = \frac{(1-y^2)^2}{b^2(z-y)^2} ,$$

$$\frac{d^2g}{dt^2} = - \frac{2(1-y^2)^2}{b^3(z-y)^3} ,$$

.....

$$\frac{d^n g}{dt^n} = (-1)^{n+1} \frac{n!(1-y^2)^2}{b^{n+1}(z-y)^{n+1}} \quad (9-12)$$

$$\left. \frac{d^n g}{dt^n} \right]_{z=1} = (-1)^{n+1} \frac{n!(1+y)^2}{b^{n+1}(1-y)^{n-1}} \quad (9-13)$$

$$\left. \frac{d^n g}{dt^n} \right]_{z=-1} = \frac{n!(1-y)^2}{b^{n-1}(1+y)^{n-1}} \quad (9-14)$$

These results in Eqs. (9-12) - (9-14) show that the higher order derivatives of $g(t,x)$ are very large at and near $z = \pm 1$ for all $y^2 < 1$. This implies that a lower order numerical integration rule may give better results than a higher order rule (see paragraph (b) in Section III) for this particular example. To check this implication, several different rules were used for some of the methods in the calculations for this example.

The matrix $[F]$ in Eq. (9-1) was calculated for 41 values of x at intervals of $\Delta x = 0.05$ for $-1 \leq x \leq 1$ using the Eq. (9-3) with $z = 5x - 3$ ($a = 0.6$ and $b = 0.2$ in Eq. (9-2)). The $[G]$ matrices as defined in Table I for the various methods were then used to give f_i at the same 41 points. The results are shown in Table II.

All of the methods located the hump and all methods, except method 3, Fourier Series A with trapezoid rule, and method 8 using Eq. (7-5) in the iteration, gave a satisfactory representation of the hump. However, a study of the Table II indicates that some of the methods gave smaller maximum deviations than others. Method 9, the inversion integral, appears to give the best results with the trapezoid and Simpson's rules giving essentially the same results. Method 1, power series B, shows slightly larger deviations in the region of the hump for a 5-point integration rule as compared to the trapezoid and Simpson's rules. This indicates that even the large higher order derivatives of Eq. (9-12) - (9-14) do not have much effect on the accuracy of the integration rules in this case. However, in this method 1, the end point values are much improved by the higher order rules. This occurs because the spacing of the points is too large to give a fair representation of x^n (n of order 20) when x approaches ± 1 at the ends. A higher order rule will naturally improve this representation near the ends. In method 5, Fourier series B, the equal Δx answer corresponds to using an interpolation matrix $[IM]$ to convert the F_i values in the Table II to equal $\Delta \theta$ values needed in the calculations, while the equal $\Delta \theta$ answer corresponds to calculating F_i at equal $\Delta \theta$ intervals directly from Eq. (9-3) and deleting the $[IM]$ matrix in $[G]$. The latter answer appears to be slightly better in this example.

Since methods 3, Fourier series A with trapezoid rule, and 8, iteration, did not produce answers as good as the other methods in the hump example, and since these methods have other drawbacks already discussed in the description of the methods, Sections V and VII, no further consideration will be given to these two methods in the remaining examples and discussion. Also, only the equal Δx case will be used for method 5, Fourier series B, in the following examples.

Example of Modified Hump. In order to examine the behavior of the solutions when a large slope change occurs in $F(x)$, a modification to the above hump example was made by taking $F(x) = -2.0$ at the points $x = 0.40, 0.45, 0.50, 0.55$ and 0.60 (see Fig. 9-1). Such a modification not only gives an extreme change in the $F(x)$ slope at $x = 0.40$ and $x = 0.60$, but also could represent a physical situation in which the light intensity is too weak to show a variation for $F(x) < -2.0$. The results for $f(x)$, the mirror surface deviation, given by the various methods for this modified $F(x)$ are shown in Fig. 9-2. The graph covers the range of $0.2 \leq x \leq 0.8$. For the remainder of the mirror line, all methods gave small values, $f(x) < 0.05$, except for power series B, which gave larger values at $x = \pm 1$, the end points. The exact answer for $f(x)$ is not known, but if the inversion integral is accepted as being the closest to the correct result, then the function methods, power series

Table II. Example of Hump Case (Eq. 9-2)

Method →	①	①	①	②	③	④	⑤	⑤	⑦	⑦	⑧	⑧	⑨	⑨		
x	f(x) Exact	Power Series B	Power Series B	Power Series B	Power Series C	Fourier Series A (Equal Δx) Trapezoid	Fourier Series A (Equal Δx) Special Rule	Fourier Series B (special rule) Equal Δx	Fourier Series B (special rule) Equal Δθ	Collocation Trapezoid	Collocation Simpson	Iteration Eq. (7-4) 5th Iteration	Iteration Eq. (7-5) 5th Iteration	Inversion Integral Trapezoid	Inversion Integral Simpson	
-1.00	-.134	0	-.066	-.024	-.017	-.015	0	.003	.003	.005	.007	.034	.142	.000	.000	
-.95	-.138	0	.001	-.001	-.000	.013	.046	-.011	.004	.004	.006	.002	.030	.000	+.001	
-.90	-.143	0	.014	.016	.020	-.004	.097	-.017	-.001	-.002	.005	.006	.020	.021	-.000	+.000
-.85	-.148	0	.022	.018	.017	-.003	.045	-.005	.005	.005	.006	.006	.029	.037	-.000	+.000
-.80	-.153	0	.003	.003	.002	.006	.074	-.014	.003	.005	.006	.006	.028	.040	-.000	.000
-.75	-.159	0	.008	.008	.011	-.003	.104	-.021	-.002	-.004	.005	.006	.026	.04c	-.000	.000
-.70	-.165	0	.021	.019	.022	-.007	.075	-.012	.000	-.001	.005	.006	.024	.039	-.000	.000
-.65	-.171	0	.018	.017	.017	.000	.043	-.005	.006	.006	.006	.022	.038	-.000	.000	
-.60	-.178	0	.007	.007	.006	.005	.058	-.010	.006	.006	.006	.020	.035	-.000	.000	
-.55	-.186	0	.004	.004	.005	.000	.094	-.020	-.001	-.001	.005	.006	.018	.033	-.000	.000
-.50	-.195	0	.012	.014	.014	-.007	.104	-.020	-.004	-.005	.006	.016	.030	-.000	.000	
-.45	-.204	0	.021	.019	.021	-.007	.075	-.012	.001	-.001	.005	.006	.014	.027	-.000	.000
-.40	-.215	0	.020	.018	.019	.001	.045	-.004	.007	.004	.006	.013	.024	-.000	.000	
-.35	-.226	0	.010	.010	.009	.006	.044	-.005	.008	.009	.005	.006	.011	.021	-.000	.000
-.30	-.239	0	.003	.003	.003	.002	.074	-.016	.002	.002	.004	.005	.009	.018	-.000	.000
-.25	-.253	0	.005	.005	.007	-.006	.106	-.023	-.005	-.006	.006	.007	.007	.017	-.000	.000
-.20	-.269	0	.015	.013	.017	-.010	.108	-.020	-.004	-.006	.003	.004	.006	.012	-.000	.000
-.15	-.287	0	.023	.021	.023	-.004	.075	-.009	.003	.002	.007	.007	.004	.009	-.000	.000
-.10	-.308	0	.021	.020	.020	.006	.029	-.001	.011	.011	.008	.003	.003	.007	-.000	.000
-.05	-.333	0	.010	.010	.009	.009	.000	-.004	.009	.011	.008	.008	0	0	-.000	.000
0	-.361	0	0	0	0	0	.006	-.017	0	0	0	-.002	-.002	0	0	0
.05	-.396	0	.000	-.001	.002	-.012	.037	-.028	-.009	-.011	.011	.010	-.003	-.006	.000	-.000
.10	-.437	0	.013	.011	.015	-.014	.070	-.007	-.007	-.010	-.003	-.004	-.005	-.008	.000	-.000
.15	-.488	0	.029	.027	.030	.000	.087	-.006	.007	.005	.015	.012	-.006	-.010	.000	-.000
.20	-.554	0	.032	.030	.030	.016	.081	-.009	.008	.020	-.008	-.010	-.008	-.012	.000	-.000
.25	-.642	0	.012	.011	.008	.013	.051	-.000	.009	.018	-.008	-.010	-.010	-.013	.000	-.001
.30	-.765	0	-.017	-.020	-.021	-.016	.044	-.032	-.015	-.015	-.016	-.021	.010	-.013	.000	-.001
.35	-.956	0	-.020	-.024	-.019	-.035	.056	-.048	-.022	-.030	.039	.031	-.015	-.009	-.002	-.005
.40	-1.333	0	.055	.053	.062	.023	.131	.019	-.051	.036	-.030	-.038	-.003	.027	.005	.004
.45	-2.214	.191	.247	.249	.256	.218	.307	.216	.248	.233	.193	.200	.184	.173	.200	.206
.50	-2.653	.562	.542	.547	.545	.535	.587	.526	.547	.543	.573	.573	.532	.532	.561	.563
.55	-2.338	.879	.850	.854	.843	.858	.900	.836	.841	.853	.890	.893	.845	.803	.874	.874
.60	-1.386	1.000	1.020	1.019	1.010	1.014	1.091	.987	.977	.999	1.013	1.020	.970	.830	.993	.997
.65	-.112	.879	.925	.922	.926	.889	1.006	.872	.862	.880	.883	.884	.862	.768	.871	.871
.70	1.059	.562	.576	.579	.595	.544	.540	.546	.549	.572	.583	.583	.568	.543	.556	.560
.75	1.656	.191	.179	.185	.196	.188	.228	.186	.211	.201	.165	.171	.220	.249	.190	.193
.80	1.333	0	-.000	-.008	-.016	.009	.056	-.000	.026	.016	.018	.017	.034	.048	.018	.015
.85	.956	0	.046	.030	.019	-.005	.122	-.014	-.003	-.003	.007	.008	.026	-.003	-.003	
.90	.765	0	.007	.029	.040	.001	.080	-.010	.004	.006	.005	.007	.001	.040	-.001	-.000
.95	.642	0	-.019	-.029	-.027	-.002	-.019	-.016	.000	-.000	.005	.006	-.096	-.191	.002	-.003
1.00	.554	0	-.272	-.104	-.076	-.003	0	.002	.002	.005	.007	--	--	.000	+.000	
Max. + deviation			+.056	+.058	+.065	+.027	+.131	+.025	+.057	+.042	+.039	+.031	+.142	+.018	+.015	
Max. - deviation			-.272	-.104	-.076	-.035	-.019	-.048	-.051	-.030	-.030	-.038	-.191	-.008	-.008	

55

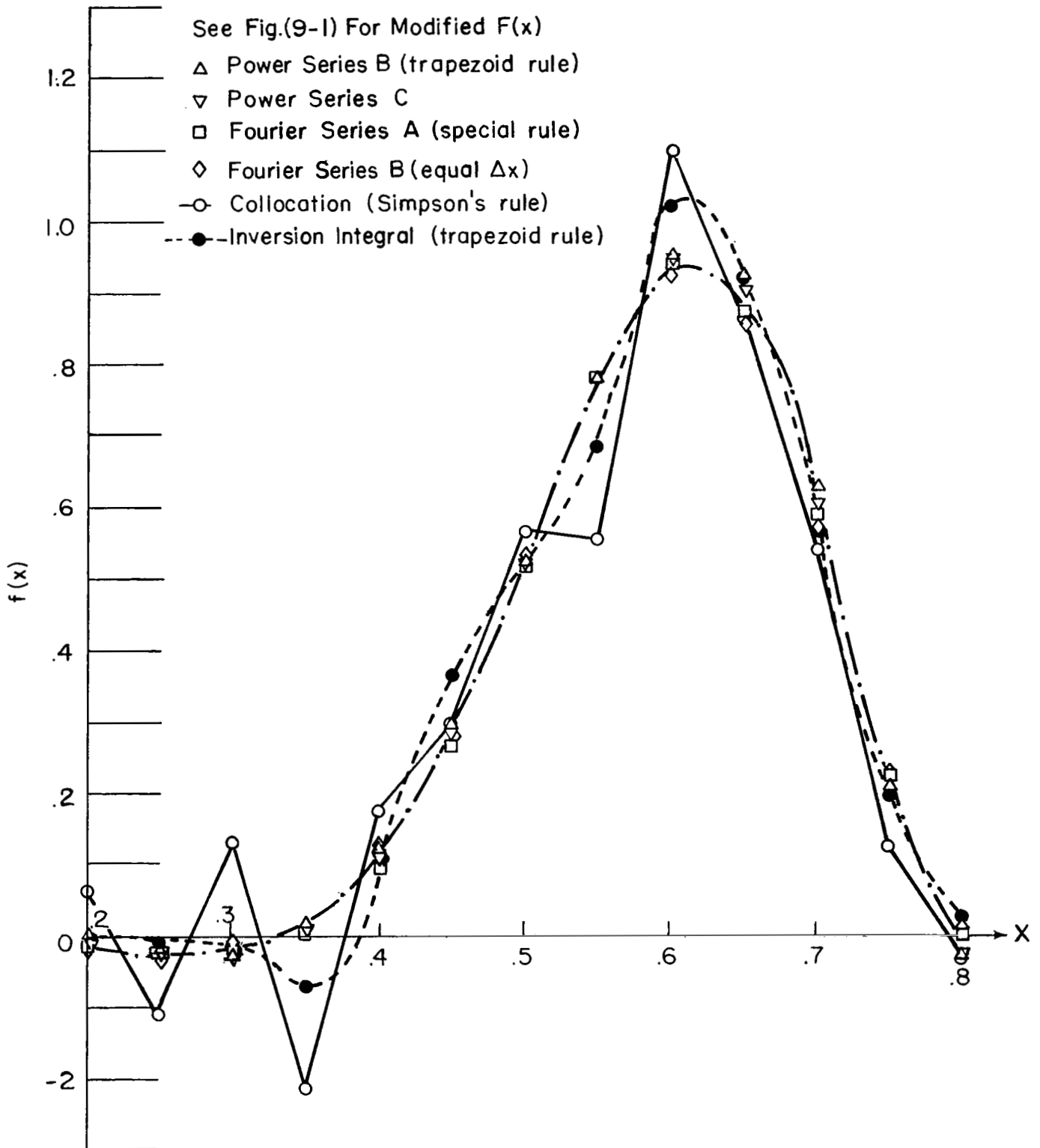


Fig. 9-2. $f(x)$ for Modified Hump Case

and Fourier series, appear to oscillate about the inversion integral curve and thus represent it approximately. The representation appears to be as good as could be expected with twenty constants in the function solutions. The collocation solution appears to represent the inversion integral solution with a high frequency large amplitude oscillation. Since the collocation method has no smoothing function effect in it, it may be expected to oscillate on functions with large slope changes or with discontinuities. Further discussion of this deficiency of the collocation method is given below in the G matrix paragraph.

Example of Straight Line. As pointed out in paragraph (f) of Section III, the method of solution should properly solve the case of a constant $F(x)$, which produces a rotation of the mirror or a straight line deviation across the mirror. To examine this case, $[F]$ in Eq. (9-1) was taken as $F_i = -40.0$ at all 41 points so that the exact slope of $f(x)$ is 20.0 with $f(-1) = -20.0$, $f(x) = 20.0$, and $f_{21} = 0$, $f_{22} = 1.0$, etc. Methods 1, 2, 4, 5, 7, 9 in Table I were used with the following results.

Method 1, power series B with trapezoid rule, gave a large oscillation with deviations of order of ± 2.0 from the straight line and with ∓ 38.78 instead of ∓ 20.0 at the ends. As pointed out above in the discussion of the hump example, this failure of the Power series B method is due to the poor representation of x^n near the ends. This affects the G matrix, which shows large effects when $f(x)$ has its largest value at the ends. See discussion of the G matrices below.

Method 2, power series C, gave the straight line to five significant figures at all 41 points.

Method 4, Fourier series A with special rule, did not give the straight line. It has large oscillations with deviations as large as ± 10.0 , with ± 20.0 deviations at the ends. This failure of Fourier series A is due to the restraints imposed by the $\sin nx$ functions being zero at the ends. This restraint gets into the G matrix, which means that for $f(x)$ odd and not zero at the ends, the method will give poor results. In this case, the series must represent a function with a discontinuity at both ends. See discussion of the G matrices below.

Method 5, Fourier series B with special rule and equal Δx 's, gave the straight line to four significant figures at all 41 points.

Method 7, collocation with Simpson's rule, gave the straight line to at least eight significant figures (only eight digits were printed out) at all 41 points.

Method 9, inversion integral with trapezoid rule, gave the straight line to four significant figures at all 41 points.

The above three examples of the hump, the modified hump, and the straight line show that all of the methods except possibly the inversion

integral, appear to have deficiencies. Some methods do better on one type of function than on other types. Although power series B and Fourier series A did satisfactorily on the hump and agreed with the other function methods on the modified hump, they failed completely on the straight line. The collocation method did very well on the hump and the straight line, but did poorly on the modified hump. The power series C, the Fourier series B, and the inversion integral methods appear to be the most consistent in the three examples considered. In order to determine which may be the better methods for all types of possible functions $f(x)$ and $F(x)$, an examination of the G matrices was made for the various methods.

The G Matrices. To study the behavior of the G matrix in Eq. (9-1) for the various methods of solution, graphs of two typical rows of the G matrices were constructed. Figure 9-3 shows row 16, which gives f_{16} at $x = -0.25$, and Fig. 9-4 shows row 33, which gives f_{33} at $x = 0.60$. Methods 1, 2, 4, 5, 7, 9 in Table I are shown in Figs. 9-3 and 9-4. Method 1, power series B with trapezoid rule, method 2, power series C, and Method 4, Fourier series A with special rule are too close to distinguish on the graph, except at the ends. For row 16, at $x = -1$, point 1, power series B gives 0.0077, power series C gives 0.0000, and Fourier series A gives 0.0538; for row 16 at $x = 1$, pt. 41, power series B gives 0.0191, power series C gives 0.0001, and Fourier series A gives 0.0520.

Since these differences in the end values occur in all the rows of the G matrices for methods 1, 2, and 4, it appears that these large end values in power series B and Fourier series A are the cause of the failure of these two methods to give the proper results in the straight line example above. Since the power series C has small end values in the G matrix, agrees with the power series B and Fourier series A elsewhere, and gives the proper straight line, it would appear to be the best of these three function methods.

In Figs. 9-3 and 9-4, the Fourier series B deviates slightly from the other three function methods and has small values at the ends ($G_{16,1} = 0.0003$, $G_{16,41} = -0.0028$). On the whole, it should give results similar to power series C.

In Figs. 9-3 and 9-4, it appears that the function methods are actually representing the inversion integral curve as well as they can with twenty constants. The inversion integral G matrix, which is limited in accuracy only by the numerical integration for each row, should be the best overall matrix (except possibly the first row and last row).

The peak values in the rows of the G matrix occur on either side of the origin ($x = 0$), which is the restraint point for the solution to make $f(0) = 0$, and on either side of the f_i point being calculated ($G_{16,15}$ and $G_{16,17}$ in Fig. 9-3 for row 16 giving f_{16}). Since the form of the integral Eq. (2-11) gives large values in the integrand for

t near x , the point at which $f(x)$ is being calculated, it is evident that these adjacent values should be emphasized in the solution. Of necessity, the function methods must smooth out these peak values and fail to give proper emphasis to them. For these reasons, the inversion integral method is considered to be the best method for all types of possible functions.

The entire G matrix for the inversion integral method using the trapezoid rule for the numerical integration is given in Appendix C. It may be noted that the inversion integral G matrix with Simpson's rule has slightly larger peak values than those shown in Figs. 9-3 and 9-4 for the trapezoid rule.

The collocation method shows a high frequency oscillation, with large amplitudes, about the inversion integral curve in Figs. 9-3 and 9-4. It is evident that if $F(x)$ has a sharp change or is discontinuous, then the large values in the collocation G matrix can magnify the discontinuity and give incorrect values for $f(x)$. Thus, the collocation method, in spite of its performance on the straight line and the hump example, it is not a good method for all types of functions, particularly those with discontinuities.

Evaluation of the Various Methods. On the basis of the above examples and examination of the G matrix, an evaluation of the nine methods of solution listed in Table I can be made. Although all the methods can solve certain problems, the best methods are those that can solve the largest class of problems. Since $F(x)$ must be measured at points, and $f(x)$ may represent any conceivable deformation of the mirror, it is essential that the method of solution handle almost any type of function, whether continuous or not. From this viewpoint, the following evaluation is made:

1. Method 9, the inversion integral, is the best overall method. It will handle most any case.
2. Power series C, method 2, and Fourier series B, methods 5 and 6, are the best function methods. They will handle most any case.
3. Collocation, method 7, is simple and satisfactory for smooth functions, but is no good on discontinuous functions. A violent oscillation in the solution indicates the method has failed.
4. Power series B, method 1, and Fourier series A, methods 3 and 4, are unsatisfactory because of end points representations and restrictions.
5. Iteration, method 8, is unsatisfactory because of end point restraints and numerical integration difficulties.

Up to this point the discussion and evaluation of the various methods has been concerned with the solid mirror. Section X takes up the Cassegrain mirror, or the mirror with a central hole.

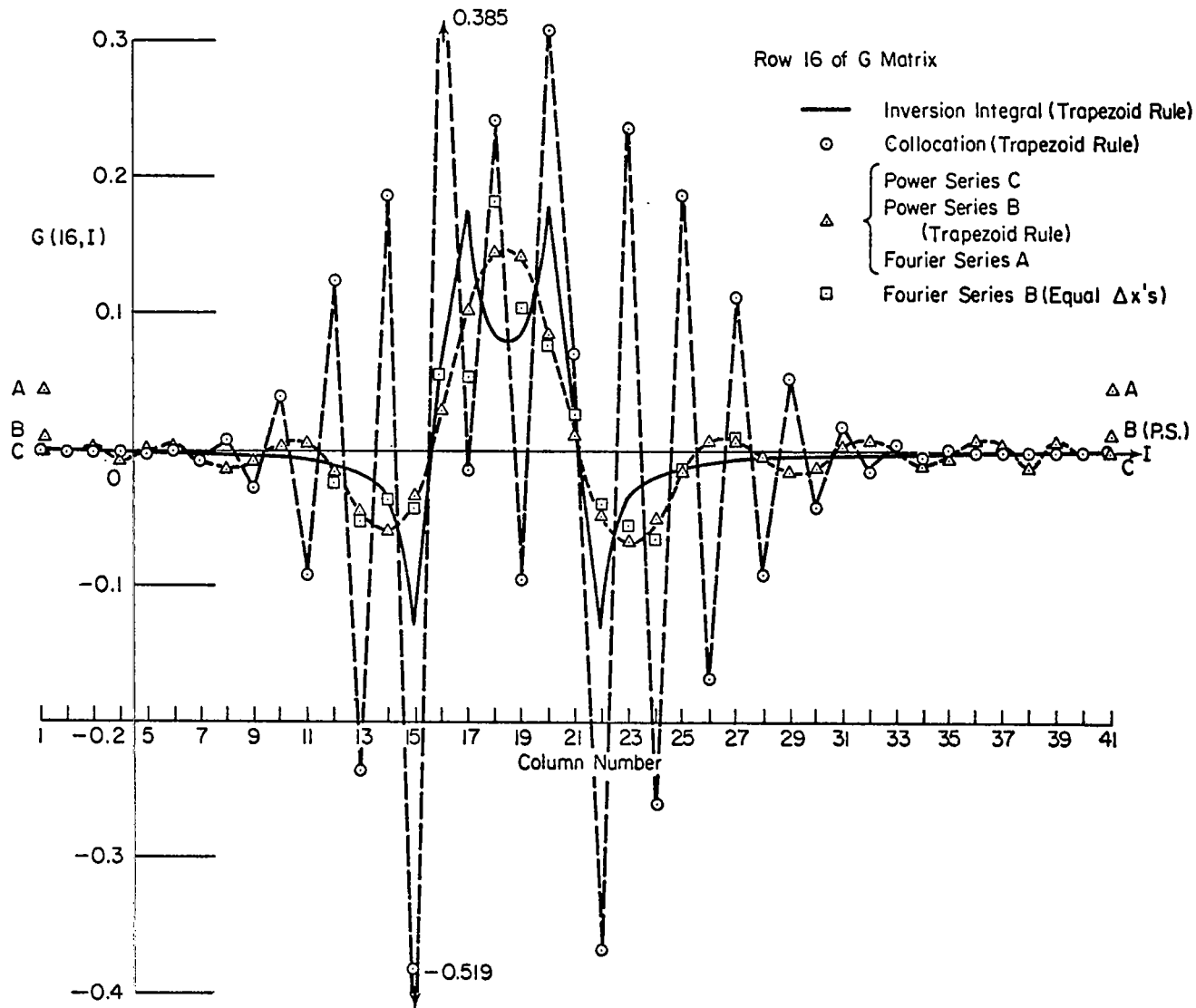


Fig. 9-3. Row 16 of G Matrix

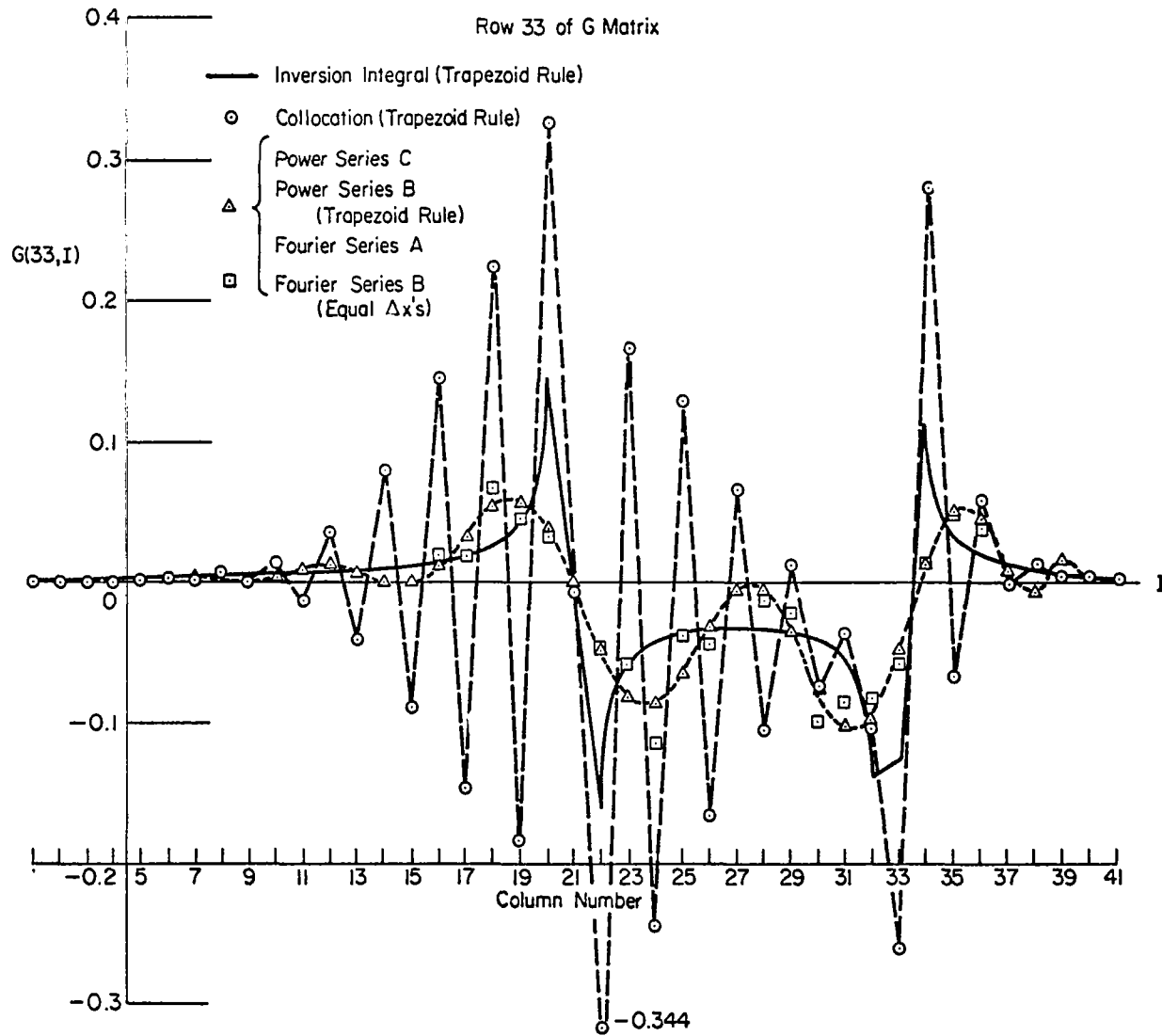


Fig. 9-4. Row 33 of G Matrix

X - SOLUTIONS FOR CASE OF A CENTRAL HOLE

The integral equations to be solved for the Cassegrain mirror are given in Eqs. (2-13) or (2-15). Take Eq. (2-15) in the following form

$$F(x) = - \left[\int_{-1}^{-R} + \int_R^1 \right] \left[\frac{f(t) - f(x)}{t - x} dt \right] \quad (10-1)$$

where R is defined in Fig. 2-3. Theoretically, this Eq. (10-1) can be solved by any of the methods described in Sections IV-VIII. However, on the premise that the evaluation of the methods for the solid mirror in Section IX holds for the Cassegrain mirror, only the better methods will be used for this case. The power series C, collocation and inversion integral methods of solution, as modified for the hole case, are described below. The Fourier series B, method 6 in Table I, is described in Ref. 2 for the hole case, together with examples. It will not be covered here.

Power Series C for Hole. As in Section IV, take

$$f(x) = \sum_{j=1}^J A_j x^j \quad (10-2)$$

in Eq. (10-1) and integrate to get

$$F(x) = - \sum_{j=1}^J A_j \sum_{k=1}^j \frac{[1 - R^{j-k+1}] [1 - (-1)^{j-k+1}] x^{k-1}}{j - k + 1} \quad (10-3)$$

whence

$$F(x_i) = F_i = \sum_{j=1}^J A_j B_j(x_i) = \sum_{j=1}^J B_{ij} A_j \quad (10-4)$$

$$B_{ij} = - \sum_{k=1}^j \frac{[1 - R^{j-k+1}] [1 - (-1)^{j-k+1}] x_i^{k-1}}{j - k + 1} \quad (10-5)$$

These Eqs. (10-4) and (10-5) correspond to Eqs. (4-22) and (4-23) so that from Eqs. (4-26) and (4-28),

$$[f] = [G][F] \quad (10-6)$$

$$[G] = [Y][B^T B]^{-1}[B]^T \quad (10-7)$$

where the elements of [Y] and [B] are given in Eqs. (4-19) and (10-5), respectively.

Results using power series C for several examples with a hole are given below and compared to the results of the other methods.

Collocation Method for Hole. For $2R$ as the width of the hole on the particular line on the mirror (see Fig. 2-3), take $(M/2)-1 = 20$ equal intervals on each side. This gives 21 points on each side, or $M = 42$ total number of points, including four edge points. Take

$$P = \Delta x = \frac{2(1-R)}{M-2}, \quad M \text{ points}, \quad (10-8)$$

whence

$$\left. \begin{aligned} x_j &= -1 + P(j-1), \quad j = 1, 2, \dots, \frac{M}{2}, \\ x_j &= R + P\left(j - 1 - \frac{M}{2}\right), \quad j = \frac{M}{2} + 1, \dots, M \end{aligned} \right\} (10-9)$$

As in Section VI, take Eq. (10-1) in matrix form

$$[A][f] = -[F] \quad (10-10)$$

where, by using Eqs. (10-9) and (6-12),

$$\left. \begin{aligned} A_{i,i-1} &= -H_{i-1} - \frac{1}{2}H_i, \quad A_{i,i+1} = H_{i+1} + \frac{1}{2}H_i, \\ &i \neq 1, \frac{M}{2}, \frac{M}{2} + 1, M, \\ A_{1,2} &= 2H_1 + H_2, \quad A_{1,3} = -\frac{1}{2}(H_1 - H_3), \\ A\left(\frac{M}{2}, \frac{M}{2} - 2\right) &= \frac{1}{2}\left[H\left(\frac{M}{2}\right) - \left(\frac{M}{2} - 2\right)\right], \\ A\left(\frac{M}{2} + 1, \frac{M}{2} + 3\right) &= -\frac{1}{2}\left[H\left(\frac{M}{2} + 1\right) - H\left(\frac{M}{2} + 3\right)\right]; \\ A\left(\frac{M}{2}, \frac{M}{2} - 1\right) &= -2H\left(\frac{M}{2}\right) - H\left(\frac{M}{2} - 1\right), \\ A\left(\frac{M}{2} + 1, \frac{M}{2} + 2\right) &= 2H\left(\frac{M}{2} + 1\right) + H\left(\frac{M}{2} + 2\right), \\ A(M, M-2) &= \frac{1}{2}[H(M) - H(M-2)], \\ A(M, M-1) &= -2H(M) - H(M-1), \\ A_{ij} &= \frac{H_j P}{x_j - x_i}, \quad \text{except above and } i \neq j \\ A_{ii} &= -\sum_{j=1, j \neq i}^M A_{ij}. \end{aligned} \right\} (10-11)$$

Now, from paragraph (e) of Section III, there are two homogeneous solutions for the hole case. Thus two points must be fixed on the mirror in order to obtain a solution by the collocation method. Any solution thus obtained will include the homogeneous solutions (3-6) and (3-7) or

$$f_h = C_1 + \frac{C_2}{x} \quad (10-12)$$

The value of C_1 is of no consequence as it represents a translation of the reference for $f(x)$, but the value of C_2 should be as small as possible to keep the apparent distortion C_2/x small. In most cases the smallest value of C_2 will be given by fixing the two points at the edges of the hole. However, if $f(x)$ is larger at the edges of the hole than at the ends, then the ends would give a smaller C_2 . Note that $C_2 = 0$ for $f(x)$ even.

Use the conditions

$$\left. \begin{aligned} f\left(\frac{M}{2}\right) &\equiv f(-R) = 0 \\ f\left(\frac{M}{2} + 1\right) &\equiv f(R) = 0 \end{aligned} \right\} \quad (10-13)$$

so that, corresponding to Eq. (6-15),

$$\left. \begin{aligned} [B] &= [A]^T[A] + [S] \\ S_{ij} &= 0, \text{ except} \\ S\left(\frac{M}{2}, \frac{M}{2}\right) &= S\left(\frac{M}{2} + 1, \frac{M}{2} + 1\right) = 1.0 \end{aligned} \right\} \quad (10-14)$$

This gives (see Section VI)

$$\begin{aligned} [f] &= [G][F] \\ [G] &= -[B]^{-1}[A]^T \end{aligned} \quad (10-15)$$

where $[A]$ is defined in Eq. (10-11) and $[B]$ in Eq. (10-14).

Results using the collocation method are given below.

Inversion Integral for Hole Case. The integral Eq. (2-13) for the Cassegrain mirror is the same as Eq. (8-29) with

$$\left. \begin{aligned} A(x) &= \log \left| \frac{1-x}{1+x} \frac{x+R}{x-R} \right|, \quad B(x) = -\pi i \\ x &= t_0, \quad L = \text{lines } -1 \text{ to } -R \text{ and } R \text{ to } 1 \end{aligned} \right\} \quad (10-16)$$

and the solution is given by Eq. (8-38) as

$$\left. \begin{aligned} f(x) &= \frac{F(x)}{D^2(x)} \log \left| \frac{1-x}{1+x} \frac{x+R}{x-R} \right| + \frac{X(x)}{D(x)} \int_L \frac{F(t)dt}{X(t)D(t)(t-x)} \\ &+ \frac{\Phi_h(x)}{D(x)}, \\ D^2(x) &= \pi^2 + \log^2 \left| \frac{1-x}{1+x} \frac{x+R}{x-R} \right|. \end{aligned} \right\} \quad (10-17)$$

To find $X(x)$, Eq. (8-23), and $\Phi_h(x)$, Eq. (8-20), to use in the above Eq. (10-17), start with Eq. (8-32) for $G(t)$, whence

$$G(t) = \frac{\log \left| \frac{1-t}{1+t} \frac{t+R}{t-R} \right| + \pi i}{\log \left| \frac{1-t}{1+t} \frac{t+R}{t-R} \right| - \pi i} = e^{2i\theta(t)} \quad (10-18)$$

where

$$\theta(t) = \arctan \left[\frac{\pi}{\log \left| \frac{1-t}{1+t} \frac{t+R}{t-R} \right|} \right] \quad (10-19)$$

From Eqs. (8-15), (8-16), (10-18), and (10-19), values of θ_k , $\log G(b_k)$, a_k , and λ_k , at the edge points can be obtained as follows:

x	θ	$\log G$	a_k	λ_k	}	(10-20)
-1	0	0	0	0		
$-R$	π	$2\pi i$	1	-1		
R	0	0	0	0		
1	π	$2\pi i$	1	-1		

Thus, Eq. (8-17) gives

$$T(z) = (z+R)^{-1}(1-z)^{-1} \quad (10-21)$$

From Eqs. (8-12) and (10-18)

$$P(x) = \frac{1}{\pi} \int_L \frac{\theta(t)dt}{t-x}, \quad (10-22)$$

where L is -1 to -R and R to 1 and $\theta(t)$ is given by Eq. (10-19). By analogy to the integration of the corresponding Eq. (8-51) for the solid mirror with the result in Eq. (8-54), the solution for Eq. (10-22) was deduced as

$$P(x) = \log \left[\left| \frac{(1-x)(x+R)}{x} \right| \sqrt{\pi^2 + \log^2 \left| \frac{1-x}{1+x} \frac{x+R}{x-R} \right|} \right] + C_1 \quad (10-23)$$

This result was verified very closely by a numerical integration of Eq. (10-22) using the trapezoid rule and the [A] matrix in Eq. (10-11). That is,

$$[P] = -\frac{1}{\pi} [A][\theta], \quad 42 \text{ points}, \quad (10-24)$$

where $A_{ii} = 0$.

Put Eqs. (10-23) and (10-21) into Eq. (8-23) to get

$$\begin{aligned} X(x) &= C_2(1-x)^{-1}(x+R)^{-1}(1-x)(x+R) x^{-1}D(x) \\ &\equiv C_2 \frac{D(x)}{x}, \end{aligned} \quad (10-25)$$

where $D(x)$ is defined in Eq. (10-17). In this case, the homogeneous solution for $f(x)$ is given by Eqs. (10-17) and (8-20) as

$$\begin{aligned} f_h(x) &= \frac{\Phi_h(x)}{D(x)} = \frac{D(x)}{xD(x)} (C_3x + C_4) \\ &= C_3 + \frac{C_4}{x} \end{aligned} \quad (10-26)$$

which agrees with the homogeneous solution given in paragraph (e) of Section III. Equation (10-17) now becomes

$$f(x) = \frac{F(x)}{D^2(x)} \log \left| \frac{1-x}{1+x} \frac{x+R}{x-R} \right| + \frac{1}{x} \int_L \frac{tF(t)dt}{D^2(t)(t-x)} + C_3 + \frac{C_4}{x} \quad (10-27)$$

$$D^2(x) = \pi^2 + \log^2 \left| \frac{1-x}{1+x} \frac{x+R}{x-R} \right| \quad (10-28)$$

which is the general inversion integral solution of Eq. (2-13).

It should be noted that this solution in Eq. (10-27) is not unique. Other forms for $X(x)$ in Eq. (10-25) are

$$X(x) = C_2 D(x) \quad \text{and} \quad X(x) = C_2 \quad (10-29)$$

whence other solutions are

$$f(x) = \frac{F(x)}{D^2(x)} \log \left| \frac{1-x}{1+x} \frac{x+R}{x-R} \right| + \int_L \frac{F(t)dt}{D^2(t)(t-x)} + C_5 + \frac{C_6}{x}, \quad (10-30)$$

$$f(x) = \frac{F(x)}{D^2(x)} \log \left| \frac{1-x}{1+x} \frac{x+R}{x-R} \right| + \frac{1}{D(x)} \int_L \frac{F(t)dt}{D(t)(t-x)} + C_7 + \frac{C_8}{x} \quad (10-31)$$

It was found that the particular integrals in the solutions (10-27), (10-30), and (10-31) behaved as if two restraints were present, or $f(\pm a) = 0$, for $x = \pm a$ points on the mirror. The value of a is different in each solution for the same function. For these reasons the mirror was restrained at the edge points, $x = \pm R$, or $f(\pm R) = 0$, which corresponds to the restraints used in the collocation method. Note that by replacing t by $t - x + x$ in the integrand in Eq. (10-27), the solution in Eq. (10-30) is obtained with a term (C_9/x) added. Since the solution in Eq. (10-31) makes $f(1) = f(-1) = 0$, it is more restricted. However, for the "hump" example given below, all three solutions are essentially the same.

The numerical integration in Eq. (10-27) was carried out in the same manner as for the solid mirror, Eqs. (8-58) - (8-65), where all log terms are approximated by $-A_{ij}$ in Eq. (10-11). Thus

$$f(x_i) = \sum_{j=1}^M \frac{H_j(\Delta x)}{x_j - x_i} \left[\frac{x_j F(x_j)}{x_j D_j^2} + \frac{F(x_j)}{D_j^2} \right] + C_3 + \frac{C_4}{x_i} \quad (10-32)$$

$$D_i^2 = \pi^2 + (A_{ii})^2 \quad (10-33)$$

$$[f] = [G_0][F] + C_3[1] + C_4 \left[\frac{1}{x_i} \right] \quad (10-34)$$

$$\left. \begin{aligned} G_{0ij} &= \frac{x_j A_{ij}}{x_i D_j^2} \quad , \quad G_{0ii} = -\frac{A_{ii}}{D_i^2} \\ [1] &= \text{column of 1's} \quad , \quad \left[\frac{1}{x_i} \right] = \text{column for } \frac{1}{x_i} \end{aligned} \right\} \quad (10-35)$$

where from Eq. (10-11) and from special integrations for the edge values (see Eqs. (8-62) and (8-65) and discussion after Eq. (8-65)):

$$\left. \begin{aligned} A_{ij} &= \frac{H_j P}{x_j - x_i} \quad , \quad i \neq j \quad , \\ A_{i,i-1} &= -H_{i-1} - \frac{1}{2} H_i \quad , \quad i \neq 1, \frac{M}{2} + 1, \\ A_{i,i+1} &= H_{i+1} + \frac{1}{2} H_i \quad , \quad i \neq \frac{M}{2}, M, \\ A_{ii} &= - \sum_{j=1, j \neq i}^M A_{ij} \quad , \quad i \neq 1, \frac{M}{2}, \frac{M}{2} + 1, M \end{aligned} \right\} \quad (10-36)$$

$$\left. \begin{aligned} D_1^2 &= D_M^2 = 28.0 \quad , \quad D^2\left(\frac{M}{2}\right) = D^2\left(\frac{M}{2} + 1\right) = 11.0 \quad , \\ G_{011} &= -G_{0MM} = 0.2060 \quad , \\ G_0\left(\frac{M}{2}, \frac{M}{2}\right) &= -G_0\left(\frac{M}{2} + 1, \frac{M}{2} + 1\right) = -0.3180, \\ G_0(2,1) &= -G_0(M-1, M) = -0.0283 \quad , \\ G_0\left(\frac{M}{2} - 1, \frac{M}{2}\right) &= -G_0\left(\frac{M}{2} + 2, \frac{M}{2} + 1\right) = 0.0432, \\ G_0\left(\frac{M}{2} - 1, \frac{M}{2} + 1\right) &= -G_0\left(\frac{M}{2} + 2, \frac{M}{2}\right) = -0.0031 \end{aligned} \right\} \quad (10-37)$$

As noted above in the collocation method, the smallest value of C_4/x in most cases will occur if the two points at the edges of the hole are fixed. Thus from Eqs. (10-13) and (10-34)

$$0 = \left[G_0\left(\frac{M}{2}, j\right) \right] [F_j] + C_3 - \frac{C_4}{R}$$

$$0 = \left[G_0\left(\frac{M}{2} + 1, j\right) \right] [F_j] + C_3 + \frac{C_4}{R}$$

whence

$$C_3 = -\frac{1}{2} \left[G_0\left(\frac{M}{2}, j\right) + G_0\left(\frac{M}{2} + 1, j\right) \right] [F_j] \quad (10-38)$$

$$C_4 = \frac{R}{2} \left[G_0\left(\frac{M}{2}, j\right) - G_0\left(\frac{M}{2} + 1, j\right) \right] [F_j]$$

Now, Eq. (10-34) becomes

$$[f] = [G][F] \quad (10-39)$$

$$G_{ij} = G_{0ij} - \frac{1}{2} \left(1 - \frac{R_1}{x_1} \right) G_0\left(\frac{M}{2}, j\right) - \frac{1}{2} \left(1 + \frac{R}{x_1} \right) G_0\left(\frac{M}{2} + 1, j\right) \quad (10-40)$$

where G_{0ij} is defined in Eqs. (10-35) - (10-37).

Results for the inversion integral method are given below and compared to the other methods.

Comparison of Solutions for Cassegrain Mirror for Selected Examples.
The three methods, power series C, collocation, and inversion integral, described above were applied to several examples and the results compared.

1. The example of a hump used above in Section IX for the solid mirror was also used for the Cassegrain mirror. In this case

$$\begin{aligned} f(x) &= (1-z^2)^2, & z^2 &\leq 1 \\ &= 0, & z^2 &> 1 \\ z &= \frac{x-a}{b}, & a &= 0.65, \quad b = 0.175, \\ R &= 0.125, \end{aligned} \quad (10-41)$$

whence

$$\left. \begin{aligned}
 F(x) &= -2z^3 + \frac{10}{3}z - (1-z^2)^2 \log \left| \frac{1-z}{1+z} \frac{1+x}{1-x} \frac{x-R}{x+R} \right|, \quad z^2 < 1 \\
 &= \pm \frac{4}{3}, \quad z = \pm 1, \\
 &= \frac{2}{3z} + \frac{2}{3z^3} - (z^2-1)^2 \left[\frac{2}{z} + \frac{2}{3z^3} + \log \left(\frac{z-1}{z+1} \right) \right], \quad z^2 > 1
 \end{aligned} \right\} (10-42)$$

This $F(x)$ was calculated at 42 points (20 equal intervals on each side) ($R = 0.125$) and the G matrices used to calculate $f(x)$ at the same 42 points. The results were similar to those in Table II for the solid mirror with the following maximum deviations from the exact answer in Eq. (10-41):

	P.S.(C)	Collocation	Inversion Integral	}	
Deviation	+0.065	+0.033	+0.017		(10-43)
	-0.048	-0.030	-0.009		

It should be noted that the restraints in the power series C solution are that $f(0) = 0$, which is not on the mirror, and $f(x)$ be continuous across the hole. This means that this solution may have to be translated. In fact, a translation of $+0.08$ was used for the power series C solution to get the best results at the hump. Even so, the power series C solution deviated more than the other two solutions. Since $f(\pm R) = 0$ was true in this example, it appears that the restraints of $f(\pm R) = 0$ used in the collocation and inversion integral solutions had essentially no effect.

2. However, in the example of $F(x) = -C = \text{constant}$, the restraints will affect the $f(x)$ solution. With no restraints or no homogeneous solutions

$$F = -C \text{ gives } f(x) = \frac{C}{2(1-R)} x \quad (10-44)$$

On the other hand, with restraints $f(\pm R) = 0$, and

$$f(x) = \frac{C}{2(1-R)} x + C_1 + \frac{C_2}{x} \quad (10-45)$$

it follows that

$$C_1 = 0 \quad , \quad C_2 = - \frac{R^2}{2(1-R)} C \quad , \quad (10-46)$$

whence

$$f(x) = \frac{C}{2(1-R)} \left(x - \frac{R^2}{x} \right) \quad . \quad (10-47)$$

The three methods were used for $F(x) = -35$ or $C = 35$, and $R = 0.125$, whence

$$f = 20x \text{ in Eq. (10-44)} \quad , \quad (10-48)$$

$$f = 20x - \frac{0.3125}{x} \text{ in Eq. (10-47)} \quad (10-49)$$

The power series C method gave $f(x)$ in Eq. (10-48) to three places. The collocation method gave $f(x)$ in Eq. (10-49) to four places. The inversion integral method gave Eq. (10-49) to three places.

The above example of $F(x) = \text{constant}$ has other implications. In paragraph (f) of Section III, it was pointed out that the reference scale for $F(x)$ may be arbitrary so that a constant change in $F(x)$ may be only an apparent rigid body rotation of the mirror and not a real distortion on the line. If an apparent rigid body rotation is occurring, then the collocation and inversion integral methods will show not only the rotation but also an apparent distortion of the form C_2/x , due to the two fixed points on the mirror surface used in these methods. The power series C and Fourier series B methods will show only the rotation, as these methods do not restrain points on the mirror. If the function methods were set up to give two restraints, they would also show the apparent C_2/x term for a constant change in $F(x)$, whether real or apparent.

On the other hand, if a real C_2/x type of distortion occurred in the Cassegrain mirror on some line, it is not evident that any of the methods of solution can detect it, since $F(x) = 0$ in this case. Apparently, some other method of measurement would have to be used to detect such a distortion. However, it seems unlikely that a distortion of the form C_2/x would occur on a mirror with R relatively small. The inherent large stiffness in the circumferential direction would tend to restrain the mirror from such a distortion.

3. The three methods were applied to the example of $F(x) = -35.0$ for $x \leq -0.125$ and $F(x) = 35.0$ for $x \geq 0.125$, a case similar to one used

by Katzoff in Ref. 2. In this case, $f(x)$ is an even function and the C_2/x term in the collocation and inversion methods is zero. After translating the power series C solution, it was found that all three solutions agreed within ± 2 in the third place. The shape of the curve is the same as that in Ref. 2.

4. The three methods were applied to the example of

$$F(x) = \frac{14}{x}, \quad f(x) = \frac{1}{x^2} \quad (10-50)$$

Here $f(\pm 1) = 1.0$ and $f(\pm 0.125) = 64.0$. After translation of all three solutions to give $f(\pm 1) = 1.0$, the maximum deviations from $1/x^2$ for the 42 points were +0.1 and -0.4 for inversion integral, +0.2 and -2.1 for collocation, +4.9 and -1.2, with considerable oscillation, for power series C. As might be expected the power series C did poorly on this negative power function. On the other hand, since $f(x)$ is even in this case, power series C was able to translate and do a reasonable representation of $f(x)$.

5. To further investigate the representation of a negative power deviation by power series C, the example

$$F(x) = \frac{14}{x^2}, \quad f(x) = \frac{1}{x^3} \quad (10-51)$$

was solved. Since this is an odd function, and power series C must be 0 at $x = 0$, it is a difficult function to represent, going from $f(1) = 1.0$ to $f(0.125) = 512.0$. As expected, it did a very poor job, giving $f(1) = 126$, $f(0.125) = 472$, $f(0.16875) = 510$ instead of 208.1, $f(0.3) = 370.0$ instead of 37.0, etc. Thus, it would appear that the function methods, both power series and Fourier series, cannot handle odd negative power type deviations. Of course, if desired, negative power terms could be added to the power series methods so that they could represent these for the Cassegrain mirror.

This example 5 in Eq. (10-51) takes the form

$$F(x) = \frac{14}{x^2}, \quad f(x) = \frac{1}{x^3} - \frac{64}{x} \quad (10-52)$$

when the points $x = \pm R$ are restrained in the collocation and inversion integral methods. In this particular example, the $C_2 = -64$ would be much smaller ($C_2 = -1$) if the end points $x = \pm 1$ were restrained instead

of the points at the edges of the hole. However, since the G matrix for the inversion integral was set up for the edges $x = \pm R$ restrained, Eq. (10-52) was compared to the inversion integral solution. The maximum deviation was at $x = \pm 0.16875$, where $f(x) = \mp 183$ instead of ∓ 172 in Eq. (10-52). By changing $C_2 = -64$ to $C_2 = -65.9$, the maximum deviation was less than ∓ 1.0 . This indicates there are slight errors in the approximations for the elements $G_o\left(\frac{M}{2}, \frac{M}{2}\right)$ and $G_o\left(\frac{M}{2} + 1, \frac{M}{2} + 1\right)$ in Eq. (10-37), which are introduced as a C/x error through Eq. (10-40) for the restraint conditions.

The conclusion is that example 5, Eqs. (10-51) and (10-52), is a rough shape to calculate numerically. It is also unlikely that the mirror could experience such a deformation. The power series can not get $f(x)$ in Eq. (10-51), but the inversion integral gets the $f(x)$ in Eq. (10-52) satisfactorily.

G Matrices for Cassegrain Mirror. To better understand why the power series C solution was very poor in some of the examples considered, the G matrices for the three methods were examined. Figure 10-1 shows a graph of row 33 for the three methods. The inversion integral row 33 in Fig. 10-1 is nearly the same as that in Fig. 9-4 for the solid mirror case. The collocation row 33 in Fig. 10-1 is quite different from Fig. 9-4, having much less oscillation. In fact, the collocation graph follows the inversion integral quite closely, except near column number 33 where it overemphasizes the local effect for point 33. Apparently, the restraint of two points in this case as compared to one point at the origin in the solid mirror case produced a damping effect on the collocation G. matrix. The power series C row 33 in Fig. 10-1 is radically different from Fig. 9-4, having much larger oscillations and failing to follow the inversion integral around column 33. This difference, which occurs in all the rows of the G matrix, explains why power series C does a poor job on certain types of functions in the hole case.

The reason why the power series C method has the large change in the G matrix from the solid mirror to the Cassegrain mirror appears to be in the restraints for the hole case. No points are fixed on the mirror. Only the origin, which is off the mirror, is fixed. With no points being specified in the hole, the power series C functions appear to be insufficiently defined to produce the proper G matrix. Also, it appears that the frequency of the oscillation in Fig. 10-1 is determined by the hole size, rather than the mirror size. This may indicate that the number of points and the value of R, or the ratio between R and interval size, affect the behavior of the G matrix for the power series C method as well as for other function methods.

Evaluation of Methods for Cassegrain Mirror. From the above examples and discussion of the G matrices, an evaluation of the three methods of solution used for the hole case is as follows:

For a specified $\eta(x)$ take

$$\left. \begin{aligned} g(x_i) &= 2\pi\eta(x_i) \quad , \\ S_i &= \sin g(x_i) \quad , \\ C_i &= \cos g(x_i) \quad , \\ [T_i] &= [A][S_i] \quad , \quad \text{and} \\ [U_i] &= [A][C_i] \quad , \end{aligned} \right\} \quad (11-3)$$

where the matrix A is the numerical integration matrix in Eq. (10-36) with rows 1, M/2, (M/2) + 1, M omitted. Since the integrals become infinite at the edge points, F(x) at $x = \pm 1$ and $x = \pm R$ cannot be calculated. However, these points are included in the numerical integration for F(x_i) at all interior points. At x_i, Eq. (11-2) gives

$$\begin{aligned} F(x_i) &= U_i^2 - \log^2 \left| \frac{1 - x_i}{1 + x_i} \frac{x_i + R}{x_i - R} \right| \\ &\quad + 2\pi S_i U_i - 2\pi C_i T_i + T_i^2 \end{aligned} \quad (11-4)$$

Assume g(x) to have the form of Eq. (9-2) as used in the linear case above

$$\left. \begin{aligned} g(x) &= p(1-z^2)^2 \quad , \quad z^2 \leq 1; \\ &= 0 \quad , \quad z^2 > 1; \quad \text{and} \\ z &= \frac{x-a}{b} \quad , \quad a = 0.6 \quad , \quad b = 0.2 \quad , \\ R &= 5/41 \quad , \quad \Delta x = 2/41 \quad , \end{aligned} \right\} \quad (11-5)$$

where p is a factor for the magnitude of the error. Note that

$$p = (2\pi)(\text{max. error in wavelengths}) \quad (11-6)$$

or

$$\eta_{\text{max}} = \text{max. error in wavelengths} = p/2\pi \quad . \quad (11-7)$$

For the linear case used above $p = 1/2\pi$ and this case was used in Eq. (11-4) to compare to the linear results. Figure 11-1 shows the comparison for $F(x)$ using 38-point numerical integration. The linear numerical integration and the nonlinear numerical are quite close.

Figure 11-2 shows results of Eq. (11-4) for several values of p ; i.e.,

$$\left. \begin{aligned}
 p &= \frac{1}{2\pi} \quad , \quad \eta_{\max} = \frac{1}{4\pi^2} \sim 0.025 \quad , \quad \text{linear;} \\
 p &= \frac{10}{2\pi} \quad , \quad \eta_{\max} = \frac{10}{4\pi^2} \sim 0.25; \\
 p &= 2\pi \quad , \quad \eta_{\max} = 1; \quad \text{and} \\
 p &= 6.25\pi \quad , \quad \eta_{\max} = 3.12 \quad .
 \end{aligned} \right\} \quad (11-8)$$

It can be concluded that large changes occur in $F(x)$ in the neighborhood of a $f(x)$ hump.

For large values of p , $g(x)$ is large and $\sin g(x)$ and $\cos g(x)$ will oscillate with many cycles over the non-zero range of $g(x)$. For the cases in Eq. (11-8) and Fig. 11-2, the approximate number of cycles in $\sin g(x)$ and $\cos g(x)$ for $0.4 \leq x \leq 0.8$ is 1/2 for $p = 1/2 \pi$ and $p = 10/2\pi$, 2 for $p = 2\pi$, 6 for $p = 6.25\pi$. These cycles are unequal in width, with the smallest width for $p = 6.25\pi$ being $\Delta x = 0.045$. Since the interval used for the numerical integration in Fig. 11-2 was $\Delta x \approx 0.05$, it is evident that the results for the $p = 6.25\pi$ case may not be very good. Either a smaller interval must be used or the numerical integration modified.

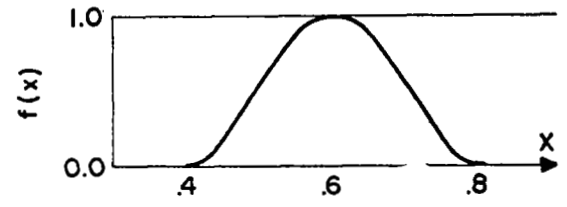
To investigate this numerical integration difficulty, $g(x)$ was approximated over any interval $x_i - \frac{\Delta x}{2} \leq x \leq x_i + \frac{\Delta x}{2}$ by

$$g(x) = g(x_i) + m(x-x_i) \quad , \quad (11-9)$$

where

$$m = \frac{g\left(x_i + \frac{\Delta x}{2}\right) - g\left(x_i - \frac{\Delta x}{2}\right)}{\Delta x} \quad (11-10)$$

If the average of $t - x$ in Eq. (11-2) is used for the interval Δt , then $\sin g(t)$ and $\cos g(t)$ can be integrated across the interval using the approximation in Eq. (11-9). The results are



78

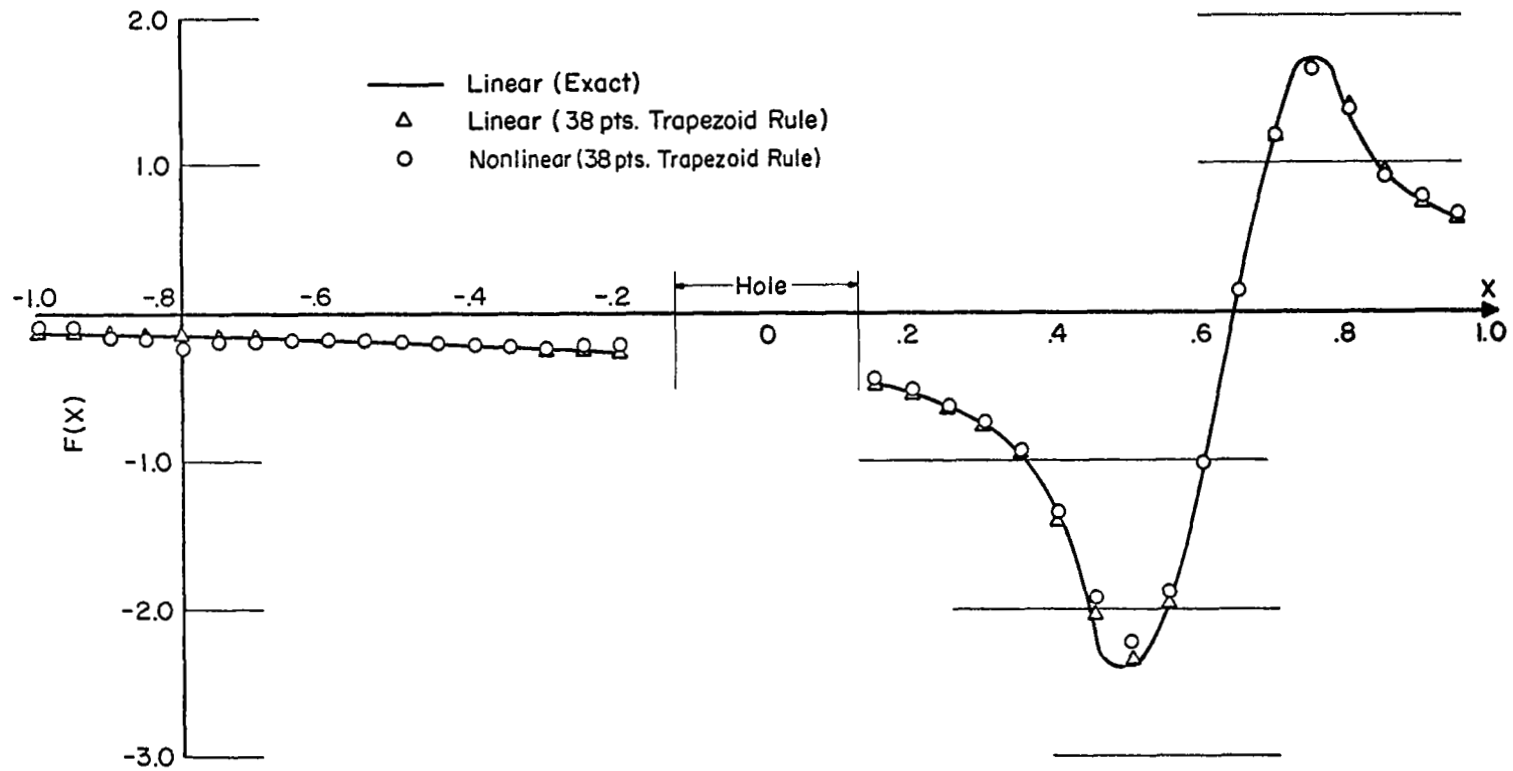


Fig. 11-1. Numerical Integration (Nonlinear Case), Comparison to Linear Case

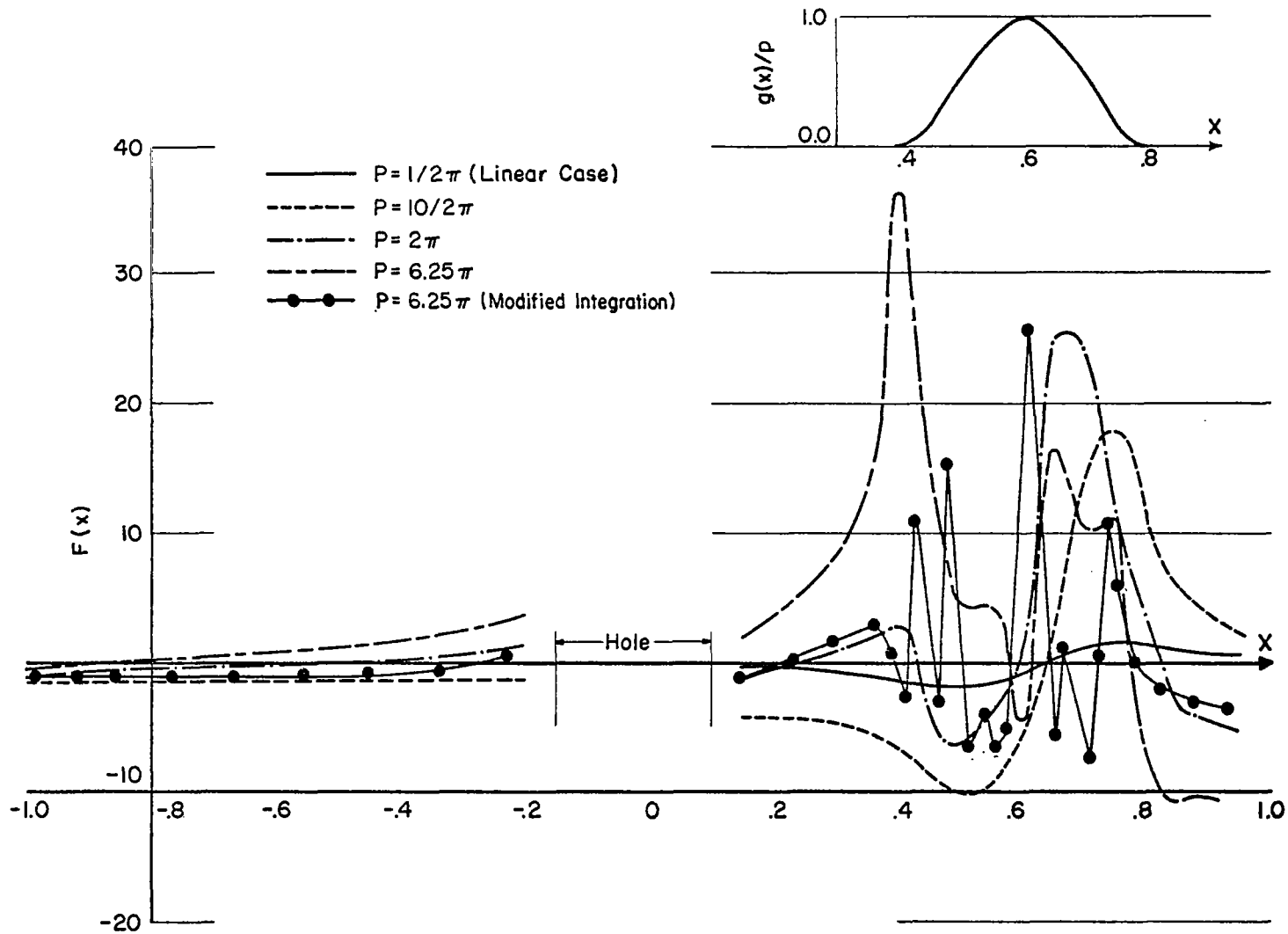


Fig. 11-2. Numerical Integration (Nonlinear Case)

$$\begin{aligned}
\int_{t_i - (\Delta t/2)}^{t_i + (\Delta t/2)} \sin g(t) dt &= - \frac{\cos g(t)}{m} \Big|_{t_i - (\Delta t/2)}^{t_i + (\Delta t/2)} \\
&= - \Delta t \frac{\left[\cos g\left(t_i + \frac{\Delta t}{2}\right) - \cos g\left(t_i - \frac{\Delta t}{2}\right) \right]}{g\left(t_i + \frac{\Delta t}{2}\right) - g\left(t_i - \frac{\Delta t}{2}\right)} \\
&= (\Delta t) D_i \quad , \qquad (11-11)
\end{aligned}$$

$$\begin{aligned}
\int_{t_i - (\Delta t/2)}^{t_i + (\Delta t/2)} \cos g(t) dt &= \frac{\Delta t \left[\sin g\left(t_i + \frac{\Delta t}{2}\right) - \sin g\left(t_i - \frac{\Delta t}{2}\right) \right]}{g\left(t_i + \frac{\Delta t}{2}\right) - g\left(t_i - \frac{\Delta t}{2}\right)} \\
&= (\Delta t) E_i \quad . \qquad (11-12)
\end{aligned}$$

The term D_i replaces S_i in the calculation of T_i in Eq. (11-3) and E_i replaces C_i in the calculation of U_i . With these terms, the results for the $p = 1/2\pi$, $10/2\pi$, and 2π cases are essentially the same. However, for the $p = 6.25\pi$ case, the peak at $x = 0.4$ is about one-half as large and more cycles appear to be present. When twice as many intervals are used with the D_i and E_i terms, the $p = 6.25\pi$ case shows about six cycles in $F(x)$ of various amplitudes and occurring in the range of the $g(x)$ hump. See $p = 6.25\pi$ (modified integration) case in Fig. 11-2. A similar cyclic result for $F(x)$ was obtained for $p = 100$.

From these results it would appear that, if $F(x)$ shows a cyclic shape in a region, then there is a large deviation in the mirror in that region.

In Section III for the linear case it was found a linear $f(x) = C_1 x$ produces a constant $F(x) = -2C_1$. Two cases for the nonlinear equation were calculated by Eq. (11-4) with

$$(a) \quad g(x) = \frac{10}{2\pi} x \quad \text{and} \quad (b) \quad g(x) = -\frac{10}{2\pi} x \qquad (11-13)$$

which is equivalent to $\eta_{\max} = \pm 1/4$ at the ends. For case (a), $F(x)$ varied from -8.0 at edges of the hole to -14.8 at the ends, being approximately constant over the middle half of the mirror. For case (b), $F(x)$ varied from $+19.6$ at edges of the hole to $+4.3$ at the ends, being approximately constant over the middle half of the mirror.

XIII - SCALE FACTOR PROBLEMS

Above, $F(x) = I - I_0$ is assumed known. I_0 is calculated for the perfect mirror. I is measured on the actual mirror. If K converts I to scale of I_0 , then

$$F(x) = \frac{I}{K} - I_0 \quad (12-1)$$

It appears that K depends on the intensity of the light source and on the instrumentation to read I . To calibrate the perfect mirror with a given light of intensity, Q_c .

$$F(x) = 0 \quad , \quad K_c = \frac{\int_L I_p dt}{\int_L I_0 dt} \quad (12-2)$$

For a different light intensity Q

$$K = \frac{Q}{Q_c} K_c \quad (12-3)$$

Thus, if K_c can be determined for the finished mirror (as perfect as possible) using the specified instrumentation and known light Q_c , then if the light Q can be determined, Eq. (12-3) would seem to hold, whence

$$F = \frac{Q_c}{Q} \frac{I}{K_c} - I_0 \quad (12-4)$$

A procedure to check K may be based on Eq. (12-1). If

$$F(x) = F_1(x) - C$$

$$\int_L F_1(x) dx = 0 \quad , \quad C = \frac{\int_L F(x) dx}{2(1-R)} \quad (12-5)$$

then from Section III, a rotation of the mirror through a slope change of $-C/2(1-R)$ will change I and make the new F be F_1 . Thus a check K is (I_R read after rotation),

$$K = \frac{\int_L I_R dx}{\int_L I_0 dx} \quad (12-6)$$

It may be possible to determine K directly by giving a small known rotation to the mirror or an equivalent displacement of the knife-edge and measuring the change in I at several points. Since the change in $F(x)$ can be calculated (linear case) as $-2C_1$, C_1 is slope, then

$$K = \frac{(\Delta I)_{\text{meas}}}{(\Delta I)_{\text{cal}}} \quad (12-7)$$

at each point. If ΔI is constant, then the K may be satisfactory.

It should be noted that an error in the origin for I shows as a rotation of $f(x)$ and also an error in K shows a rotation in $f(x)$. Thus, if $f(x)$ shows a large rotation, it probably means I and K are not compatible, or the knife-edge is not central.

Finally, in the Eqs. (12-2) and (12-6)

$$\left. \begin{aligned} \int_{-1}^1 I_0 dx &= \frac{8}{3} \pi^2, \quad \text{no hole,} \\ &= 2\pi^2(1-R) + 2 \int_R^1 \log^2 \left| \frac{1-x}{1+x} \frac{x+R}{x-R} \right| dx, \end{aligned} \right\} \quad (12-8)$$

for hole of radius R.

XIII - CONCLUSIONS AND RECOMMENDATIONS

The linear integral equation for the Foucault test of a mirror, solid or Cassegrain type, can be solved by several different methods. Since the methods of solution are approximate due to numerical integration and/or finite function representations, they are not unique. Although the methods may agree on results for some examples, they disagree on other examples. The inversion integral method appears to cover the largest range of possible problems with good results for both the solid and Cassegrain mirrors. The collocation method does well on many examples, particularly for the Cassegrain mirror, but it fails for functions with discontinuities. The function methods, power series and Fourier series, do well on some functions but have various deficiencies, particularly for the Cassegrain mirror. The iteration method is very poor and is not recommended.

There appears to be several possible procedures for calibrating and scaling the input data for the integral equation solutions. The simplest procedure may be to give the knife-edge a small displacement and measure the change in the light intensity. Since the change can be calculated in the linear case, the scaling can be made by comparing the measured and calculated results.

For various assumed functions for the errors on the mirror, the light distribution on the mirror can be calculated from the nonlinear equation by numerical integration. Large changes occur in the light intensity in the neighborhood of a local surface deviation, whether linear or nonlinear. However, for a large nonlinear deviation, large changes may occur in other regions somewhat removed from the local deviation.

It is recommended that further investigation of the nonlinear equation be conducted, particularly with regard to

- (a) input of a nonlinear $F(x)$ solution into the linear equation and comparison of solution to original assumed $f(x)$ in the nonlinear equation;
- (b) scaling and calibration in the nonlinear case; and
- (c) possible iteration solutions of the nonlinear equation.

REFERENCES

1. Linfoot, E. H.: Recent Advances in Optics. Clarendon Press (Oxford), 1958.
2. Katzoff, Samuel: Quantitative Determination of Optical Imperfections by Mathematical Analysis of the Foucault Knife-Edge Test Pattern. NASA TN D-6119, 1971.
3. Kopal, Zdenek: Numerical Analysis. John Wiley & Sons, Inc., 1955.
4. Westlake, J. R.: Handbook of Numerical Matrix Inversion and Solution of Linear Equations. John Wiley & Sons, Inc., 1968.
5. Glauert, H.: The Elements of Aerofoil and Airscrew Theory. Second ed., Cambridge Univ. Press, 1948, pp. 92-93.
6. Muskhelishvili, N. I. (J. R. M. Radok, Transl.): Singular Integral Equations. Second ed., P. Noordhoff, Ltd. (Groningen), 1953.
7. Niedenfuhr, F. W.; Leissa, Arthur W.; and Lo, C. C.: A Study of the Point Matching Method as Applied to Thermally and Transversely Loaded Plates and Other Boundary Value Problems. AFFDL-TR-64-159, U. S. Air Force, Oct. 1964. (Available from DDC as AD 610 146.)

APPENDIX A

Approximation in the Sense of Least Squares for a System of Simultaneous Equations

Consider the system of simultaneous equations

$$\sum_{j=1}^N a_{ij}x_j = b_i \quad , \quad i = 1, 2, \dots, M \quad (A-1)$$

or in matrix form

$$AX = B \quad (A-2)$$

If $M = N$, the A matrix is square and, if it is nonsingular, the system of equations can be solved directly.

If $M > N$, the A matrix is rectangular, as there are more equations than unknowns. This system of equations can be solved in the sense of least squares in the following manner (see p. 8 of Ref. 7).

Let \bar{x}_j be a column vector that does not identically satisfy Eq. (A-1), but gives a residual error vector e_i in

$$\sum_{j=1}^N a_{ij}\bar{x}_j - b_i = e_i \quad , \quad i = 1, 2, \dots, M \quad (A-3)$$

Now

$$\sum_{i=1}^M e_i^2 = \sum_{i=1}^M \left(\sum_{j=1}^N a_{ij}\bar{x}_j - b_i \right) \left(\sum_{k=1}^N a_{ik}\bar{x}_k - b_i \right) \quad (A-4)$$

and for a minimum

$$\begin{aligned} \frac{\partial}{\partial \bar{x}_p} \left(\sum_{i=1}^M e_i^2 \right) &= \sum_{i=1}^M a_{ip} \left(\sum_{k=1}^N a_{ik}\bar{x}_k - b_i \right) \\ &\quad + \sum_{i=1}^M a_{ip} \left(\sum_{j=1}^N a_{ij}\bar{x}_j - b_i \right) \\ &= 2 \sum_{i=1}^M a_{ip} \left(\sum_{j=1}^N a_{ij}\bar{x}_j - b_i \right) = 0 \end{aligned} \quad (A-5)$$

$$p = 1, 2, \dots, M$$

This set of equations for a minimum of the square of the error can be written in matrix form as

$$2[A^T(AX - B)] = 0$$

or

$$A^TAX = A^TB \tag{A-6}$$

Since A^TA is a square matrix, symmetric, positive diagonal elements, and nonsingular, it can be inverted to give

$$X = [A^TA]^{-1}A^TB \tag{A-7}$$

as the solution of the system in the sense of least squares.

As a simple example, consider the system

$$2X_1 + 3X_2 = 0$$

$$2X_1 - 4X_2 = 1$$

$$X_1 - X_2 = 0$$

Equation (A-7) gives $X_1 = 8/45$ and $X_2 = -6/45$ with the residuals

$$e_1 = -\frac{2}{45}, \quad e_2 = -\frac{5}{45}, \quad e_3 = \frac{14}{45},$$

$$e_1^2 + e_2^2 + e_3^2 = \frac{1}{9}$$

None of the three equations are satisfied exactly, but the X_1 and X_2 values are the best values in the sense of least squares. Any other values of X_1 and X_2 will give

$$e_1^2 + e_2^2 + e_3^2 > \frac{1}{9}$$

It is evident that if one or more of the equations have mistakes in them, these mistakes will affect all the results and residuals. The mistakes or errors are spread out over all the results. Such an effect

can occur if incompatible conditions or restrictions are present in the system of equations. For example, suppose the third equation in the simple example above is

$$1000X_1 - X_2 = 0.$$

Then, there results from Eq. (A-7) $X_1 \sim -4/25,000$ and $X_2 \sim -4/25$. Thus the equation with the large change is still approximately satisfied, but the solution is completely changed.



APPENDIX B

Evaluation of an Integral in Fourier Series Solution*

The integral in Eq. (5-11)

$$\frac{\pi^2}{4} K_{mn} = \int_0^\pi \log\left(\frac{\sin \theta}{1 + \cos \theta}\right) \sin n\theta \cos m\theta \, d\theta \quad (B-1)$$

can be written as

$$\frac{\pi^2}{2} K_{mn} = \int_0^\pi \log\left(\frac{\sin \theta}{1 + \cos \theta}\right) [\sin(m+n)\theta - \sin(m-n)\theta] \, d\theta \quad (B-2)$$

Now consider the integral

$$I_{2i} = \int_0^\pi \log\left(\frac{\sin \theta}{1 + \cos \theta}\right) \sin 2i\theta \, d\theta \quad , \quad i = 1, 2, 3, \dots, N \quad (B-3)$$

Introduce the constant $1/2i$ and integrate by parts to get

$$\begin{aligned} I_{2i} &= \frac{1 - \cos 2i\theta}{2i} \log \frac{\sin \theta}{1 + \cos \theta} \Big|_0^\pi - \frac{1}{2i} \int_0^\pi \frac{1 - \cos 2i\theta}{\sin \theta} \, d\theta \\ &= - \frac{1}{2i} \int_0^\pi \frac{1 - \cos 2i\theta}{\sin \theta} \, d\theta \end{aligned} \quad (B-4)$$

Consider the difference form

$$\begin{aligned} 2iI_{2i} - (2i-2)I_{2i-2} &= \int_0^\pi \frac{\cos 2i\theta - \cos (2i-2)\theta}{\sin \theta} \, d\theta \\ &= - 2 \int_0^\pi \sin(2i-1)\theta \, d\theta \\ &= - \frac{2}{2i-1} [1 - \cos (2i-1)\pi] \\ &= - \frac{4}{2i-1} \end{aligned}$$

*Thanks are due to Dr. Keith Stewartson, Visiting Professor at The Ohio State University, Summer 1969, and Goldsmid Professor of Mathematics and Joint Head of Mathematics Department, University of London, for this integration.

Since $I_0 = 0$, it follows that

$$\begin{aligned}
 I_0 &= 0 \quad , \\
 I_2 &= -2 \quad , \\
 I_4 &= -\frac{4}{2(2)} \left[\frac{1}{3} + \frac{1}{1} \right] = -\frac{4}{3} \\
 &\vdots \\
 I_{2i} &= -\frac{2}{i} \sum_{k=1}^i \frac{1}{2k-1} \quad (B-6)
 \end{aligned}$$

Put this result in Eq. (B-6) into Eq. (B-2) and use $2i = m + n$ or $m - n$ to get

$$K_{mn} = -\frac{8}{\pi^2(m+n)} \sum_{k=1}^{(m+n)/2} \frac{1}{2k-1} + \frac{8}{\pi^2(m-n)} \sum_{k=1}^{|(m-n)/2|} \frac{1}{2k-1} \quad (B-7)$$

where $m + n$ is even. If $m = n$, Eq. (B-2) gives

$$K_{mm} = -\frac{4}{\pi^2 m} \sum_{k=1}^m \frac{1}{2k-1} \quad , \quad m = n \quad (B-8)$$

For $m + n$ odd, $\sin(m+n)\theta$ is even in the interval 0 to π . Since the log term in Eq. (B-2) is odd on the interval 0 to π , the value of the integral is zero for $m + n$ odd, or

$$K_{mn} = 0 \quad , \quad \text{for } m + n \text{ odd} \quad . \quad (B-9)$$

APPENDIX C

G Matrix for Inversion Integral Method

G MATRIX

ROW 1	0.20320	0.04411	0.02977	0.02417	0.02123	0.01951	0.01848
	0.01790	0.01766	0.01772	0.01805	0.01869	0.01968	0.02112
	0.02322	0.02632	0.03114	0.03937	0.05606	0.15715	0.00507
	-0.14701	-0.04587	-0.02910	-0.02076	-0.01579	-0.01250	-0.01017
	-0.00843	-0.00709	-0.00602	-0.00514	-0.00442	-0.00380	-0.00326
	-0.00279	-0.00236	-0.00196	-0.00157	-0.00113	-0.00042	
ROW 2	-0.02500	0.15897	0.08337	0.03444	0.02689	0.02317	0.02106
	0.01984	0.01918	0.01894	0.01906	0.01953	0.02039	0.02174
	0.02376	0.02679	0.03156	0.03974	0.05639	0.15745	0.00533
	-0.14677	-0.04565	-0.02890	-0.02058	-0.01563	-0.01235	-0.01003
	-0.00831	-0.00697	-0.00591	-0.00505	-0.00433	-0.00372	-0.00319
	-0.00273	-0.00230	-0.00191	-0.00153	-0.00110	-0.00041	
ROW 3	-0.00750	-0.06065	0.16187	0.09606	0.03821	0.02926	0.02494
	0.02255	0.02120	0.02050	0.02031	0.02056	0.02125	0.02247
	0.02438	0.02733	0.03203	0.04016	0.05676	0.15778	0.00563
	-0.14650	-0.04541	-0.02868	-0.02038	-0.01545	-0.01219	-0.00989
	-0.00817	-0.00685	-0.00580	-0.00495	-0.00424	-0.00364	-0.00312
	-0.00266	-0.00225	-0.00186	-0.00149	-0.00107	-0.00039	
ROW 4	-0.00472	-0.01875	-0.07741	0.15901	0.10615	0.04146	0.03141
	0.02662	0.02402	0.02259	0.02192	0.02184	0.02230	0.02334
	0.02512	0.02797	0.03258	0.04063	0.05718	0.15815	0.00596
	-0.14620	-0.04514	-0.02844	-0.02017	-0.01526	-0.01201	-0.00973
	-0.00803	-0.00672	-0.00568	-0.00484	-0.00414	-0.00355	-0.00304
	-0.00259	-0.00219	-0.00181	-0.00145	-0.00104	-0.00038	
ROW 5	-0.00333	-0.01176	-0.02382	-0.08881	0.15386	0.11462	0.04434
	0.03341	0.02826	0.02551	0.02407	0.02349	0.02361	0.02441
	0.02601	0.02872	0.03322	0.04119	0.05766	0.15858	0.00633
	-0.14587	-0.04485	-0.02818	-0.01993	-0.01504	-0.01182	-0.00955
	-0.00787	-0.00658	-0.00555	-0.00472	-0.00404	-0.00346	-0.00296
	-0.00252	-0.00212	-0.00176	-0.00140	-0.00101	-0.00037	
ROW 6	-0.00250	-0.00827	-0.01489	-0.02719	-0.09766	0.14748	0.12195
	0.04698	0.03533	0.02990	0.02708	0.02570	0.02530	0.02574
	0.02709	0.02961	0.03397	0.04183	0.05822	0.15906	0.00675
	-0.14550	-0.04452	-0.02789	-0.01967	-0.01481	-0.01161	-0.00936
	-0.00770	-0.00642	-0.00542	-0.00460	-0.00393	-0.00336	-0.00287
	-0.00244	-0.00205	-0.00170	-0.00135	-0.00097	-0.00036	
ROW 7	-0.00194	-0.00618	-0.01042	-0.01692	-0.02972	-0.10486	0.14033
	0.12842	0.04946	0.03721	0.03159	0.02878	0.02755	0.02746
	0.02845	0.03071	0.03488	0.04259	0.05886	0.15961	0.00724
	-0.14508	-0.04415	-0.02756	-0.01938	-0.01455	-0.01138	-0.00915
	-0.00751	-0.00626	-0.00527	-0.00447	-0.00380	-0.00325	-0.00277
	-0.00235	-0.00198	-0.00164	-0.00130	-0.00094	-0.00034	

ROW 8	-0.00155	-0.00478	-0.00774	-0.01178	-0.01840	-0.03170	-0.11086
	0.13268	0.13424	0.05183	0.03912	0.03340	0.03069	0.02975
	0.03019	0.03208	0.03599	0.04350	0.05963	0.16026	0.00779
	-0.14460	-0.04373	-0.02719	-0.01905	-0.01426	-0.01112	-0.00892
	-0.00731	-0.00607	-0.00510	-0.00432	-0.00367	-0.00313	-0.00267
	-0.00226	-0.00190	-0.00157	-0.00125	-0.00090	-0.00033	
ROW 9	-0.00125	-0.00378	-0.00595	-0.00870	-0.01274	-0.01951	-0.03326
	-0.11590	0.12470	0.13953	0.05416	0.04111	0.03542	0.03295
	0.03251	0.03384	0.03737	0.04462	0.06055	0.16103	0.00844
	-0.14404	-0.04325	-0.02677	-0.01869	-0.01394	-0.01084	-0.00867
	-0.00708	-0.00587	-0.00492	-0.00416	-0.00353	-0.00301	-0.00256
	-0.00217	-0.00182	-0.00150	-0.00119	-0.00085	-0.00031	
ROW 10	-0.00102	-0.00303	-0.00468	-0.00665	-0.00934	-0.01341	-0.02032
	-0.03446	-0.12011	0.11653	0.14443	0.05653	0.04329	0.03776
	0.03576	0.03619	0.03915	0.04601	0.06167	0.16195	0.00921
	-0.14339	-0.04269	-0.02629	-0.01827	-0.01357	-0.01052	-0.00839
	-0.00683	-0.00565	-0.00473	-0.00399	-0.00338	-0.00287	-0.00244
	-0.00206	-0.00173	-0.00142	-0.00113	-0.00081	-0.00030	
ROW 11	-0.00083	-0.00245	-0.00372	-0.00518	-0.00708	-0.00975	-0.01386
	-0.02088	-0.03533	-0.12359	0.10826	0.14903	0.05903	0.04577
	0.04064	0.03948	0.04152	0.04781	0.06307	0.16307	0.01013
	-0.14263	-0.04205	-0.02574	-0.01780	-0.01316	-0.01016	-0.00808
	-0.00656	-0.00541	-0.00451	-0.00380	-0.00321	-0.00272	-0.00231
	-0.00195	-0.00163	-0.00134	-0.00106	-0.00076	-0.00028	
ROW 12	-0.00068	-0.00199	-0.00298	-0.00408	-0.00546	-0.00732	-0.00998
	-0.01410	-0.02120	-0.03588	-0.12637	0.10000	0.15347	0.06179
	0.04877	0.04442	0.04485	0.05020	0.06487	0.16448	0.01126
	-0.14171	-0.04128	-0.02510	-0.01725	-0.01269	-0.00975	-0.00772
	-0.00625	-0.00514	-0.00428	-0.00359	-0.00303	-0.00256	-0.00217
	-0.00183	-0.00153	-0.00125	-0.00099	-0.00071	-0.00026	
ROW 13	-0.00056	-0.00160	-0.00238	-0.00322	-0.00425	-0.00557	-0.00739
	-0.01002	-0.01413	-0.02126	-0.03611	-0.12848	0.09187	0.15790
	0.06502	0.05264	0.04983	0.05354	0.06727	0.16629	0.01267
	-0.14058	-0.04036	-0.02434	-0.01661	-0.01215	-0.00929	-0.00732
	-0.00590	-0.00484	-0.00401	-0.00336	-0.00283	-0.00239	-0.00202
	-0.00170	-0.00142	-0.00116	-0.00092	-0.00065	-0.00024	
ROW 14	-0.00045	-0.00129	-0.00189	-0.00254	-0.00330	-0.00427	-0.00554
	-0.00731	-0.00989	-0.01395	-0.02106	-0.03597	-0.12986	0.08402
	0.16255	0.06910	0.05813	0.05856	0.07064	0.16870	0.01447
	-0.13918	-0.03924	-0.02342	-0.01585	-0.01152	-0.00875	-0.00687
	-0.00551	-0.00450	-0.00372	-0.00310	-0.00260	-0.00219	-0.00185
	-0.00155	-0.00129	-0.00106	-0.00083	-0.00059	-0.00022	
ROW 15	-0.00036	-0.00102	-0.00149	-0.00198	-0.00255	-0.00325	-0.00416
	-0.00537	-0.00707	-0.00957	-0.01354	-0.02056	-0.03542	-0.13044
	0.07666	0.16781	0.07474	0.06693	0.07568	0.17207	0.01689
	-0.13737	-0.03784	-0.02231	-0.01495	-0.01077	-0.00813	-0.00634
	-0.00506	-0.00411	-0.00339	-0.00281	-0.00236	-0.00198	-0.00166
	-0.00139	-0.00116	-0.00095	-0.00074	-0.00053	-0.00019	

ROW 16

-0.00028 -0.00079 -0.00115 -0.00151 -0.00193 -0.00244 -0.00308
 -0.00392 -0.00505 -0.00664 -0.00903 -0.01285 -0.01968 -0.03433
 -0.13004 0.07019 0.17440 0.08366 0.08409 0.17713 0.02026
 -0.13496 -0.03604 -0.02091 -0.01384 -0.00987 -0.00739 -0.00572
 -0.00454 -0.00367 -0.00301 -0.00249 -0.00208 -0.00174 -0.00146
 -0.00122 -0.00101 -0.00082 -0.00065 -0.00046 -0.00017

ROW 17

-0.00021 -0.00059 -0.00085 -0.00112 -0.00142 -0.00177 -0.00222
 -0.00278 -0.00353 -0.00456 -0.00602 -0.00822 -0.01181 -0.01831
 -0.03251 -0.12832 0.06534 0.18405 0.10091 0.18557 0.02533
 -0.13158 -0.03364 -0.01912 -0.01246 -0.00877 -0.00650 -0.00499
 -0.00394 -0.00316 -0.00258 -0.00213 -0.00177 -0.00147 -0.00123
 -0.00103 -0.00085 -0.00069 -0.00054 -0.00038 -0.00014

ROW 18

-0.00015 -0.00041 -0.00060 -0.00078 -0.00098 -0.00122 -0.00151
 -0.00188 -0.00236 -0.00299 -0.00387 -0.00514 -0.00708 -0.01030
 -0.01626 -0.02961 -0.12457 0.06382 0.20182 0.20244 0.03377
 -0.12652 -0.03027 -0.01673 -0.01068 -0.00740 -0.00542 -0.00412
 -0.00322 -0.00257 -0.00208 -0.00171 -0.00141 -0.00117 -0.00098
 -0.00081 -0.00067 -0.00054 -0.00043 -0.00030 -0.00011

ROW 19

-0.00009 -0.00026 -0.00037 -0.00048 -0.00061 -0.00075 -0.00092
 -0.00114 -0.00141 -0.00177 -0.00226 -0.00294 -0.00394 -0.00549
 -0.00813 -0.01316 -0.02491 -0.11712 0.07071 0.30366 0.05066
 -0.11809 -0.02523 -0.01339 -0.00830 -0.00564 -0.00406 -0.00305
 -0.00236 -0.00187 -0.00150 -0.00123 -0.00101 -0.00084 -0.00069
 -0.00057 -0.00047 -0.00038 -0.00030 -0.00021 -0.00008

ROW 20

-0.00004 -0.00012 -0.00018 -0.00023 -0.00028 -0.00035 -0.00043
 -0.00052 -0.00064 -0.00080 -0.00100 -0.00128 -0.00169 -0.00229
 -0.00325 -0.00494 -0.00830 -0.01673 -0.10091 0.16196 0.15198
 -0.10122 -0.01682 -0.00837 -0.00498 -0.00329 -0.00232 -0.00172
 -0.00131 -0.00103 -0.00082 -0.00066 -0.00054 -0.00045 -0.00037
 -0.00030 -0.00025 -0.00020 -0.00016 -0.00011 -0.00004

ROW 21

0.0 0.0 0.0 0.0 0.0 0.0 0.0
 0.0 0.0 0.0 0.0 0.0 0.0 0.0
 0.0 0.0 0.0 0.0 0.0 0.0 0.0
 0.0 0.0 0.0 0.0 0.0 0.0 0.0
 0.0 0.0 0.0 0.0 0.0 0.0 0.0
 0.0 0.0 0.0 0.0 0.0 0.0 0.0

ROW 22

0.00004 0.00011 0.00016 0.00020 0.00025 0.00030 0.00037
 0.00045 0.00054 0.00066 0.00082 0.00103 0.00131 0.00172
 0.00232 0.00329 0.00498 0.00837 0.01682 0.10122 -0.15198
 -0.16196 0.10091 0.01673 0.00830 0.00494 0.00325 0.00229
 0.00169 0.00128 0.00100 0.00080 0.00064 0.00052 0.00043
 0.00035 0.00028 0.00023 0.00018 0.00012 0.00004

ROW 23

0.00008 0.00021 0.00030 0.00038 0.00047 0.00057 0.00069
 0.00084 0.00101 0.00123 0.00150 0.00187 0.00236 0.00305
 0.00406 0.00564 0.00830 0.01339 0.02523 0.11809 -0.05066
 -0.30366 -0.07071 0.11712 0.02491 0.01316 0.00813 0.00549
 0.00394 0.00294 0.00226 0.00177 0.00141 0.00114 0.00092
 0.00075 0.00061 0.00048 0.00037 0.00026 0.00009

ROW 24

0.00011	0.00030	0.00043	0.00054	0.00067	0.00081	0.00098
0.00117	0.00141	0.00171	0.00208	0.00257	0.00322	0.00412
0.00542	0.00740	0.01068	0.01673	0.03027	0.12652	-0.03377
-0.20244	-0.20182	-0.06382	0.12457	0.02961	0.01626	0.01030
0.00708	0.00514	0.00387	0.00299	0.00236	0.00188	0.00151
0.00122	0.00098	0.00078	0.00060	0.00041	0.00015	

ROW 25

0.00014	0.00038	0.00054	0.00069	0.00085	0.00103	0.00123
0.00147	0.00177	0.00213	0.00258	0.00316	0.00394	0.00499
0.00650	0.00877	0.01246	0.01912	0.03364	0.13158	-0.02533
-0.18557	-0.10091	-0.18405	-0.06534	0.12832	0.03251	0.01831
0.01181	0.00822	0.00602	0.00456	0.00353	0.00278	0.00222
0.00177	0.00142	0.00112	0.00085	0.00059	0.00021	

ROW 26

0.00017	0.00046	0.00065	0.00082	0.00101	0.00122	0.00146
0.00174	0.00208	0.00249	0.00301	0.00367	0.00454	0.00572
0.00739	0.00987	0.01384	0.02091	0.03604	0.13496	-0.02026
-0.17713	-0.08409	-0.08366	-0.17440	-0.07019	0.13004	0.03433
0.01968	0.01285	0.00903	0.00664	0.00505	0.00392	0.00308
0.00244	0.00193	0.00151	0.00115	0.00079	0.00028	

ROW 27

0.00019	0.00053	0.00074	0.00095	0.00116	0.00139	0.00166
0.00198	0.00236	0.00281	0.00339	0.00411	0.00506	0.00634
0.00813	0.01077	0.01495	0.02231	0.03784	0.13737	-0.01689
-0.17207	-0.07568	-0.06693	-0.07474	-0.16781	-0.07666	0.13044
0.03542	0.02056	0.01354	0.00957	0.00707	0.00537	0.00416
0.00325	0.00255	0.00198	0.00149	0.00102	0.00036	

ROW 28

0.00022	0.00059	0.00083	0.00106	0.00129	0.00155	0.00185
0.00219	0.00260	0.00310	0.00372	0.00450	0.00551	0.00687
0.00875	0.01152	0.01585	0.02342	0.03924	0.13918	-0.01447
-0.16870	-0.07064	-0.05856	-0.05813	-0.06910	-0.16255	-0.08402
0.12986	0.03597	0.02106	0.01395	0.00989	0.00731	0.00554
0.00427	0.00330	0.00254	0.00189	0.00129	0.00045	

ROW 29

0.00024	0.00065	0.00092	0.00116	0.00142	0.00170	0.00202
0.00239	0.00283	0.00336	0.00401	0.00484	0.00590	0.00732
0.00929	0.01215	0.01661	0.02434	0.04036	0.14058	-0.01267
-0.16629	-0.06727	-0.05354	-0.04983	-0.05264	-0.06502	-0.15790
-0.09187	0.12848	0.03611	0.02126	0.01413	0.01002	0.00739
0.00557	0.00425	0.00322	0.00238	0.00160	0.00056	

ROW 30

0.00026	0.00071	0.00099	0.00125	0.00153	0.00183	0.00217
0.00256	0.00303	0.00359	0.00428	0.00514	0.00625	0.00772
0.00975	0.01269	0.01725	0.02510	0.04128	0.14171	-0.01126
-0.16448	-0.06487	-0.05020	-0.04485	-0.04442	-0.04877	-0.06179
-0.15347	-0.10000	0.12637	0.03588	0.02120	0.01410	0.00998
0.00732	0.00546	0.00408	0.00298	0.00199	0.00068	

ROW 31

0.00028	0.00076	0.00106	0.00134	0.00163	0.00195	0.00231
0.00272	0.00321	0.00380	0.00451	0.00541	0.00656	0.00808
0.01016	0.01316	0.01780	0.02574	0.04205	0.14263	-0.01013
-0.16307	-0.06307	-0.04781	-0.04152	-0.03948	-0.04064	-0.04577
-0.05903	-0.14903	-0.10826	0.12359	0.03533	0.02088	0.01386
0.00975	0.00708	0.00518	0.00372	0.00245	0.00083	

ROW 32	0.00030	0.00081	0.00113	0.00142	0.00173	0.00206	0.00244
	0.00287	0.00338	0.00399	0.00473	0.00565	0.00683	0.00839
	0.01052	0.01357	0.01827	0.02629	0.04269	0.14339	-0.00921
	-0.16195	-0.06167	-0.04601	-0.03915	-0.03619	-0.03576	-0.03776
	-0.04329	-0.05653	-0.14443	-0.11653	0.12011	0.03446	0.02032
	0.01341	0.00934	0.00665	0.00468	0.00303	0.00102	

ROW 33	0.00031	0.00085	0.00119	0.00150	0.00182	0.00217	0.00256
	0.00301	0.00353	0.00416	0.00492	0.00587	0.00708	0.00867
	0.01084	0.01394	0.01869	0.02677	0.04325	0.14404	-0.00844
	-0.16103	-0.06055	-0.04462	-0.03737	-0.03384	-0.03251	-0.03295
	-0.03542	-0.04111	-0.05416	-0.13953	-0.12470	0.11590	0.03326
	0.01951	0.01274	0.00870	0.00595	0.00378	0.00125	

ROW 34	0.00033	0.00090	0.00125	0.00157	0.00190	0.00226	0.00267
	0.00313	0.00367	0.00432	0.00510	0.00607	0.00731	0.00892
	0.01112	0.01426	0.01905	0.02719	0.04373	0.14460	-0.00779
	-0.16026	-0.05963	-0.04350	-0.03599	-0.03208	-0.03019	-0.02975
	-0.03069	-0.03340	-0.03912	-0.05183	-0.13424	-0.13268	0.11086
	0.03170	0.01840	0.01178	0.00774	0.00478	0.00155	

ROW 35	0.00034	0.00094	0.00130	0.00164	0.00198	0.00235	0.00277
	0.00325	0.00380	0.00447	0.00527	0.00626	0.00751	0.00915
	0.01138	0.01455	0.01938	0.02756	0.04415	0.14508	-0.00724
	-0.15961	-0.05886	-0.04259	-0.03488	-0.03071	-0.02845	-0.02746
	-0.02755	-0.02878	-0.03159	-0.03721	-0.04946	-0.12842	-0.14033
	0.10486	0.02972	0.01692	0.01042	0.00618	0.00194	

ROW 36	0.00036	0.00097	0.00135	0.00170	0.00205	0.00244	0.00287
	0.00336	0.00393	0.00460	0.00542	0.00642	0.00770	0.00936
	0.01161	0.01481	0.01967	0.02789	0.04452	0.14550	-0.00675
	-0.15906	-0.05822	-0.04183	-0.03397	-0.02961	-0.02709	-0.02574
	-0.02530	-0.02570	-0.02708	-0.02990	-0.03533	-0.04698	-0.12195
	-0.14748	0.09766	0.02719	0.01489	0.00827	0.00250	

ROW 37	0.00037	0.00101	0.00140	0.00176	0.00212	0.00252	0.00296
	0.00346	0.00404	0.00472	0.00555	0.00658	0.00787	0.00955
	0.01182	0.01504	0.01993	0.02818	0.04485	0.14587	-0.00633
	-0.15858	-0.05766	-0.04119	-0.03322	-0.02872	-0.02601	-0.02441
	-0.02361	-0.02349	-0.02407	-0.02551	-0.02826	-0.03341	-0.04434
	-0.11462	-0.15386	0.08881	0.02382	0.01176	0.00333	

ROW 38	0.00038	0.00104	0.00145	0.00181	0.00219	0.00259	0.00304
	0.00355	0.00414	0.00484	0.00568	0.00672	0.00803	0.00973
	0.01201	0.01526	0.02017	0.02844	0.04514	0.14620	-0.00596
	-0.15815	-0.05718	-0.04063	-0.03258	-0.02797	-0.02512	-0.02334
	-0.02230	-0.02184	-0.02192	-0.02259	-0.02402	-0.02662	-0.03141
	-0.04146	-0.10615	-0.15901	0.07741	0.01875	0.00472	

ROW 39	0.00039	0.00107	0.00149	0.00186	0.00225	0.00266	0.00312
	0.00364	0.00424	0.00495	0.00580	0.00685	0.00817	0.00989
	0.01219	0.01545	0.02038	0.02868	0.04541	0.14650	-0.00563
	-0.15778	-0.05676	-0.04016	-0.03203	-0.02733	-0.02438	-0.02247
	-0.02125	-0.02056	-0.02031	-0.02050	-0.02120	-0.02255	-0.02494
	-0.02926	-0.03821	-0.09606	-0.16187	0.06065	0.00750	

ROW 40

0.00041	0.00110	0.00153	0.00191	0.00230	0.00273	0.00319
0.00372	0.00433	0.00505	0.00591	0.00697	0.00831	0.01003
0.01235	0.01563	0.02058	0.02890	0.04565	0.14677	-0.00533
-0.15745	-0.05639	-0.03974	-0.03156	-0.02679	-0.02376	-0.02174
-0.02039	-0.01953	-0.01906	-0.01894	-0.01918	-0.01984	-0.02106
-0.02317	-0.02689	-0.03444	-0.08337	-0.15897	0.02500	

ROW 41

0.00042	0.00113	0.00157	0.00196	0.00236	0.00279	0.00326
0.00380	0.00442	0.00514	0.00602	0.00709	0.00843	0.01017
0.01250	0.01579	0.02076	0.02910	0.04587	0.14701	-0.00507
-0.15715	-0.05606	-0.03937	-0.03114	-0.02632	-0.02322	-0.02112
-0.01968	-0.01869	-0.01805	-0.01772	-0.01766	-0.01790	-0.01848
-0.01951	-0.02123	-0.02417	-0.02977	-0.04411	-0.20520	

APPENDIX D

Computer Program for Inversion Integral Method (Cassegrain Mirror)

The computer program listed here is a Fortran program written for the IEM SYSTEM 360-75. The program solves the integral equation for the Foucault Test using the inversion integral method of solution for the case of a mirror with a central hole. All operations are performed in double precision (approximately 16 decimal places).

The main program reads in M and $MODE$ under a (215) format. M is the number of evenly spaced points on the mirror and must be even. The end points and points on the edge of the hole are among these M points. $MODE$ determines which method of numerical integration is to be used ($MODE = 1$, trapezoid rule; $MODE = 2$, Simpson's rule; $MODE = 3$, 5-point rule). Also in the main program R , the radius of the central hole, is read in under a (E 12.8) format. Next the subroutine $GMAT$ is called. $GMAT$ generates the G matrix which is stored in $G(I, J)$. The subroutine $GMAT$ calls subroutine $AMAT$, which calculates the $A(I, J)$ matrix (Eq. 10-36). $AMAT$ in turn calls the subroutine $HMAT$, which calculates the numerical integration matrix $H(I)$. $H(I)$ is used in $A(I, J)$ and $A(I, J)$ is used in calculating $G(I, J)$, Eqs. (10-35), (10-33), (10-37), and (10-40). Control then returns to the main program where $NRUN$, the number of cases to be solved, is read in under an (I5) format. Next the subroutine $CAPF$ is called. $CAPF$ calculates the light intensity difference $F(x)$ from a functional representation at the M points on the Mirror (Eqs. 10-42, 10-44, 10-50, 10-51). The M values of $F(x)$ are stored in $FBIG(I)$ in the main program and $F(I)$ in subroutine $CAPF$. Subroutine $DGMPRD$ then matrix multiplies F into $FBIG$ to return $FLIT$, Eq. (10-39). The matrix $FLIT$ contains M values of the surface error $f(x)$ calculated at the same points as $F(x)$. $DGMPRD$ is an external IEM subroutine contained in the Scientific-Subroutine Package. If the "hump case" for $f(x)$ is to be run, as in case 4 of this listing, A and B , the location and size of the hump, must be given values in $CAPF$. If $F(x)$ is to be input data rather than functionally represented, then $CAPF$ may be replaced by a $READ$ statement.

```

      IMPLICIT REAL*8 (A-Z)
      DIMENSION A(42,42),H(42),G(42,42),FRIG(42),FLIT(42)
C   ***INVERSION INTEGRAL METHOD FOR HOLE CASE***
      WRITE(6,109)
109  FORMAT(/,10X,'***INVERSION INTEGRAL METHOD FOR HOLE CASE**')
      READ(5,101) M,MODE
101  FORMAT(2I5)
      READ(5,102) R
102  FORMAT(3E12.8)
      WRITE(6,107) M,MODE,R
107  FORMAT(///,10X,'NO. OF POINTS = ',I5,/,10X,'MODE = ',I5,13X,'R = ',
      *,E16.8)
      CALL GMAT(M,MODE,G,R)
      WRITE(6,104)
104  FORMAT(///,10X,'G MATRIX')
      DO 2 I=1,M
        2  WRITE(6,103) I,(G(I,J),J=1,M)
103  FORMAT(1H,5X,'ROW',I3/(10X,5E16.8))
      READ(5,101) MRUN
      WRITE(6,110) MRUN
110  FORMAT(10X,'NO. OF CASES RUN = ',I5)
      DO 3 I=1,MRUN
        CALL CAPF(H,FRIG,R,I)
        CALL DGIPRD(G,FRIG,FLIT,M,M,1)
        WRITE(6,105)
105  FORMAT(///,10X,'LITTLE F')
        3  WRITE(6,106) (FLIT(J),J=1,M)
106  FORMAT(1H,(10X,5E16.8))
      STOP
      END

```

```

SUBROUTINE GMAT(M,MODE,G,R)
IMPLICIT REAL*8(A-H,O-Z)
DIMENSION G(42,42),H(42),D(42),GT(42),A(42,42),X(42)
PI=3.1415926535897900
PI2=PI*PI
CALL AMAT(M,MODE,A,H,R,X)
DO 1 J=1,M
1 D(J)=      PI2+(A(J,J))**2
MH=M/2
MH1=MH+1
M1=M-1
MHM1=MH-1
MH2=MH+2
D(1)=28.000
D(M)=28.000
D(MH)=11.000
D(MH1)=11.000
DO 5 I=1,M
DO 2 J=1,M
IF(J .EQ. I) GO TO 2
G(I,J)=X(J)*A(I,J)/(X(I)*D(J))
2 CONTINUE
G(I,I)=-A(I,I)/D(I)
5 CONTINUE
G(1,1)=0.206000
G(M,M)=-0.206000
G(MH,MH)=-0.318000
G(MH1,MH1)=0.318000
G(2,1)=-0.028300
G(M1,M)=0.028300
G(MHM1,MH)=0.043200
G(MH2,MH1)=-0.043200
G(MHM1,MH1)=-0.003100
G(MH2,MH)=0.003100
DO 9 I=1,M
H(I)=G(MH,I)
9 GT(I)=G(MH1,I)
DO 8 I=1,M
DO 8 J=1,M
8 G(I,J)=G(I,J) -((1.000-R/( X(I)))*H(J)  +(1.000+R/( X(I)))*GT(J
*)))/2.000
RETURN
END

```

```

SUBROUTINE AMAT(M,MODE,A,H,R,X)
IMPLICIT REAL*8 (A-H,O-Z)
DIMENSION A(M,M),H(M),AT(42,42),B(42,42),X(42)
MH=M/2
CALL HMAT(MH,MODE,H)
M1=M-1
M2=M-2
MH1=MH+1
MH2=MH+2
MH3=MH+3
MHM1=MH-1
MHM2=MH-2
P=2*(1.000-R)/DFLOAT(M2)
DO 1 J=1,MH
1 X(J)=-1.000+P*(J-1)
DO 2 J=MH1,M1
2 X(J)=R+P*(J-MH1)
DO 3 I=1,M
DO 3 J=1,M
IF(J .EQ. I) GO TO 3
A(I,J)=(P*H(J))/(X(J)-X(I))
3 CONTINUE
DO 4 I=2,M1
IP1=I+1
IM1=I-1
A(I,IM1)=-H(IM1)-0.500*H(I)
A(I,IP1)=H(IP1)+0.500*H(I)
ADD=0.000
DO 5 J=1,M
IF(I .EQ. J) GO TO 5
ADD=ADD+A(I,J)
5 CONTINUE
4 A(I,I)=-ADD
A(MH,MH1)=(P*H(MH1))/(X(MH1)-X(MH))
A(MH1,MH)=(P*H(MH))/(X(MH)-X(MH1))
A(MH,MHM1)=(P*H(MHM1))/(X(MHM1)-X(MH))
A(MH1,MH2)=(P*H(MH2))/(X(MH2)-X(MH1))
A(1,1)=1.000
A(1,M)=1.000
WRITE(6,102)
102 FOR FMT(///,10X,'A MATRIX')
DO 10 I=1,M
10 WRITE(6,101) I,(A(I,J),J=1,M)
101 FORMAT(1H ,5X,'ROW ',I3,'/(10X,5E16.8))
RETURN
END

```

```

SUBROUTINE FNAT(N,MODE,H)
IMPLICIT REAL*8(A-H,O-Z)
DIMENSION H(N)
M1=N-1
M2=M-2
GO TO (1,2,3),MODE
1 DO 10 I=2,M1
10 H(I)=1.000
F(1)=0.500
H(M)=0.500
GO TO 7
2 DO 11 I=2,M1,2
11 H(I)=4.000/3.000
DO 12 I=3,M2,2
12 H(I)=2.000/3.000
H(1)=1.000/3.000
H(M)=1.000/3.000
GO TO 7
3 DO 16 I=2,M1,2
16 H(I)=32.000/45.000
DO 17 I=3,M2,4
17 H(I)=12.000/45.000
M4=M-4
DO 18 I=5,M4,4
18 H(I)=14.000/45.000
H(1)=7.000/45.000
H(M)=7.000/45.000
7 CONTINUE
DO 4 I=1,M
M1=M-I
M2=M-M
4 H(M1)=H(I)
M2=M-M
WRITE(6,101)
101 FORMAT(///,10X,'H MATRIX')
WRITE(6,102) (H(I),I=1,M2)
102 FORMAT(1H ,(10X,5E16.8))
RETURN
END

```

```

SUBROUTINE CAPE (N, F, K, J)
IMPLICIT REAL*8 (A-H, O-Z)
DIMENSION F(N)
M2=N/2
P=2.000*(1.000-R)/(M-2.000)
X=-1.000-P
A=0.6500
R=0.17500
WRITE(6,103) A,R
103 FORMAT(//,10X,'A = ',F16.8,/,10X,'R = ',F16.8)
DO 52 I=1,M
X=X+P
GO TO (1,2,3,4,5,6,7),J
1 F(I)=-35.000
GO TO 52
2 F(I)=-35.000*X
GO TO 52
3 F(I)=-35.000*X*X
GO TO 52
4 Z=(X-A)/R
IF (Z**2 .GE. 1.00001) GO TO 53
IF (Z**2 .LT. 1.00001 .AND. Z**2 .GT. .99990) GO TO 55
F(I)=-2.0*Z**3+(10.0/3.0)*Z-((1.0-Z**2)**2)*DLOG(DABS(((1.0-Z)/(1.0+Z))*((1.0+X)/(1.0-X))*((X-R)/(X+R))))
GO TO 52
53 F(I)=2.0/(3.0*Z)+2.0/(3.0*Z**3)-((Z**2-1.0)**2)*(2.0/Z+2.0/(3.0*Z*
1*3)+DLOG(DABS((Z-1.0)/(Z+1.0))))
GO TO 52
55 F(I)=DSIGN((4.0/3.000),Z)
GO TO 52
5 F(I)=14.000/X
GO TO 52
6 F(I)=DSIGN(35.000,X)
GO TO 52
7 F(I)=14.000/(X*X)
52 IF(I .EQ. M2) X=R-P
WRITE(6,101) (F(I),I=1,M)
101 FORMAT(//,10X,'BIG F',/, (6D16.8))
RETURN
/ END

```